

**THE UNIVERSITY OF ALABAMA**  
**COLLEGE OF ENGINEERING**  
**BUREAU OF ENGINEERING RESEARCH**

M.S. Thesis

Contract Number MASG-R / ER3



**HYDRODYNAMICS OF  
MOBILE BAY AND  
MISSISSIPPI SOUND -  
PASS EXCHANGE STUDIES**

by  
John P. Jarrell  
graduate research assistant

directed by  
Gary C. April  
Donald C. Raney  
co-principal investigators

prepared for  
Mississippi-Alabama Sea Grant Consortium

July 1981

BER Report No. 271-112

MASGP-80-023

### **BUREAU OF ENGINEERING RESEARCH**

Members of the faculty who teach at the undergraduate and graduate levels, along with their graduate students, generate and conduct the investigations that make up the College's research program. The College of Engineering of The University of Alabama believes that research goes hand in hand with teaching. Early in the development of its graduate program, the College recognized that men and women engaged in research should be as free as possible of the administrative duties involved in sponsored research. Therefore, the Bureau of Engineering Research (BER) was established and assigned the administrative responsibility for such research within the College.

The director of BER—himself a faculty member and researcher—maintains familiarity with the support requirements of both proposals and research in progress. He is aided by the College of Engineering Research Committee which is made up of faculty representatives from the academic departments of the College. This committee serves to inform BER of the needs and perspectives of the research program.

In addition to administrative support, BER is charged with providing certain technical assistance. Because it is not practical for each department to become self-sufficient in all phases of the supporting technology essential to present-day research, BER makes services available through support groups such as the machine shop, the electronics shop, and publication services.

HYDRODYNAMICS OF MOBILE BAY AND MISSISSIPPI SOUND  
PASS-EXCHANGE STUDIES

by John P. Jarrell

A THESIS

Submitted in partial fulfillment of the requirements for the  
Degree of Master of Science in the Department of  
Chemical and Metallurgical Engineering  
in the Graduate School of  
The University of Alabama

University, Alabama

1981

HYDRODYNAMICS OF MOBILE BAY AND MISSISSIPPI SOUND  
PASS-EXCHANGE STUDIES

Preface

This document contains the results of a mathematical modeling study of Mobile Bay/East Mississippi Sound. The study was supported by the Mississippi-Alabama Sea Grant Consortium under contract number MASG-R/ER3 and is complementary to the information contained in BER Report No. 247-112 (MASG-R/ES4) dated March 1980.

Additionally, this work also satisfies, in part, the degree requirements for a Master of Science in Chemical Engineering for John Phillip Jarrell, a graduate research assistant on the project.

## ABSTRACT

The purpose of this research is to develop a mathematical model of Mobile Bay and East Mississippi Sound, Alabama capable of describing the hydrodynamics in Pass aux Herons and Main Pass. The elucidation of the complex interaction of these passes is necessary to further the knowledge of the Alabama coastal system gained through previous modeling efforts.

The inadequacies of the existing Mobile Bay models for the description of pass hydrodynamics necessitate the use of a different model. The recently developed WES Implicit Flooding Model, Version II (WIFM II) is applied to the Mobile Bay-East Mississippi Sound system. This model is suitable for the indicated purpose because of the implicit solution format and variable grid size capabilities which it possesses.

Calibration and verification of the model with available field data is accomplished. The model is determined to be an effective trend analysis tool for the study of the pass hydrodynamics on the basis of these studies.

Parametric studies are then undertaken to determine the relative effects of tide range, river flow, and a constant wind on Pass aux Herons and Main Pass flows. Tide range variation produced the most significant effects in the water transport in the passes. Changing river flows and a constant wind also alter the flow patterns in the passes.

Utilization of WIFM II for the study of the trend behavior in the passes of Mobile Bay-East Mississippi Sound is presented. Continued efforts toward field data collection studies are recommended to develop this and other Mobile Bay models from trend analysis tools to fully predictive models for the improved management of the coastal Alabama system.

## VITA

John P. Jarrell, son of Col. (Ret) Vernon H. and E. Jean Jarrell, was born in Sacramento, California, on November 5, 1956. He completed his high school education at Douglas High School, Rapid City, South Dakota, in May, 1975. He entered the University of Alabama in August, 1975. He graduated with a degree of Bachelor of Science, summa cum laude, in Chemistry in May, 1979. The author is currently a M.S. candidate at the Department of Chemical and Metallurgical Engineering of The University of Alabama.

## NOMENCLATURE

$a_1, b_1, c_1$  = arbitrary constants defining expansion coefficients for variable grid of WIFM II on x-axis

$a_2, b_2, c_2$  = arbitrary constants defining expansion coefficients for variable grid of WIFM II on y-axis

$b$  = barrier height

cfs = cubic feet per second

cu = cubic

$C$  = Chezy friction coefficient

$C_o$  = admittance coefficient for water flowing over a barrier

CST = Central Standard Time

$d = \eta - h$  = total water depth

$d_H$  = depth of water over the crest of a barrier

$e$  = eddy viscosity coefficient

$f$  = Coriolis parameter

$F$  = external force factor

fps = feet per second

ft = feet

$g$  = gravitational acceleration

$h$  = still water elevation

hr = hour

$H_{\max}$  = maximum depth of any grid cell

k = knot  
km = kilometer  
LWD = Low Water Datum  
m = meter  
mi = mile  
M = WIFM II direction corresponding to x-axis  
MLW = Mean Low Water  
MP = Main Pass  
MSL = Mean Sea Level  
n = Manning friction factor  
N = WIFM II direction corresponding to y-axis  
ppt = parts per thousand  
P = pressure  
PaH = Pass aux Herons  
 $Q_N$  = normal component of water transport  
R = rate of water accumulation  
sec = second  
sq = square  
t = time  
u = velocity in x-direction  
U = flow per unit width in M-direction  
v = velocity in y-direction  
V = flow per unit width in N-direction  
w = velocity in z-direction  
WES = Waterways Experiment Station  
WIFM II = WES Implicit Flooding Model Version II

$x, y, z$  = Cartesian coordinate system axes  
 $\alpha_1$  = WIFM II computational space dimension of x-axis  
 $\alpha_2$  = WIFM II computational space dimension of y-axis  
 $\Delta s$  = spatial step size  
 $\Delta t$  = time step size  
 $\epsilon$  = height of water defining a wet or dry cell  
 $\eta$  = surface water elevation relative to  $h$   
 $\eta_a$  = surface water elevation corresponding to atmospheric pressure  
 $\mu$  = viscosity  
 $\rho$  = density

## ACKNOWLEDGEMENTS

The author is obliged to Dr. Gary C. April and Dr. Donald C. Raney for providing the opportunity to participate in this research project. Their guidance, encouragement, and suggestions during the course of this work are greatly appreciated.

Financial support from the Mississippi-Alabama Sea Grant Program and the Graduate School of the University of Alabama is gratefully acknowledged.

The author also wishes to thank the persons who unselfishly assisted in this study: to Lynn Kopp, Pat Moore, Joyce Donley, Carolyn Trent, and others, at The University of Alabama Seebeck Computer Center without whose help this project could not have been completed; to Dr. William W. Schroeder and Dr. William C. Clements, Jr. for their interest and concern; to Col. and Mrs. Vernon H. Jarrell for their continued encouragement and love; to Susan A. Penny for her presence; and to Woodie D. Mordecai whose moral support and friendship are invaluable.

## TABLE OF CONTENTS

ABSTRACT . . . . .	iii
VITA . . . . .	v
NOMENCLATURE . . . . .	vi
ACKNOWLEDGEMENTS . . . . .	ix
LIST OF TABLES . . . . .	xiii
LIST OF FIGURES . . . . .	xiv
CHAPTER	
I. INTRODUCTION . . . . .	1
II. BACKGROUND . . . . .	6
Study Area . . . . .	6
Mobile Bay . . . . .	6
East Mississippi Sound . . . . .	7
Passes . . . . .	7
Main Pass. . . . .	7
Petit Bois Pass. . . . .	8
Pass aux Herons . . . . .	8
Effect of Pass Exchange on Oyster	
Productivity . . . . .	10
Methods for Studying Estuarine	
Hydrodynamics . . . . .	12
Field data . . . . .	12
Models . . . . .	13
Physical models . . . . .	13
Mathematical models . . . . .	15
Use of Mathematical Models in Mobile Bay . . . . .	16
Hydrodynamics and salinity . . . . .	16
Non-conservative species transport . . . . .	16
Sedimentation study . . . . .	18
Effects of river flooding and storm	
surges . . . . .	18
Limitations of Existing Mobile Bay Models	
for Pass-exchange Study . . . . .	19
Reasons for Use of WIFM II Model . . . . .	21
Variable grid . . . . .	21
Implicit solution technique . . . . .	21

Objectives of Study . . . . .	22
III. DESCRIPTION OF WIFM II . . . . .	24
General Equations . . . . .	24
Assumptions and Limitations of WIFM II . . . . .	26
Variable-grid Equations . . . . .	29
Alternating-Direction, Implicit Formulation . . . . .	31
Boundary Conditions . . . . .	31
Open boundaries . . . . .	31
Water-land boundaries . . . . .	33
Subgrid boundaries . . . . .	33
External Forces . . . . .	36
IV. APPLICATION OF WIFM II TO MOBILE BAY-EAST MISSISSIPPI SOUND . . . . .	37
Development of Variable Grid . . . . .	37
Limits of system . . . . .	37
Description of variable grid . . . . .	39
Grid cell size . . . . .	39
Boundaries . . . . .	41
Depths . . . . .	44
Flood cells . . . . .	46
Manning friction factors . . . . .	46
Pass flow calculations . . . . .	47
Field Data for Calibration/Verification . . . . .	47
Description of field data . . . . .	47
Comparison of model data to field data . . . . .	48
Calibration/Verification . . . . .	49
Case study of field data from May 15 and 16, 1972 . . . . .	49
Results of case study of May 15 and 16, 1972 . . . . .	55
Tide elevation . . . . .	55
Velocity magnitude and direction . . . . .	62
Pass flow rates . . . . .	62
Case study of field data from June 13 and 14, 1973 . . . . .	63
Results of case study of June 13 and 14, 1973 . . . . .	67
Tide elevation . . . . .	67
Velocity magnitude and direction . . . . .	73
Re-evaluation of the 1972 case study . . . . .	74
Results of model run using astronomical tides from May 15 and 16, 1972 . . . . .	76
Tide elevation . . . . .	76
Velocity magnitude and direction . . . . .	83
Pass flow rates . . . . .	83

Results of model run using Dauphin Island Gulf gage from May 15 and 16, 1972 delayed 2 hrs . . . . .	83
Tide elevation . . . . .	90
Velocity magnitude and direction . . . . .	90
Pass flow rates . . . . .	90
Conclusion of calibration/ verification study . . . . .	91
V. PARAMETRIC STUDY . . . . .	93
Tide Range, River Flow, and Wind . . . . .	93
Effects on Flows through Passes . . . . .	93
Effects on Current Velocities in the Passes	102
VI. CONCLUSIONS AND RECOMMENDATIONS . . . . .	135
Concluding Observations . . . . .	135
Recommendations for Further Study . . . . .	137
LIST OF REFERENCES . . . . .	139
APPENDICES . . . . .	143
A. Sample Input Data to WIFM II . . . . .	144
B. Sample Output from WIFM II . . . . .	152

LIST OF TABLES

1.	Tide Range, River Flow, and Wind for Each Model Run . . . . .	94
2.	Total Incoming and Outgoing Pass Flows for Each Model Run . . . . .	97

## LIST OF FIGURES

Figure		
1.	Map of Mobile Bay-East Mississippi Sound Area on the Gulf of Mexico Coast of Alabama (3)	2
2.	Grid Used for All Mobile Bay Model Studies Based on the Work of Hill (12)	17
3.	Definition of Grid Cell Variables for WIFM II	32
4.	Flood Cell Treatment by WIFM II (17)	34
5.	Barrier Conditions Treated by WIFM II (17)	35
6.	Boundaries of Mobile Bay-East Mississippi Sound Model	38
7.	Variable Grid for Mobile Bay-East Mississippi Sound--Cell Number (N,M)	40
8.	Grid Formulation in Pass aux Herons	42
9.	Grid Formulation in Main Pass	43
10.	Significant Water Levels Relative to Low Water Datum	45
11.	Velocity Calculation for Field Data Station at Grid Cell (N,M)--Four-point Average	50
12.	Location of Field Data Stations for May 15-16, 1972 (26)	51
13.	Grid Representation of Field Data Stations for 1972	53
14.	Comparison of Model Results with 1972 Data A. Dauphin Island Gulf Tide Gage B. Dauphin Island Marine Lab Tide Gage	56
15.	Comparison of Model Results with 1972 Data A. Cedar Point Tide Gage B. Fowl River Tide Gage	57

16.	Comparison of Model Results with 1972 Data .	58
	A. State Docks Tide Gage	
	B. Point Clear Tide Gage	
17.	Comparison of Model Results with 1972 Data .	59
	A. Bon Secour Tide Gage	
	B. East Main Pass Velocity Station	
18.	Comparison of Model Results with 1972 Data .	60
	A. West Main Pass Velocity Station	
	B. Buoy 12 Velocity Station	
19.	Comparison of Model Results with 1972 Data .	61
	A. Main Pass Flow Rate	
	B. Pass aux Herons Flow Rate	
20.	Location of Field Data Stations for June 13-14, 1973 (26) . . . . .	64
21.	Grid Representation of Field Data Stations for 1973 . . . . .	66
22.	Comparison of Model Results with 1973 Data .	68
	A. Dauphin Island Marine Lab Tide Gage	
	B. Cedar Point Tide Gage	
23.	Comparison of Model Results with 1973 Data .	69
	A. State Docks Tide Gage	
	B. Point Clear Tide Gage	
24.	Comparison of Model Results with 1973 Data .	70
	A. Bon Secour Tide Gage	
	B. East Main Pass Velocity Station	
25.	Comparison of Model Results with 1973 Data .	71
	A. Dauphin Island Bridge Velocity Station	
	B. Buoy 12 Velocity Station	
26.	Comparison of Model Results with 1973 Data .	72
	A. Buoy 32 Velocity Station	
	B. State Docks Velocity Station	
27.	Comparison of Astronomical Tide with Tide Record . . . . .	75
	A. Bayou La Batre (BLB)-Cedar Point (CP)	
	B. Dauphin Island (Fort Gaines) (DI(FG))- Dauphin Island Gulf (DIG)	

28.	Comparison of Astronomical-tide Model Results with 1972 Data . . . . .	77
	A. Dauphin Island Gulf Tide Gage	
	B. Dauphin Island Marine Lab Tide Gage	
29.	Comparison of Astronomical-tide Model Results with 1972 Data . . . . .	78
	A. Cedar Point Tide Gage	
	B. Fowl River Tide Gage	
30.	Comparison of Astronomical-tide Model Results with 1972 Data . . . . .	79
	A. State Docks Tide Gage	
	B. Point Clear Tide Gage	
31.	Comparison of Astronomical-tide Model Results with 1972 Data . . . . .	80
	A. Bon Secour Tide Gage	
	B. East Main Pass Velocity Station	
32.	Comparison of Astronomical-tide Model Results with 1972 Data . . . . .	81
	A. West Main Pass Velocity Station	
	B. Buoy 12 Velocity Station	
33.	Comparison of Astronomical-tide Model Results with 1972 Data . . . . .	82
	A. Main Pass Flow Rate	
	B. Pass aux Herons Flow Rate	
34.	Comparison of Dauphin Island Gulf Record Delayed 2 hrs with 1972 Data . . . . .	84
	A. Dauphin Island Gulf Tide Gage	
	B. Dauphin Island Marine Lab Tide Gage	
35.	Comparison of Dauphin Island Gulf Record Delayed 2 hrs with 1972 Data . . . . .	85
	A. Cedar Point Tide Gage	
	B. Fowl River Tide Gage	
36.	Comparison of Dauphin Island Gulf Record Delayed 2 hrs with 1972 Data . . . . .	86
	A. State Docks Tide Gage	
	B. Point Clear Tide Gage	
37.	Comparison of Dauphin Island Gulf Record Delayed 2 hrs with 1972 Data . . . . .	87
	A. Bon Secour Tide Gage	
	B. East Main Pass Velocity Station	

38.	Comparison of Dauphin Island Gulf Record Delayed 2 hrs with 1972 Data . . . . .	88
	A. West Main Pass Velocity Station	
	B. Buoy 12 Velocity Station	
39.	Comparison of Dauphin Island Gulf Record Delayed 2 hrs with 1972 Data . . . . .	89
	A. Main Pass Flow Rate	
	B. Pass aux Herons Flow Rate	
40.	Tide Elevations Used as Boundary Conditions for Parametric Studies . . . . .	95
	A. Low Tide Range	
	B. Medium Tide Range	
	C. High Tide Range	
41.	Comparison of Pass Flow Rates of Run 6 with Run 1 . . . . .	99
42.	Comparison of Pass Flow Rates of Run 2 and Run 3 with Run 1 . . . . .	100
43.	Comparison of Pass Flow Rates of Run 4 and Run 5 with Run 1 . . . . .	101
44.	Velocity Vector Plot of Mobile Bay-East Mississippi Sound--Run 1 (Ebb Tide) . . . . .	103
45.	Velocity Vector Plot of Mobile Bay-East Mississippi Sound--Run 1 (Low Tide) . . . . .	104
46.	Velocity Vector Plot of Mobile Bay-East Mississippi Sound--Run 1 (Flood Tide) . . . . .	105
47.	Velocity Vector Plot of Mobile Bay-East Mississippi Sound--Run 1 (High Tide) . . . . .	106
48.	Velocity and Flow-rate Vector Plots--Run 1 (Ebb Tide) . . . . .	111
49.	Velocity and Flow-rate Vector Plots--Run 1 (Low Tide) . . . . .	112
50.	Velocity and Flow-rate Vector Plots--Run 1 (Flood Tide) . . . . .	113
51.	Velocity and Flow-rate Vector Plots--Run 1 (High Tide) . . . . .	114

52.	Velocity Vector Plots--Run 2 . . . . .	115
	(Medium Tide Range, Low River, No Wind)	
	Ebb Tide--A. Pass aux Herons B. Main Pass	
	Flood Tide--C. Pass aux Herons D. Main Pass	
53.	Velocity Vector Plots--Run 2 . . . . .	117
	(Medium Tide Range, Low River, No Wind)	
	Low Tide--A. Pass aux Herons B. Main Pass	
	High Tide--C. Pass aux Herons D. Main Pass	
54.	Velocity Vector Plots--Run 3 . . . . .	119
	(Medium Tide Range, High River, No Wind)	
	Ebb Tide--A. Pass aux Herons B. Main Pass	
	Flood Tide--C. Pass aux Herons D. Main Pass	
55.	Velocity Vector Plots--Run 3 . . . . .	121
	(Medium Tide Range, High River, No Wind)	
	Low Tide--A. Pass aux Herons B. Main Pass	
	High Tide--C. Pass aux Herons D. Main Pass	
56.	Velocity Vector Plots--Run 4 . . . . .	123
	(Low Tide Range, Medium River, No Wind)	
	Ebb Tide--A. Pass aux Herons B. Main Pass	
	Flood Tide--C. Pass aux Herons D. Main Pass	
57.	Velocity Vector Plots--Run 5 . . . . .	124
	(Low Tide Range, Medium River, No Wind)	
	Low Tide--A. Pass aux Herons B. Main Pass	
	High Tide--C. Pass aux Herons D. Main Pass	
58.	Velocity Vector Plots--Run 5 . . . . .	127
	(High Tide Range, Medium River, No Wind)	
	Ebb Tide--A. Pass aux Herons B. Main Pass	
	Flood Tide--C. Pass aux Herons D. Main Pass	
59.	Velocity Vector Plots--Run 5 . . . . .	129
	(High Tide Range, Medium River, No Wind)	
	Low Tide--A. Pass aux Herons B. Main Pass	
	High Tide--C. Pass aux Herons D. Main Pass	
60.	Velocity Vector Plots--Run 6 . . . . .	131
	(Medium Tide Range, Medium River,	
	15 k Wind from Southwest)	
	Ebb Tide--A. Pass aux Herons B. Main Pass	
	Flood Tide--C. Pass aux Herons D. Main Pass	
61.	Velocity Vector Plots--Run 6 . . . . .	133
	(Medium Tide Range, Medium River,	
	15 k Wind from Southwest)	
	Low Tide--A. Pass aux Herons B. Main Pass	
	High Tide--C. Pass aux Herons D. Main Pass	

## CHAPTER I

### INTRODUCTION

The principal components of estuarine Alabama are Mobile Bay, the Mobile River delta, and Mississippi Sound east of Petit Bois Island, Figure 1. These bodies of water are separated from the Gulf of Mexico by barrier islands. This coastal region also possesses large areas of salt marsh consistent with estuarine systems. The system has been a valuable resource since the establishment of the Port of Mobile in the early 1700s. Several man-made modifications dating from the 1820s, when channels were dredged to facilitate waterborne transportation, have affected water movement and circulation patterns in the Bay. These changes, providing deep-water access from the Bay to the Gulf, have led to the continued development of many industries in the area.

Mobile Harbor and the Gulf Intracoastal Waterway serve as avenues for over 60 million tons of commercial freight traffic yearly (1). The commercial seafood industry is vital to the economy of the coast with nearly 35 million pounds of seafood landed in Alabama valued at over 35 million dollars in 1976 (2). The area also

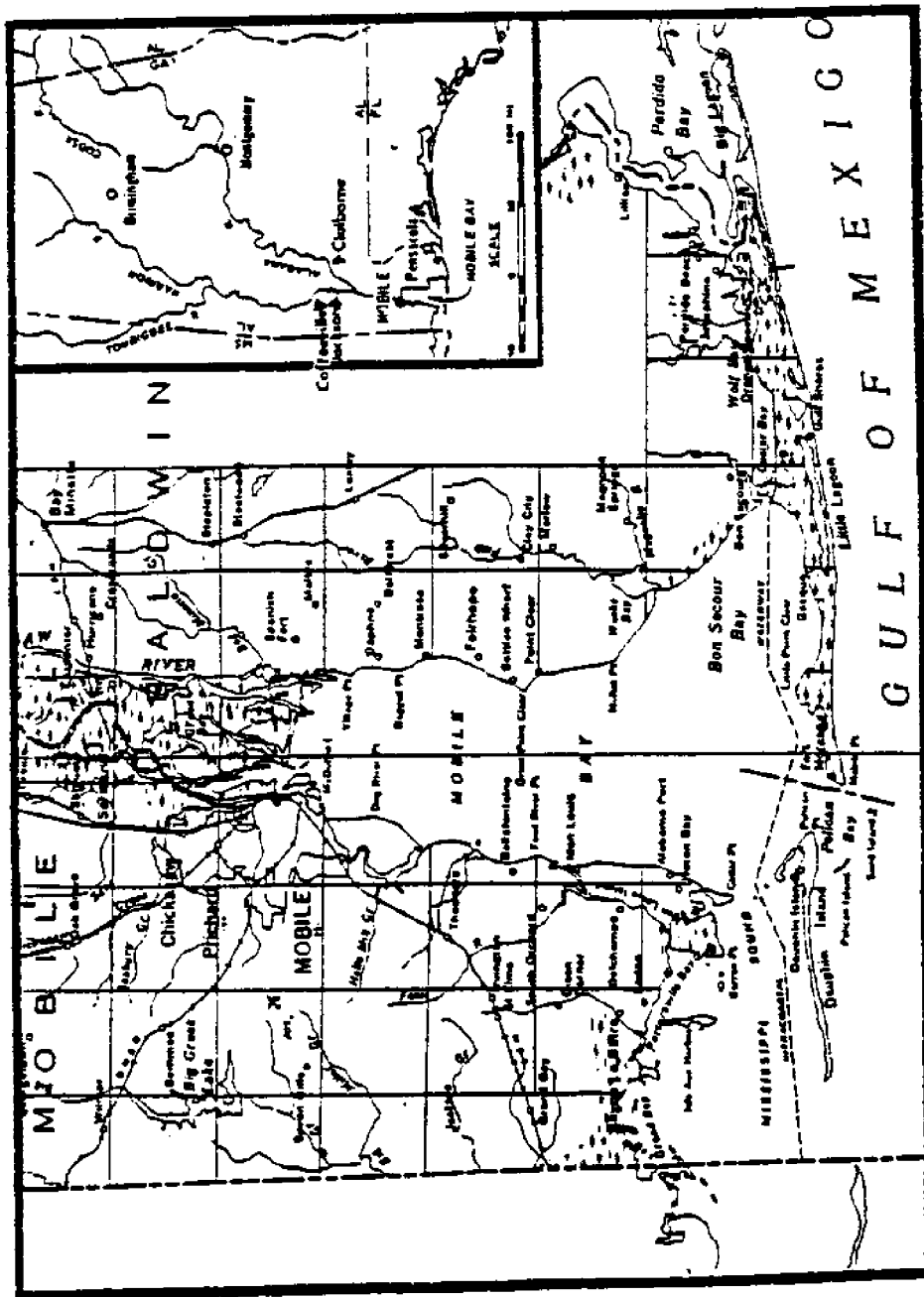


Figure 1. Map of Mobile Bay-East Mississippi Sound Area on the Gulf of Mexico Coast of Alabama (3).

supports many recreational activities typical of a coastal zone. In addition, estuarine Alabama provides many unique habitats for wildlife, some of which are endangered species. Chermock and LaMoreaux (4) state that the salt marshes are particularly delicate ecological systems whose importance is only recently being fully realized. The mutual coexistence and prosperity of these diverse interests in coastal Alabama depend upon the wise management of the estuarine system.

The first step in the efficient use of such a system is the elucidation of the water circulation patterns of the area. The understanding of estuarine hydrodynamics provides insight into the impact of man-made or natural changes to the system. Numerical models of estuarine systems such as coastal Alabama have been increasingly used as tools for describing hydrodynamic patterns. These models consist of mathematical representations of the laws of conservation, mass, and energy. Solution of the resulting equations by high-speed computer can greatly extend the data base for a system, provided the model is properly applied and suitably verified with field data (5-10).

A two-dimensional, depth-averaged model was developed and applied to Mobile Bay by Hill (11) to describe the hydrodynamic and salinity patterns within Mobile Bay proper. This work was extended by other researchers to

simulate non-conservative and conservative species transport, and the impact of river flooding and storm surges in the Bay (3,12-14). In all cases the studies were limited to Mobile Bay and excluded the waters of East Mississippi Sound.

Recent field data collection studies by Schroeder (15) and Eleuterius (16) indicate that water from Mobile Bay flowing through Pass aux Herons has a large impact on the hydrodynamic behavior of East Mississippi Sound. This is due to the large fresh water inflow from the Mobile River to Mobile Bay, coupled with the lack of direct fresh water input to East Mississippi Sound from surrounding land masses. The intrusion of salt water from the Main Pass into Mobile Bay and from Petit Bois Pass into East Mississippi Sound further affects the behavior of East Mississippi Sound and Mobile Bay. Because of the interaction of East Mississippi Sound and Mobile Bay, the transport of water through the passes is one of the controlling factors influencing the physical, chemical, and biological environment of the area.

This study proposes to apply a recently developed numerical model, the Waterways Experiment Station Implicit Flooding Model Version II (WIFM II), formulated by the U.S. Army Corps of Engineers at the Waterways Experiment Station, Vicksburg, Mississippi (17), to the Mobile Bay-East Mississippi Sound system. The model has features

including variable grid size and implicit solution format which facilitate its use for pass-exchange study. The purpose of this work is to extend the knowledge gained from previous studies to include the description of the exchange of water through the passes. The continued investigation, systematic development, and application of mathematical models from Mobile Bay to East Mississippi Sound and surrounding areas are essential to the proper management of these resources.

## CHAPTER II

### BACKGROUND

#### Study Area

##### Mobile Bay

Mobile Bay is the terminus of the Mobile River system, with the fourth largest flow rate of the rivers in the United States. The Bay is a pear-shaped estuary about 49 km (31 mi) long from the Main Pass, Figure 1, to the Mobile Delta at its northern end. The width varies from 12 km (8 mi) at the northern end to 37 km (23 mi) between Pass aux Herons and the eastern shore of Bon Secour Bay. The principal source of fresh water to the area is the Mobile River system. The Bay has a surface area of about 1000 sq km (390 sq mi) and a volume of 3.48 billion cu m (122 billion cu ft). The Bay is shallow, with an average depth of 3 m (9 ft), except for the Mobile Ship Channel. The channel is 47 km (29 mi) long by 120 m (400 ft) wide with a controlling depth of 11.3 m (37 ft). Hollinger's Island Channel in the northwest Bay is maintained at a controlling depth of 3.1 m (10 ft). The Bay is separated from the Gulf of Mexico by Fort Morgan Peninsula to the southeast and Dauphin Island to the southwest. The 6.4 km (4.1 m) wide

Main Pass connects Mobile Bay to the Gulf of Mexico between these barriers.

### East Mississippi Sound

The coastal Alabama portion of Mississippi Sound extends 26 km (16 mi) from the Mississippi-Alabama state line eastward to Pass aux Herons. East Mississippi Sound is 19 km (12 mi) at its widest point along the state line. The surface area is 38 sq km (14 sq mi) with a volume of 1.16 billion cu m (40.8 billion cu ft). The average depth is 3.1 m (10 ft). Pass aux Herons, including the dredged Intracoastal Channel, connects the Bay and the Sound through a 3.1 km (1.9 mi) wide opening. Petit Bois Pass opens to the Gulf of Mexico from East Mississippi Sound and is 8.2 km (5.1 mi) wide.

### Passes

#### Main Pass

The Main Pass is the opening through which most of the salt water enters the Bay from the Gulf via tidal action. West Main Pass is fairly shallow, with depths ranging from 1.2 m (4 ft) to 3 m (10 ft), for a distance of 4.0 km (2.5 mi) along a line from Pelican Point on Dauphin Island to Mobile Point on Fort Morgan Peninsula. East Main Pass, the remaining 2.4 km (1.5 mi) along this line, slopes sharply to a depth of 13.7 m (45 ft) at the Main Channel (18,19). Because of the greater depths in East Main Pass,

most of the flow occurs here during the tidal cycle. Schroeder (20), in field data collection studies conducted during 1973-6, showed maximum velocities in West Main Pass to be 1.4 k during flood tide and 1.8 k during ebb tide. Current speeds from 0.6-1.0 k were noted in over 40% of the observations for West Main Pass. In East Main Pass maximum surface and bottom current speeds were 1.9 k during ebb tide. During flood tide maximum velocities of 2.4 k and 1.9 k were noted for surface and bottom, respectively.

#### Petit Bois Pass

East Mississippi Sound opens to the Gulf via Petit Bois Pass. The pass is 8.2 km (5.1 mi) wide, with a maximum depth of 3.7 km (12 ft), just off the western end of Dauphin Island. Little field work has been done to characterize the flows between East Mississippi Sound and Petit Bois Pass. Eleuterius (16) stated that the flow from Mobile Bay enters East Mississippi Sound mainly through Pass aux Herons and exits entirely through Petit Bois Pass. He also stated that flows from the Pascagoula River are deflected westward or flow directly out to the Gulf through Horn Island Pass or Dog Keys Pass to the west. These facts leave Mobile Bay as a controlling factor in determining the hydrography of East Mississippi Sound.

#### Pass aux Herons

The most current, detailed description of the

bathymetry in this area exists in a study of the oyster resources of Alabama by May in 1971 (21). It should be noted however that this area underwent significant changes due to the impact of Hurricane Frederic in September 1980. This study utilizes the data presented by May (21) and a Mobile Bay nautical chart (18) and is therefore limited to describing conditions in Pass aux Herons before the hurricane. With the acquisition of new bathymetric data for the pass, the study can be extended to show the changes in flow regime caused by the hurricane.

The interaction of Mobile Bay and East Mississippi Sound show Pass aux Herons to be important to the understanding of these bodies of water. According to May (21), Pass aux Herons is about 3.1 km (1.9 mi) wide along a line between Cedar Point and North Point of Little Dauphin Island. The majority of the pass is shallow with depths ranging from 0-1.2 m (4 ft). The area contains Cedar Point Reef, a productive oyster reef, some sections of which are exposed at sufficiently low tides. The Gulf Intracoastal Channel, dredged through Pass aux Herons, has a controlling depth of 3.7 m (12 ft). Dauphin Island Bridge connected the mainland to Dauphin Island before being destroyed by Hurricane Frederic. The bridge is currently being rebuilt.

Schroeder (15) conducted a field study to determine the effects of the 1973 flood of the Mobile River system on

lower Mobile Bay and East Mississippi Sound. He noted that East Mississippi Sound does not receive any direct fresh water flow and is dependent on Mobile Bay for fresh water input. As previously stated, Eleuterius (16) also noted the interaction of Mobile Bay and East Mississippi Sound.

#### Effect of Pass Exchange on Oyster Productivity

An example of the importance of the hydrodynamics of Pass aux Herons and the effects of man's activities is illustrated by the investigation of the oyster productivity in the area. May (22) examined the effects of channel dredging, sedimentation, salinity, predators, and other factors, on the oyster population in Mobile Bay and East Mississippi Sound. He noted that Pass aux Herons was dredged through productive oyster bottom for the construction of Dauphin Island Bridge. This action destroyed or altered an unknown amount of the bottom. Silting was noted to kill spat (larval oysters) in East Mississippi Sound in 1969. These direct effects, however, were found to be less important than the changes in salinity and current patterns caused by dredging and spoil deposition.

The salinity of the waters inhabited by oysters affects their survival in a number of ways. May (23) noted the mortality of oyster spat caused by periods of low salinity. Lower than normal salinity in lower Mobile Bay

and East Mississippi Sound was caused by floods of the Mobile River system as reported by Schroeder (15) and May (22). It was observed that while mortality rates of up to 100% can occur during floods, these effects may be, by low-salinity water, overshadowed by the deterrence of disease and predators of the oyster.

The abundance of the most serious oyster predator in Alabama, the oyster drill (Thais haemostoma), is directly related to salinity. The drill is prevalent in waters of salinity higher than 20 ppt. The density of the drill ranges from 0 in lower salinity portions of upper Mobile Bay to nearly 3 per sq m in East Mississippi Sound. Oyster mortality rates of 80-90% in lower Mobile Bay and East Mississippi Sound have been attributed to the drill by May (22). Hoese et al. (24) determined the settling of spat to be 200 per sq m per day in East Mississippi Sound compared to 5 per sq m per day east of Pass aux Herons in 1967. The higher settling rate in East Mississippi Sound did not favor survival, however, because of the increased drill predation due to high salinity.

May (22) further cited evidence that Portersville Bay in East Mississippi Sound once supported oysters in abundance. The area is now unfit for oyster growth due to changes leading to increased salinity. The higher salinity was attributed partly to the westward migration of Petit Bois Island, which resulted in the increased width of Petit

Bois Pass. This allows Gulf water to penetrate further into East Mississippi Sound. Chermock and LaMoreaux (4) mentioned that the construction of the Dauphin Island Bridge could be responsible for restricting water exchange between Mobile Bay and East Mississippi Sound. The restricted flow would contribute to increased salinity in the area.

Since the salinity regime in East Mississippi Sound is a direct function of the pass exchange between East Mississippi Sound and Mobile Bay, the description of this exchange would be advantageous. Better understanding of the pass hydrodynamics could give insight into design parameters affecting optimum utilization of this vital natural resource for the benefit of all Alabamians.

#### Methods for Studying Estuarine Hydrodynamics

##### Field data

Due to the complexity and dynamic behavior of estuarine systems, field-data studies are limited in their ability to describe the water bodies. In order to adequately relate the interactions among parts of the system, such as pass exchange, many sampling stations must be simultaneously monitored. Large expenditures must be made to provide the research vessels and man-hours necessary. Bad weather conditions can unpredictably disrupt a field survey. Mathematical and physical models

of estuarine systems are not subject to these problems and can extend limited field data.

### Models

Models attempt to represent the real system under study. An acceptable model must be able to accurately describe specific responses to variations in system parameters. The suitability of a model for a particular application is shown through calibration and verification procedures. The model is calibrated by first applying it, within certain limitations, to the study system. The model variables must then be manipulated so as to best describe the system with all its attendant idiosyncrasies. Once the system seems to be adequately described within the model framework, it must be verified. Verification is established by the use of sound field data to show that model results can, in fact, describe system behavior over a wide variation in conditions. Unacceptable results at this stage lead to recalibration of the model, collection of additional field data, or the utilization of a different model. All models must satisfy these basic elements to be useful.

### Physical models

Shallow estuaries have been represented by several types of models, including physical and mathematical models. A physical model is an imitation of the real

system scaled according to the laws of dynamic similitude. These models have the advantage of visually depicting the circulation patterns of the system under study. The effects of various input conditions such as tide elevation and river flow can be studied. Masch et al. noted (25), however, that it is rarely possible to satisfy all the scaling criteria simultaneously.

The modeling of a shallow estuary is a problem of free surface flow in which gravitational and inertial forces are important. The equality of the Froude number, which is the ratio of these forces, in the model and the prototype system is therefore the modeling criterion. After establishing a suitable linear ratio between the model and prototype, the ratios of the area, volume, velocity, flow rate, etc., are determined.

Viscous and diffusional forces may also be important in the model of a tidal estuary. These forces cannot be held in proportion between the model and the prototype if the model is built according to Froude similarity. The vertical scale must be much larger than the horizontal scale to compensate for the viscous forces. The bottom roughness elements, usually simulated by metal strips adjusted to reproduce prototype data, must be distorted as well. Because of these necessary distortions, a physical model cannot be expected to simultaneously represent processes which are gravitationally influenced, and those

more related to frictional forces. Surface wind conditions also cannot be represented with a physical model.

Another limitation of physical models of estuaries is their high construction and operation costs. A physical model of Mobile Bay exists at the Waterways Experiment Station in Vicksburg, Mississippi (26). The model was built in 1973 at a cost of \$1,000,000 (12), a large investment compared to the benefits derived from the model.

#### Mathematical models

The mathematical model is a functional representation of the real system in a form that can be solved using mathematical methods. With the development of high-speed digital computers, finite-difference methods for solving the partial differential equations describing the system have been widely used. Hydrodynamic models for simulation of estuarine and coastal systems are based on some form of the equations of continuity and momentum. The models, many of which are reviewed in the literature (5-10), use a variety of solution techniques for these equations. Mathematical models have been applied to Mobile Bay for the investigation of hydrodynamic and salinity profiles, conservative and non-conservative mass transport, the effects of river flooding and storm surges, and the description of the salinity profiles in the Main Pass area during flooding of the Mobile River system (3,11-14).

## Use of Mathematical Models in Mobile Bay

### Hydrodynamics and salinity

Hill (11) adapted and applied a form of the Reid-Bodine numerical model to Mobile Bay. The model was based on the depth-averaged, two-dimensional equations of change. The model used an explicitly solved, finite-difference form of the equations, including terms for Coriolis forces and advective acceleration. The model represented the Bay using a constant size grid, Figure 2, and yielded tide elevations, current patterns, and salinity distribution profiles. After calibration and verification, the model was used to predict changes in output parameters caused by varying input conditions. The inputs consisted of wind field, river flow rates, and other parameters peculiar to this model. The simulation of the intrusion of salt water (known as the salt wedge) into lower Mobile Bay was effected on the two-dimensional format of the model.

### Non-conservative species transport

A non-conservative-species transport model was developed by Liu (12) for the simulation of coliform bacteria loading in the Bay. The two-dimensional surface model used the hydrodynamic and salinity model of Hill (11) to provide basic current and dispersion-coefficient data. These data were necessary for simulating non-conservative species transport. A die-off rate constant based on water

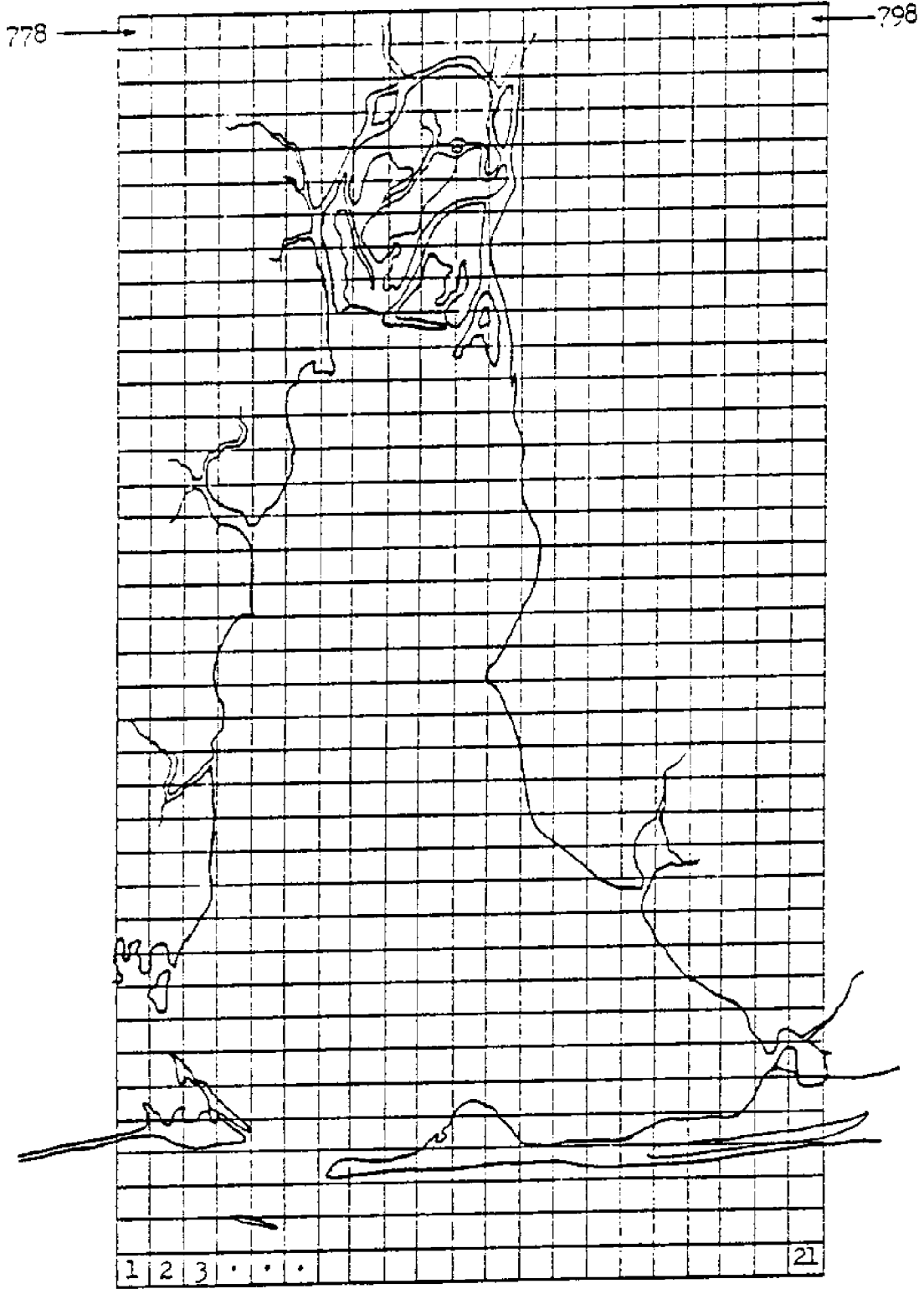


Figure 2. Grid Used for All Mobile Bay Model Studies Based on the Work of Hill (12).

temperature was used for the bacteria. The model provided monthly-averaged coliform bacteria concentrations corresponding to the data base used for verification. A parametric study was undertaken to determine the effects of changing river flows, wind field, coliform-loading concentration, and water temperature on coliform bacteria distribution in the Bay.

#### Sedimentation study

Sediment transportation in Mobile Bay was studied by Ng (13) using the hydrodynamic model of Hill (11). The study used LANDSAT-1 satellite images of Mobile Bay, coupled with the model, to establish a correlation between observed turbidity patterns, river-flow rates, and wind conditions. Varying degrees of success were attained in predicting sediment transportation depending on the wind and river-flow conditions imposed.

#### Effects of river flooding and storm surges

Hu (14) studied the effects of river flooding and storm surges on Mobile Bay. The study involved the use of a modified form of Hill's model (11). The effects of flooding and storm surge on salinity regimes, tide elevations, and velocities within the Bay were simulated. The study used the open-coast model of Wanstrath (27) to obtain a storm-surge hydrograph for input into the model.

April et al. (3) later applied this model to the description of the salinity profile at Main Pass during flooding of the Mobile River. The hydrodynamic model was exercised to provide the basic velocity data to drive the salinity model. Salinity profiles at the Main Pass were reproduced in this manner.

#### Limitations of Existing Mobile Bay Models for Pass-exchange Study

These applications of numerical models in Mobile Bay showed the variety of information which can be obtained from their use. However, these studies were in all cases limited to Mobile Bay itself, with no inclusion of East Mississippi Sound. The inclusion of East Mississippi Sound is important to the more complete understanding of the Mobile Bay-East Mississippi Sound interaction.

The previous studies in Mobile Bay all used the hydrodynamic model of Hill (11) as a basis. This model was determined to be too restrictive for the detailed description of pass exchange between the Bay and East Mississippi Sound. A grid size small enough to provide the needed detail of the passes caused severe problems with solution stability and excessive computer time requirements.

The grid system of Hill (11) used a 2 km grid size with 798 cells representing Mobile Bay, Figure 2. This region included only that portion of East Mississippi Sound 4 km west of Pass aux Herons. A 2 km grid size resulted in

just over one cell encompassing the entire pass. For any detailed description of the pass exchange, this was obviously too coarse a grid mesh.

Reduction of the grid size was not feasible. Any reduction in grid size must be made uniformly over the entire model area. Decreasing the grid size by a factor of four, to 0.5 km (a more reasonable scale for the pass), resulted in 12,768 cells for the entire Bay area. Much larger computer memory requirements were imposed by this increase in number of grid cells. The stability criterion of the explicitly solved, finite-difference form of the equations used by Hill's model (11) required the time step to be decreased with the grid size. For a stable solution the time increment must satisfy the following inequality:

$$1. \quad \Delta t < \frac{\Delta s}{(2gH_{\max})^{1/2}}$$

Thus the time step must then be decreased from 120 seconds, as used by Hill, to 30 seconds. The increased computer time necessary to effect a solution under these conditions was significant and costly. In light of these facts, a different model was used in this study to circumvent these problems.

### Reasons for Use of WIFM II Model

This study used the two-dimensional, depth-averaged Waterways Experiment Station Implicit Flooding Model, Version II (WIFM II), developed at the U.S. Army Engineer Waterways Experiment Station, Vicksburg, Mississippi (17). This model had several features not available in Hill's model (11). The variable-grid capability and implicit solution scheme were especially important to the pass-exchange study.

#### Variable grid

WIFM II allowed the grid size to smoothly vary from small increments to much larger increments in either of the two spatial dimensions. This enabled the use of a small mesh in complex, rapidly changing areas such as the passes. The mesh size could be expanded in large areas of fairly constant bathymetry such as in Bon Secour Bay. Thus the model provided for both the spatial accuracy necessary for pass description and, in appropriate regions, the savings in computer requirements resulting from a coarse grid mesh.

#### Implicit solution technique

Another factor weighing in the selection of this model was the use of an implicit solution technique for the finite-difference equations. The implicit formulation was unconditionally stable, providing a great computational

### Reasons for Use of WIFM II Model

This study used the two-dimensional, depth-averaged Waterways Experiment Station Implicit Flooding Model, Version II (WIFM II), developed at the U.S. Army Engineer Waterways Experiment Station, Vicksburg, Mississippi (17). This model had several features not available in Hill's model (11). The variable-grid capability and implicit solution scheme were especially important to the pass-exchange study.

#### Variable grid

WIFM II allowed the grid size to smoothly vary from small increments to much larger increments in either of the two spatial dimensions. This enabled the use of a small mesh in complex, rapidly changing areas such as the passes. The mesh size could be expanded in large areas of fairly constant bathymetry such as in Bon Secour Bay. Thus the model provided for both the spatial accuracy necessary for pass description and, in appropriate regions, the savings in computer requirements resulting from a coarse grid mesh.

#### Implicit solution technique

Another factor weighing in the selection of this model was the use of an implicit solution technique for the finite-difference equations. The implicit formulation was unconditionally stable, providing a great computational

advantage over the explicit technique. This fact allowed a choice of a time step based on the time scale of the physical phenomena simulated. The implicit formulation has produced reductions in cost per simulation by as much as a factor of 15 over explicit formulations (28). These factors showed WIFM II to be much more suitable for the present study than the existing model of Mobile Bay.

#### Objectives of Study

It is proposed in this study to investigate the water transport in the Pass aux Herons area of coastal Alabama. This area has been shown to be critical in the behavior of East Mississippi Sound, a water body rich in oyster growing potential and in natural habitat. The interaction of Pass aux Herons and Main Pass will be investigated to determine the effects of this interaction on the hydrodynamics of the Pass aux Herons area.

The method to be used to study this interaction will involve the use of a mathematical representation of the system. Although many studies of Mobile Bay using mathematical modeling have been made (3,11-14), there is no detailed description of this critical pass-exchange behavior reported. Field-data surveys by Schroeder (15) and Eleuterius (16) indicate the importance of this area to the coastal environment and provide a basis from which a detailed study can be made. Specifically, this study will:

1. Apply the equations of change describing water movement and elevation to the Mobile Bay-East Mississippi Sound area
2. Solve these equations, after suitable simplification, using a two-dimensional, implicitly defined numerical model (WIFM II)
3. Calibrate and verify the model with available field data from the area
4. Analyze the interactions that occur between Mobile Bay and East Mississippi Sound through Pass aux Herons under a wide range of conditions

Successful completion of these objectives will provide a much needed source of knowledge about this system upon which sound decisions can be made concerning its use.

## CHAPTER III

### DESCRIPTION OF WIFM II

#### General Equations

The hydrodynamic equations used in WIFM II were derived from the continuity equation and the Navier-Stokes equations of momentum:

#### CONTINUITY

$$2. \quad \frac{\delta u}{\delta x} + \frac{\delta v}{\delta y} + \frac{\delta w}{\delta z} = 0$$

#### MOMENTUM

$$3. \quad \rho \left( \frac{\delta u}{\delta t} + u \frac{\delta u}{\delta x} + v \frac{\delta u}{\delta y} + w \frac{\delta u}{\delta z} \right) = \mu \left( \frac{\delta^2 u}{\delta x^2} + \frac{\delta^2 u}{\delta y^2} + \frac{\delta^2 u}{\delta z^2} \right) - \frac{\delta P}{\delta x} + \rho g_x$$

$$4. \quad \rho \left( \frac{\delta v}{\delta t} + u \frac{\delta v}{\delta x} + v \frac{\delta v}{\delta y} + w \frac{\delta v}{\delta z} \right) = \mu \left( \frac{\delta^2 v}{\delta x^2} + \frac{\delta^2 v}{\delta y^2} + \frac{\delta^2 v}{\delta z^2} \right) - \frac{\delta P}{\delta y} + \rho g_y$$

$$5. \quad \rho \left( \frac{\delta w}{\delta t} + u \frac{\delta w}{\delta x} + v \frac{\delta w}{\delta y} + w \frac{\delta w}{\delta z} \right) = \mu \left( \frac{\delta^2 w}{\delta x^2} + \frac{\delta^2 w}{\delta y^2} + \frac{\delta^2 w}{\delta z^2} \right) - \frac{\delta P}{\delta z} + \rho g_z$$

The equations were integrated from sea bottom to water surface resulting in the two-dimensional form of the equations of continuity and momentum:

### CONTINUITY

$$6. \quad \frac{\delta \eta}{\delta t} + \frac{\delta U}{\delta x} + \frac{\delta V}{\delta y} = R$$

### MOMENTUM

$$7. \quad \frac{\delta U}{\delta t} + \frac{\delta}{\delta x} \left( \frac{U^2}{d} \right) + \frac{\delta}{\delta y} \left( \frac{UV}{d} \right) - fV + gd \frac{\delta}{\delta x} (\eta - \eta_a) + F_x$$

$$+ \frac{gU}{C^2 d^2} (U^2 + V^2)^{\frac{1}{2}} - e \left( \frac{\delta^2 U}{\delta x^2} + \frac{\delta^2 U}{\delta y^2} \right) = 0$$

$$8. \quad \frac{\delta V}{\delta t} + \frac{\delta}{\delta x} \left( \frac{UV}{d} \right) + \frac{\delta}{\delta y} \left( \frac{V^2}{d} \right) + fU + gd \frac{\delta}{\delta y} (\eta - \eta_a) + F_y$$

$$+ \frac{gV}{C^2 d^2} (U^2 + V^2)^{\frac{1}{2}} - e \left( \frac{\delta^2 V}{\delta x^2} + \frac{\delta^2 V}{\delta y^2} \right) = 0$$

For a detailed derivation see Leendertse (29).

### Assumptions and Limitations of WIFM II

WIFM II was derived with the following assumptions:

1. The advective and momentum-flux terms may be omitted from the general two-dimensional equations of change (7-8 above) with negligible effect on the results
2. The fluid is homogeneous and incompressible
3. The horizontal flows are reasonably uniform from surface to bottom (i.e. accelerations in the vertical direction are negligibly small)
4. The depth of the water is small compared to the wavelength of of the tidal forcing function

The first assumption was necessary due to mathematical instabilities in the solution of the implicitly formed equations if these terms were included. When formulating the equations for the implicit, finite-difference method, Roache (30) reported that the presence of the non-linear advective terms (second and third terms of the momentum equations) caused mathematical instabilities which rendered the solution meaningless. The last terms of the momentum equations represent the internal-stress resultants due to turbulent and dispersive momentum flux. The terms provide a means of dissipating wave energy with a wavelength on the order of twice the spatial step size. Since this energy is transmitted by the advective terms, the flux terms were also omitted (17).

Masch et al. (25) developed an explicit numerical model and studied the effects of the advective terms on computed tidal elevations and velocities. The model was exercised in a simplified one-dimensional, shallow estuary with and without the advective terms. The effects of these terms were observed to be negligibly small.

Rather than omitting the flux terms outright, they were included in an overall energy-gradient term. The gradient terms were used to derive expressions for bottom friction and wind stress. The resulting equations were the same as those used in WIFM II.

Hill (11) assessed the effects of the advective terms in the Mobile Bay model. The model was exercised with and without the advective terms while maintaining all other parameters constant. Tidal elevations showed a slight effect from the omission of the advective terms. In all cases the phase of the tidal curves remained virtually unchanged. The only change noted was that the elevations at low tide were approximately 0.1 ft (about 4%) lower when the advective terms were omitted. A much more significant effect was noted in the salinity model results. This was to be expected due to the important role of advection in mass transport.

Since this study was limited to hydrodynamic simulation only, use of the WIFM II model with the advective terms omitted was made in a first attempt for

describing pass exchange. The determination of the significance of the advective terms in estuarine modeling is an area of continued study (17).

The remaining assumptions are satisfied in shallow, well-mixed estuaries. Mobile Bay and East Mississippi Sound fit this criterion well except in the ship channels and in East Main Pass. The intrusion of a wedge of saline water from the Gulf into the ship channel and East Main Pass, with the resultant stratification of the water column, is well documented. A two-dimensional model cannot reproduce the variation of current velocity with depth, which is found in these regions. The model gives a representation of the net flows over the depth in a stratified water column, instead. The relatively small size of the ship channel in comparison to the width of the Bay and the successful use of the two-dimensional model of Hill (11) to simulate the occurrence of the salt wedge in lower Mobile Bay, led to the conclusion that the use of a two-dimensional, depth-averaged model such as WIFM II was justified in this study. It should be realized, however, that the model gives a representation of the net flows in the ship channels and East Main Pass and not the actual velocity profile as a function of depth in these areas.

### Variable-grid Equations

As previously stated, WIFM II had the capability of incorporating a continuously varying grid to the system. A piecewise-reversible transformation was used to map the real space of the system into the computational space of WIFM II. The transformation is of the form:

$$9. \quad x = a_1 + b_1 \alpha_1^{c_1}$$

$$10. \quad y = a_2 + b_2 \alpha_2^{c_2}$$

where a, b, and c are arbitrary constants. The constants were fit such that the function and the first derivative of the spacing of the variable grid were continuous. This scheme removed many difficulties associated with variable-grid models (17). An interactive program was used to map real space into computational space for WIFM II.

Omitting the advective and momentum flux terms from equations 7-8 and applying the variable grid equations yielded a modified form of the two-dimensional equations of momentum and continuity:

## CONTINUITY

$$11. \quad \frac{\delta n}{\delta t} + \frac{1}{u_1} \left( \frac{\delta U}{\delta \alpha_1} \right) + \frac{1}{u_2} \left( \frac{\delta V}{\delta \alpha_2} \right) = R$$

## MOMENTUM

$$12. \quad \frac{\delta U}{\delta t} - pV + \frac{\hbar d}{u_1} \left( \frac{\delta}{\alpha_1} (\eta - \eta_a) \right) + F_{\alpha_1} +$$

$$\frac{\hbar U}{c^2 d^2} (U^2 + v^2)^{\frac{3}{2}} = 0$$

$$13. \quad \frac{\delta V}{\delta t} + pU + \frac{\hbar d}{u_2} \left( \frac{\delta}{\alpha_2} (\eta - \eta_a) \right) + F_{\alpha_2} +$$

$$\frac{\hbar V}{c^2 d^2} (U^2 + v^2)^{\frac{3}{2}} = 0$$

where

$$14. \quad u_1 = \frac{\delta x}{\delta \alpha_1} = b_1 c_1 \alpha_1^{c_1 - 1}$$

$$15. \quad u_2 = \frac{\delta y}{\delta \alpha_2} = b_2 c_2 \alpha_2^{c_2 - 1}$$

### Alternating-Direction, Implicit Formulation

These equations were cast in finite-difference form using a space-staggered grid defining flows and water levels at different points, Figure 3. A multi-operational, alternating-direction, implicit technique, first developed by Leendertse (29), was used to develop a computational algorithm. Computations were performed in two cycles. In the first cycle,  $u$  and  $V$  were computed implicitly along a grid line parallel to the  $x$  axis. A centered-difference operator was applied to the momentum and continuity equations (11-13). This resulted in a system of linear algebraic equations whose coefficient matrix was tridiagonal. The matrix was solved most economically by a series of recursion formulas. Each grid line was solved until all the columns were computed. The second cycle solved for  $u$  and  $V$  implicitly along grid lines parallel to the  $y$  axis in a similar treatment. For a detailed derivation see Butler (17) and Leendertse (29).

### Boundary Conditions

The boundary conditions available to the model were of three general types: open boundaries, water-land boundaries, and subgrid boundaries.

#### Open boundaries

These were the seaward boundaries terminating the computational grid, or channels exiting the grid at any

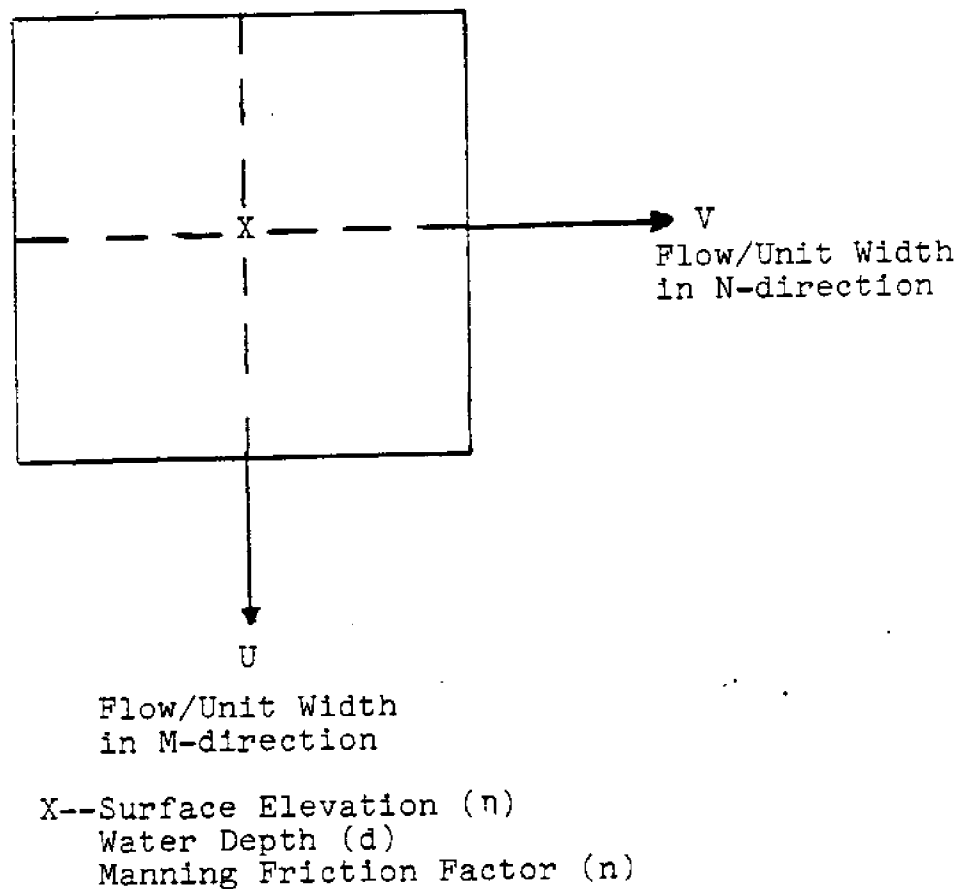


Figure 3. Definition of Grid Cell Variables  
for WIFM II.

point in the system. Water levels corresponding to tidal cycles or storm surges were specified as functions of location and time. Flow rates could also be prescribed to simulate river inputs to the system.

#### Water-land boundaries

The usual condition for these boundaries was that of no flow in the direction perpendicular to the boundary. In other words,  $U$  or  $V$  was set to zero at the appropriate cell face. In addition, the model permitted flooding and drying of low-lying land areas. This was accomplished by checking water levels in cells adjacent to land cells. The land-cell face was opened to flow when the water level in the adjacent cell reached a prescribed height. The cell could dry in the inverse manner, Figure 4. The flooding capability permitted a realistic representation of the movement of water across low-lying, tidal flood plains and marsh areas. This boundary treatment was not available in Hill's model (11).

#### Subgrid boundaries

These barriers were defined along cell faces and could be exposed, overtopping, or submerged. Exposed barriers imposed a no-flow condition along a cell face. Submerged barriers were simulated by the use of a time-dependent frictional coefficient. Overtopping barriers could alternately be submerged or exposed, Figure 5.

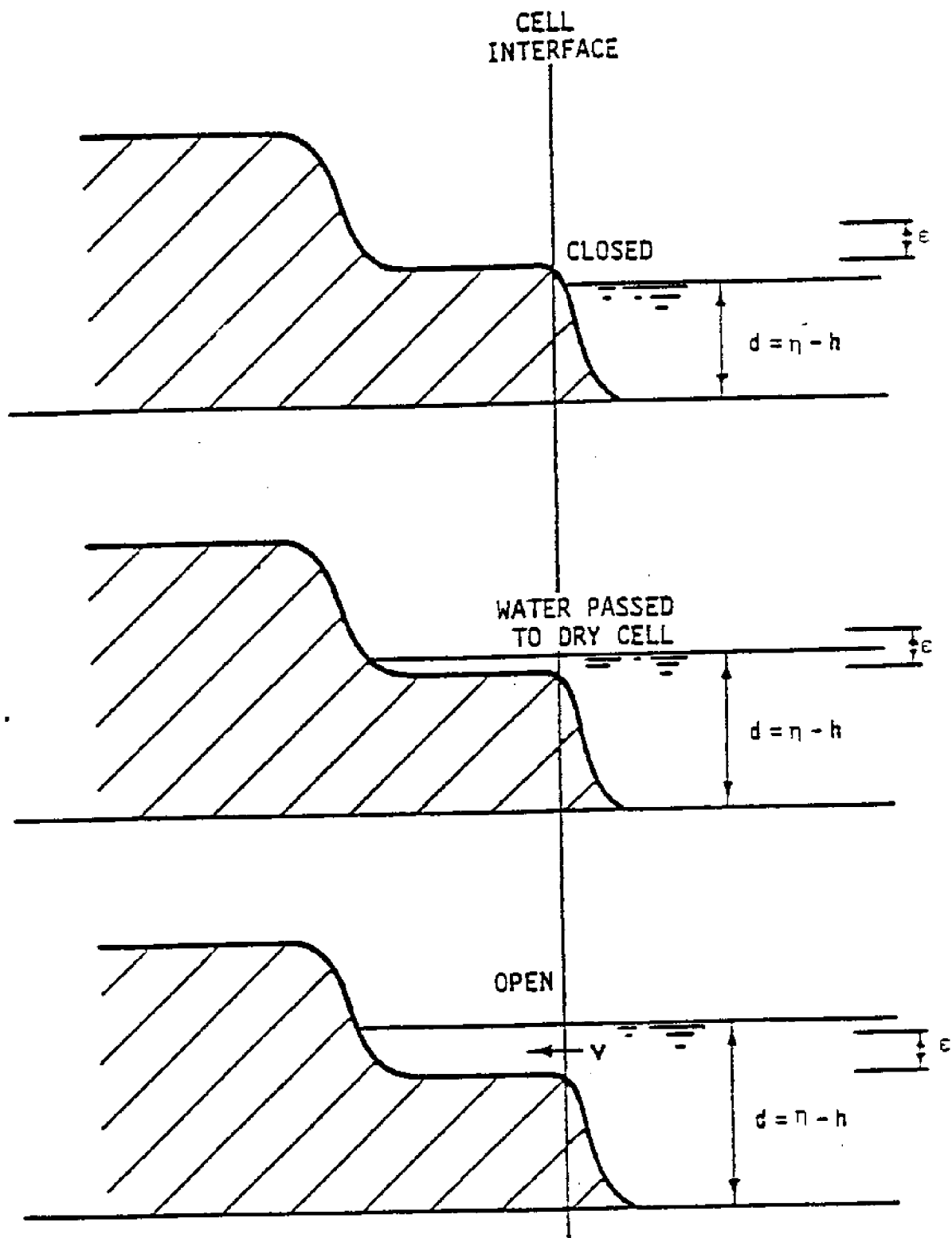
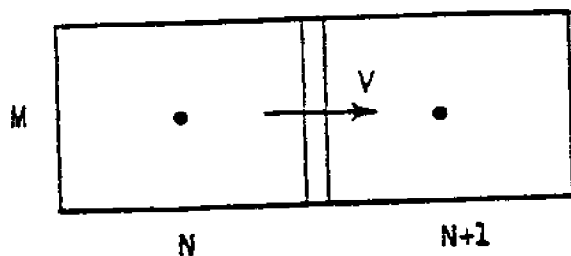
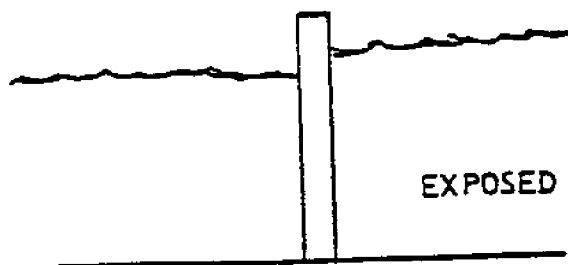


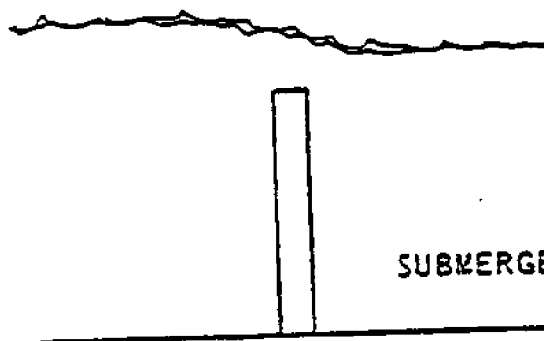
Figure 4. Flood Cell Treatment by WIFM II (17).

BARRIER AT CELL INTERFACE (HEIGHT  $b$ )

$$V = 0$$

$$\eta_N < b + \epsilon$$

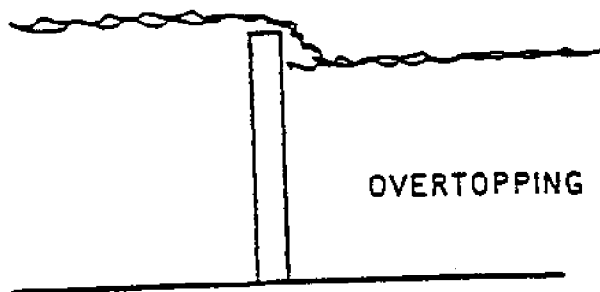
$$\eta_{N+1} < b + \epsilon$$



$$\eta_N > b + \epsilon$$

$$\eta_{N+1} > b + \epsilon$$

$V$  CONTROLLED BY  
SPECIAL CHEZY  
COEFFICIENT



$$\eta_N > b + \epsilon$$

$$\eta_{N+1} < b + \epsilon$$

$$V = C_d d_H \sqrt{g H}$$

WATER IS PASSED TO  
LOW SIDE ACCORDING  
TO FLOW RATE  $V$

Figure 5. Barrier Conditions Treated by WIFM II (17).

Water levels were checked in the cells adjacent to the barrier. If the water elevation overtopped the barrier, water was permitted to flow to the low side according to the broad-crested weir equation:

$$16. \quad V = C_o d_H (d_H)^{\frac{1}{2}}$$

When the barrier became submerged or exposed it was treated as above. These subgrid boundaries allowed the simulation of features too small to be incorporated into the normal grid size. Such features could include islands, dredge spoil banks, jetties, and others.

#### External Forces

Wind stress, gravity, and Coriolis forces were the external forces included in WIFM II. The model accepted wind input as constant in direction and speed, variable in speed and direction as a function of time, or variable in speed and direction as a function space and time. The last option required a subroutine which must be developed for each system being studied.

## CHAPTER IV

### APPLICATION OF WIFM II TO MOBILE BAY- EAST MISSISSIPPI SOUND

#### Development of Variable Grid

##### Limits of system

The area of Mobile Bay and East Mississippi Sound chosen for representation by a variable-size, finite-difference grid, Figure 6, included Mobile Bay, the Mobile River delta up to 20.8 km (12.9 mi) north of the Interstate 10 causeway, East Mississippi Sound to 11.2 km (6.9 mi) west of Dauphin Island Bridge, and the Gulf of Mexico southward to 13.7 km (8.5 mi) south of Fort Morgan. This area was bounded on the east by  $87^{\circ} 45'$  longitude, on the west by  $88^{\circ} 15'$  longitude, on the south by  $29^{\circ} 07'$  latitude, and on the north by  $30^{\circ} 52'$  latitude.

The Mobile River delta was included in the model because of the importance of this area as a capacitance. The results of experiments with a grid system extending northward only to the mouth of the Mobile River proved to be inadequate. Reasonable reproduction of available field data could not be achieved with such a grid.

Schroeder (15) defined the western limit of East Mississippi Sound as  $88^{\circ} 30'$  longitude. This area included

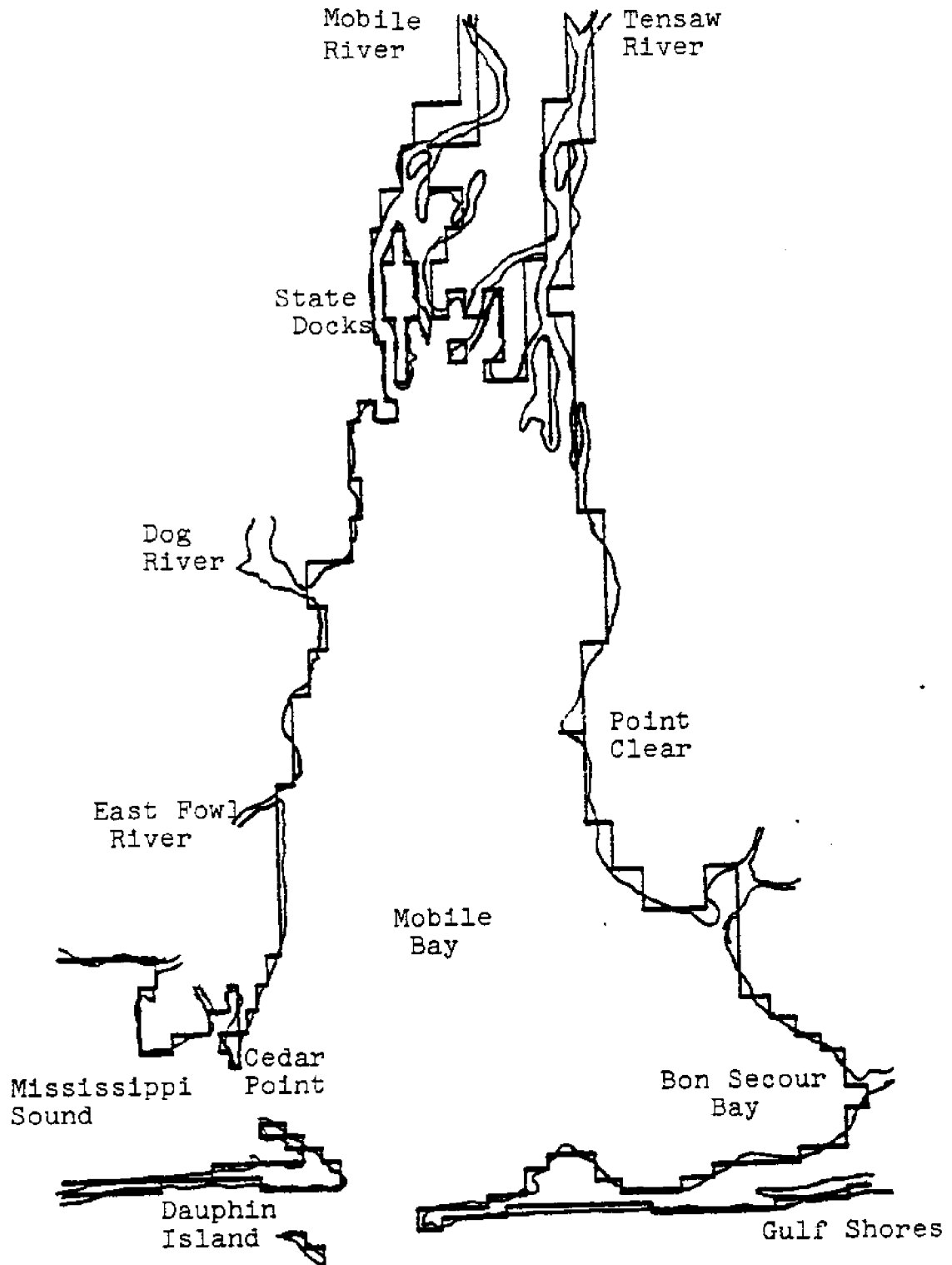


Figure 6. Boundaries of Mobile Bay-East Mississippi Sound Model.

Petit Bois Pass and the east end of Petit Bois Island, Figure 1. The model was not extended to include this area. No field data were available at Petit Bois Island for establishing boundary conditions at this point. Without accurate boundary conditions based on good field data, adequate calibration and verification of the model could not be attained. For this reason the model was limited to 88° 15' longitude, thus excluding Petit Bois Pass.

The southern boundary was extended to a point in the Gulf of Mexico so that the depths of the grid cells at the southern edge of the model did not vary drastically over the range of the boundary. This permitted the complex bathymetry of the Main Pass area to be represented by the model.

#### Description of variable grid

##### Grid cell size

All field data, nautical chart measurements (18), and Tide Tables (31) predictions were given in the English system of units. The English system was therefore used in all the model studies to facilitate the comparison of field data and model results.

The grid, Figure 7, used for the model of Mobile Bay-East Mississippi Sound was developed with the aid of the Mobile Bay nautical chart (18). The chart scale was 1:80000. A variable grid was mapped based on a minimum

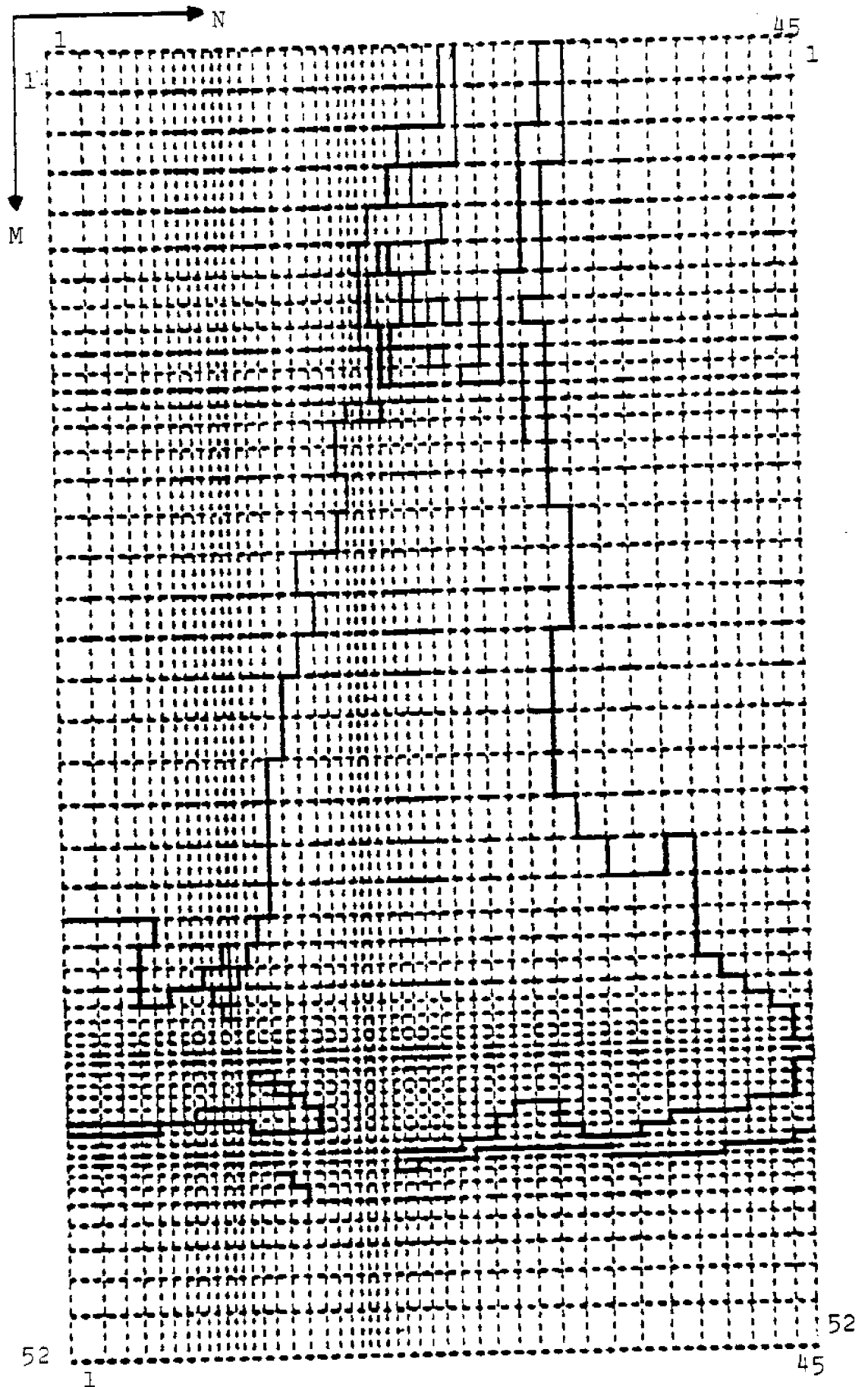


Figure 7. Variable Grid for Mobile Bay-East Mississippi Sound--Cell Number (N,M).

grid-cell dimension of 0.25 in on the chart. This value corresponds to 1666.7 ft of prototype distance. The dimensions of the resulting grid were 45 by 52 cells or 2340 cells. The computer memory requirements for this application of WIFM II on the UNIVAC 1100/61 computer system at The University of Alabama was 21,504 words of memory. After mapping the grid, it was overlaid on the chart in order to assign boundaries, depths, and Manning coefficients for each cell.

The smallest cells were used in Pass aux Herons and Main Pass, Figures 8-9. Greater resolution was needed in these areas to represent their complexity and to study the hydrodynamics of these areas in detail. Large cells were used in regions of relatively constant bathymetry. These regions were Bon Secour Bay, the Gulf of Mexico boundary, and upper Mobile Bay. Relatively large cells were also used in the Mobile River delta although this region is more intricate than anywhere else in the model area. The Mobile River delta was included for its capability to dissipate water from a constant river flow and an incoming tide in a manner similar to the actual marsh. The model was not intended to describe the delta in detail.

#### Boundaries

The shore line of the system was defined as closely as possible within the grid framework, Figure 6. Features

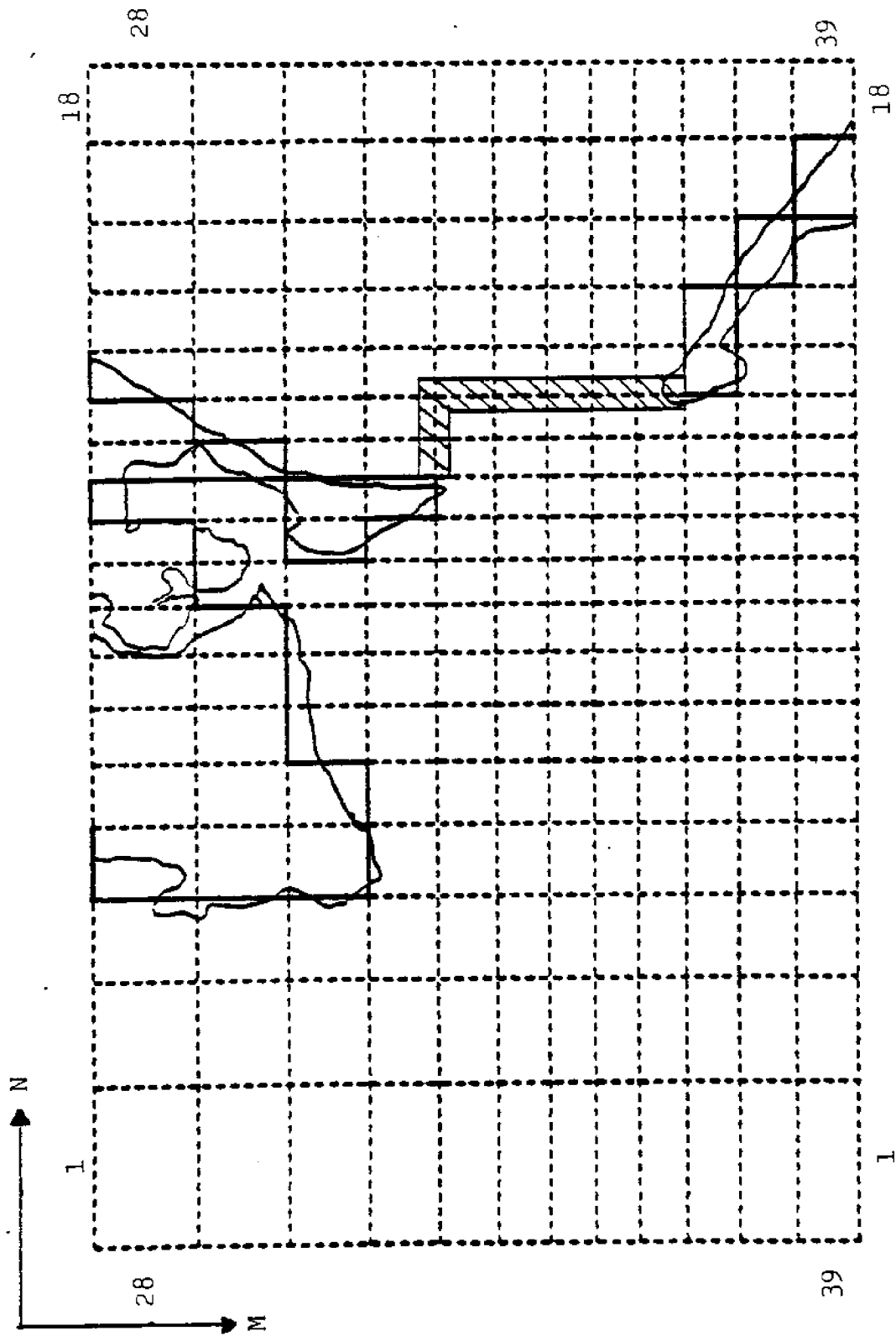


Figure 8. Grid Formulation in Pass aux Herons.

////// Flow Calculations

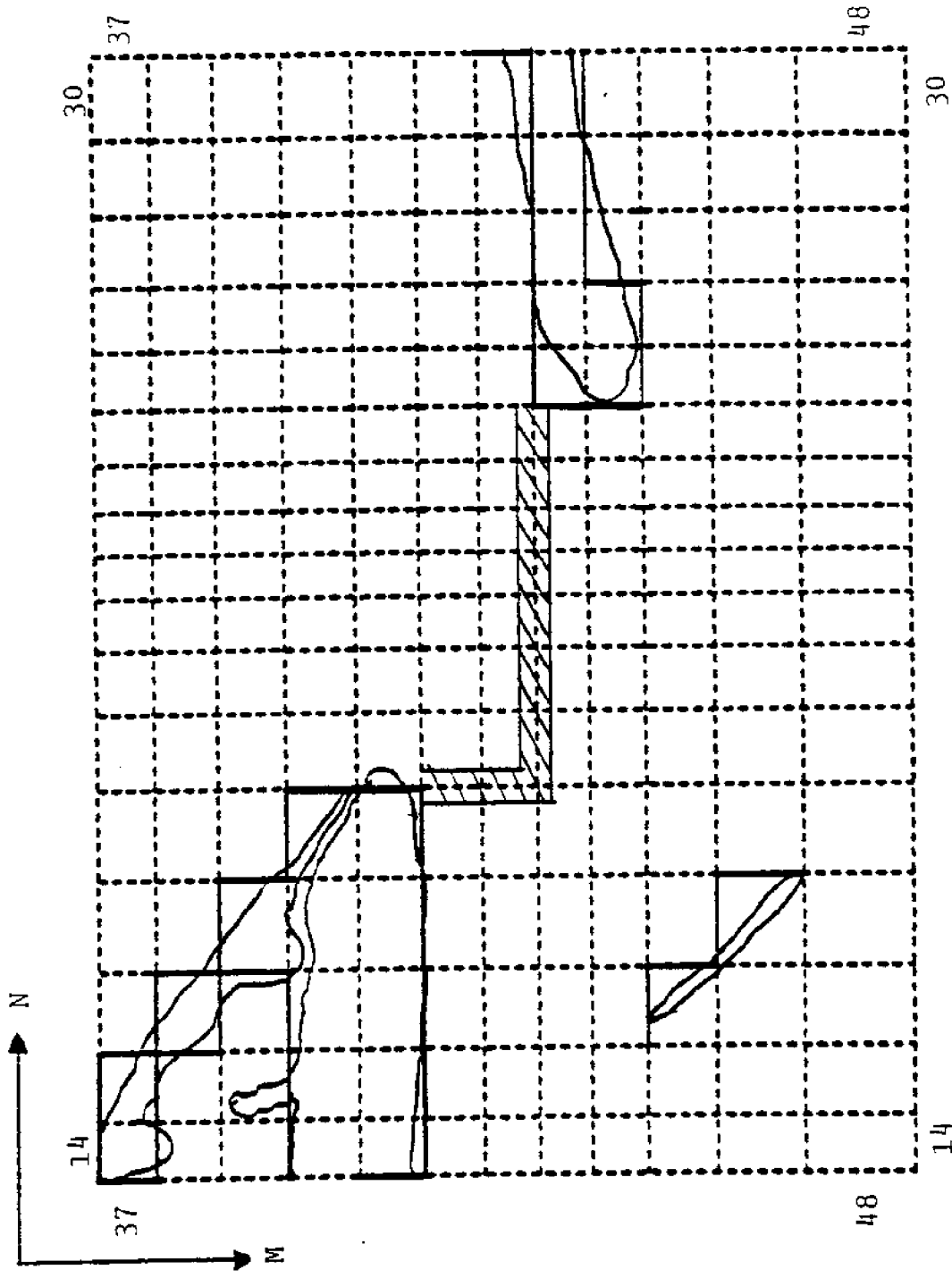


Figure 9. Grid Formulation in Main Pass.

Flow Calculations

too small to be represented within the grid were described by exposed subgrid barriers. Point Clear, Sand Island, part of Dauphin Island, and some of the islands at the mouth of the Mobile River delta were represented by subgrid barriers.

Tide-elevation boundary conditions were specified at the Gulf of Mexico boundary and the East Mississippi Sound boundary. River-flow boundary conditions were specified for the Mobile and Tensaw Rivers. River flows were not included for Dog River, Fowl River, or any of the other small rivers emptying into the model region. The flows from these rivers are insignificant with respect to the overall hydrodynamics of the Mobile Bay-East Mississippi Sound region as stated above. Some of these flows could be important with respect to mass transport modeling (i.e. salinity or dissolved oxygen).

#### Depths

The datum of the nautical chart was the Gulf Coast Low Water Datum (LWD) which was established in 1880 as an average of 60 consecutive low-water readings according to MacPhearson (32), Figure 10. The datum of the Tide Tables (31) was Mean Low Water (MLW). The datum of the field data used in this study was Mean Sea Level (MSL). In applying the model, the depth of each cell was corrected to MSL to correspond to the field data.

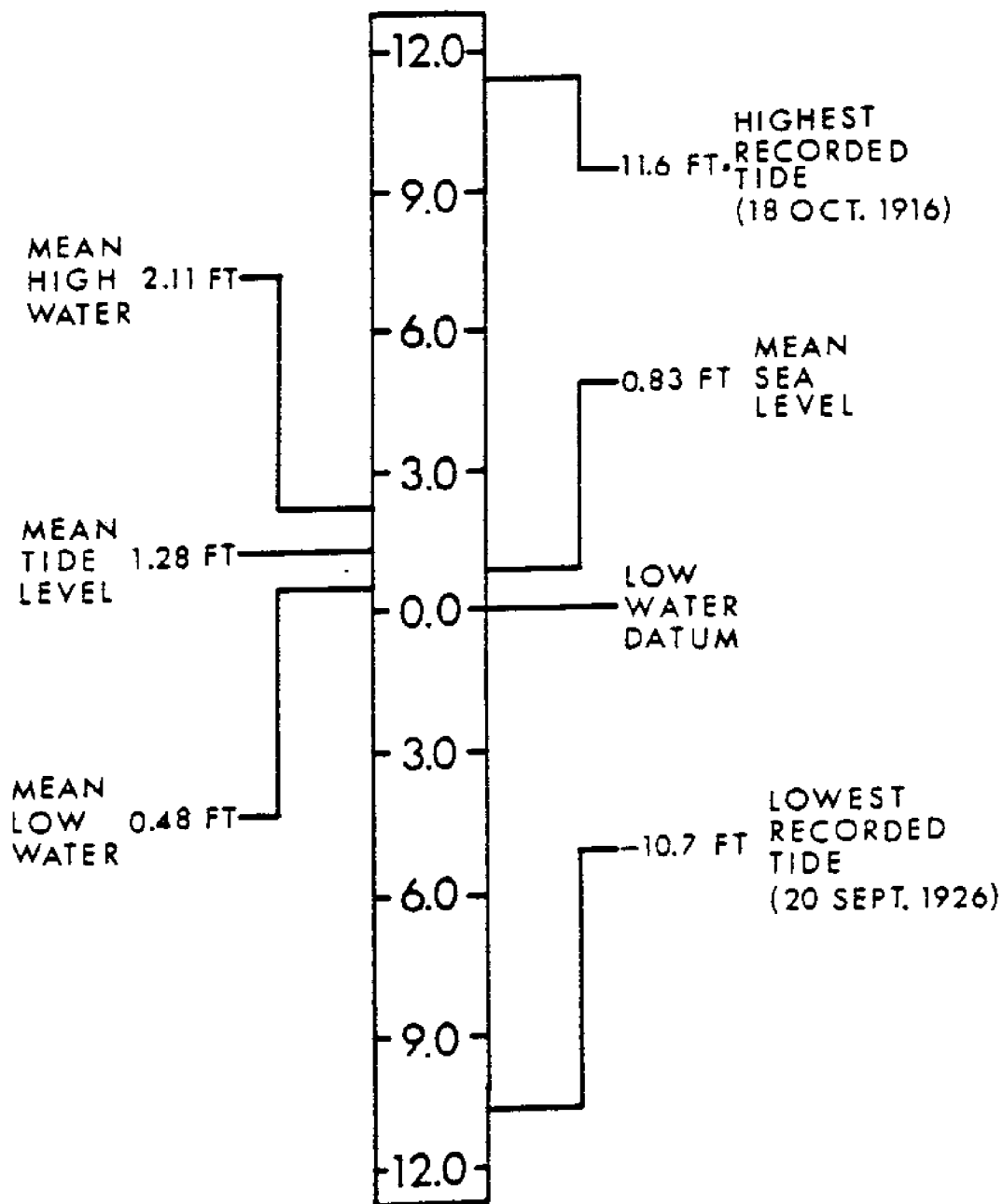


Figure 10. Significant Water Levels Relative to Low Water Datum. (32).

Depths were assigned to each water cell as delineated by the land boundary. The depth of each cell was determined as a weighted average of the charted depths within that cell. Due to the slowly varying bottom depth over large portions of the Bay, most of the depths assigned to the grid cells reflected the actual bathymetry of the Bay. This did not hold for the grid cells in which the ship channel was located. The ship channel is 400 ft wide, and therefore much smaller than the minimum grid dimension of 1667 ft. Its 40 ft depth is deeper than the average 10 ft depth of the Bay. Depths for these cells were assigned by a careful weighted average.

#### Flood cells

Land cells with an elevation of less than 0.5 ft were specified to be subject to flooding. Such a cell would flood if the water elevation of an adjacent water cell became 0.3 ft higher than the land-cell elevation. Various cells along the water-land boundary and in the Mobile River delta were subject to flooding.

#### Manning friction factors

Manning's  $n$  values for bottom roughness were assigned on a relative basis according to the bottom type specified by the nautical chart (18). The Manning coefficients ranged from 0.10 in Bon Secour Bay to 0.35 in the river-marsh area of the Mobile River delta.

## Pass flow calculations

WIFM II had the capability of calculating the flow across any cell face specified. This feature was utilized to calculate the flows through Main Pass and Pass aux Herons as shown in Figures 8-9. The results of the calculation were used in the calibration and verification of the model and in the evaluation of the parametric studies below.

### Field Data for Calibration/Verification

#### Description of field data

Two sets of tidal elevation and current velocity data were used for calibrating and verifying the model. These data were obtained from the U.S. Army Corps of Engineers, Mobile, Alabama (33). The data were originally used for the calibration and verification of the physical model of Mobile Bay located at the Waterways Experiment Station, U.S. Army Corps of Engineers, Vicksburg, Mississippi (26). An additional tide elevation record from Hill (11) that was not included with the Corps of Engineers data was also used.

The data were collected over two 25 hr time periods. The first period was from 1200 CST May 15, 1972 to 1300 CST May 16, 1972. The second data set was collected from 0900 CST June 13, 1973 to 1000 CST June 14, 1973. The locations of some of the tide-elevation and current-velocity stations vary between the two data sets. The average flow rates

(cfs) during these two time periods for the Mobile and Tensaw Rivers were included in the data. The 1972 data also included flow-rate calculations for Main Pass and Pass aux Herons over the data collection period.

The tide-elevation data consisted of a continuous paper-tape record of elevation (ft) over time (hrs). A correction factor was supplied by the Corps of Engineers with each elevation record to correct the data to the MSL datum. The current-velocity data consisted of readings of the current-velocity magnitude and compass direction at hourly intervals over the 25 hr collection periods. For the velocity stations located in the deep water of the ship channel or East Main pass, these measurements were made at graduated depth intervals from the surface to the bottom.

#### Comparison of model data to field data

For comparison to the model, the tide elevations at each gage were read from the tape at hourly intervals corresponding to the times of the velocity data. In most cases the elevation could be read to  $\pm 0.20$  ft at any given hour. At stations where the current velocity and direction were measured at depth intervals, the velocity magnitude and direction were taken as the average of these measurements.

The locations of the tide gages and velocity stations on the model grid were designated as a grid cell as close

as possible to the actual location. The tide elevation for each gage was the elevation of the designated grid cell as calculated by the model. The velocity magnitude and direction of each station were determined by a four-point average of the velocity vectors at the designated cell, Figure 11.

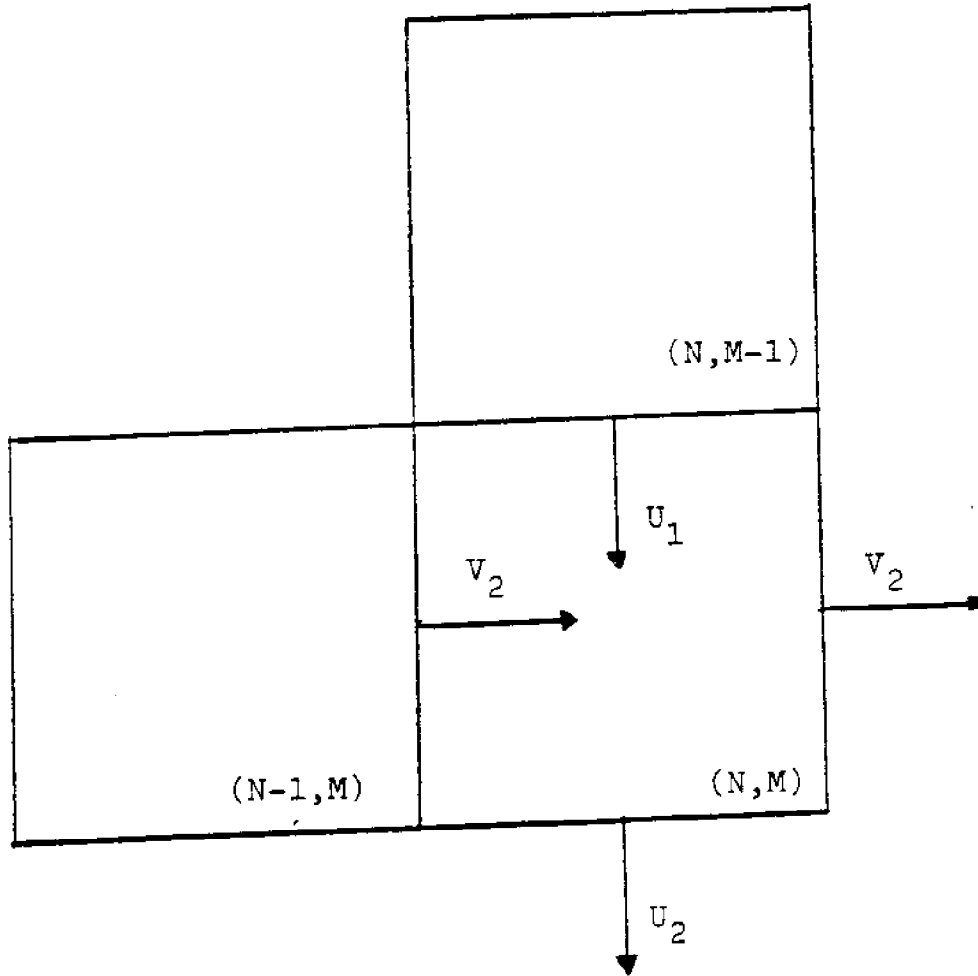
The flow-rate calculations from WIFM II mentioned above were given in total flow (cu ft) at any specified time interval. The data were divided by the chosen time interval of 1800 sec (0.5 hr) to obtain flow rates (cfs) for comparison to the discharge-rate data from 1972 and for evaluation of the parametric studies below.

#### Calibration/Verification

##### Case study of field data from May 15 and 16, 1972

As stated above, tide-elevation, current-velocity, and pass flow-rate data were available for the 25 hr period starting 1200 CST May 15, 1972. Notes on the raw velocity data indicated the presence of a variable wind of 5-20 k. The actual locations of each gage station are shown in Figure 12. The model representation of these gage positions is shown in Figure 13.

A constant, total river flow of 63,500 cfs was used. Of this amount, 33,270 cfs was introduced into the Mobile River and 30,230 cfs into the Tensaw River as suggested by Lawing et al.

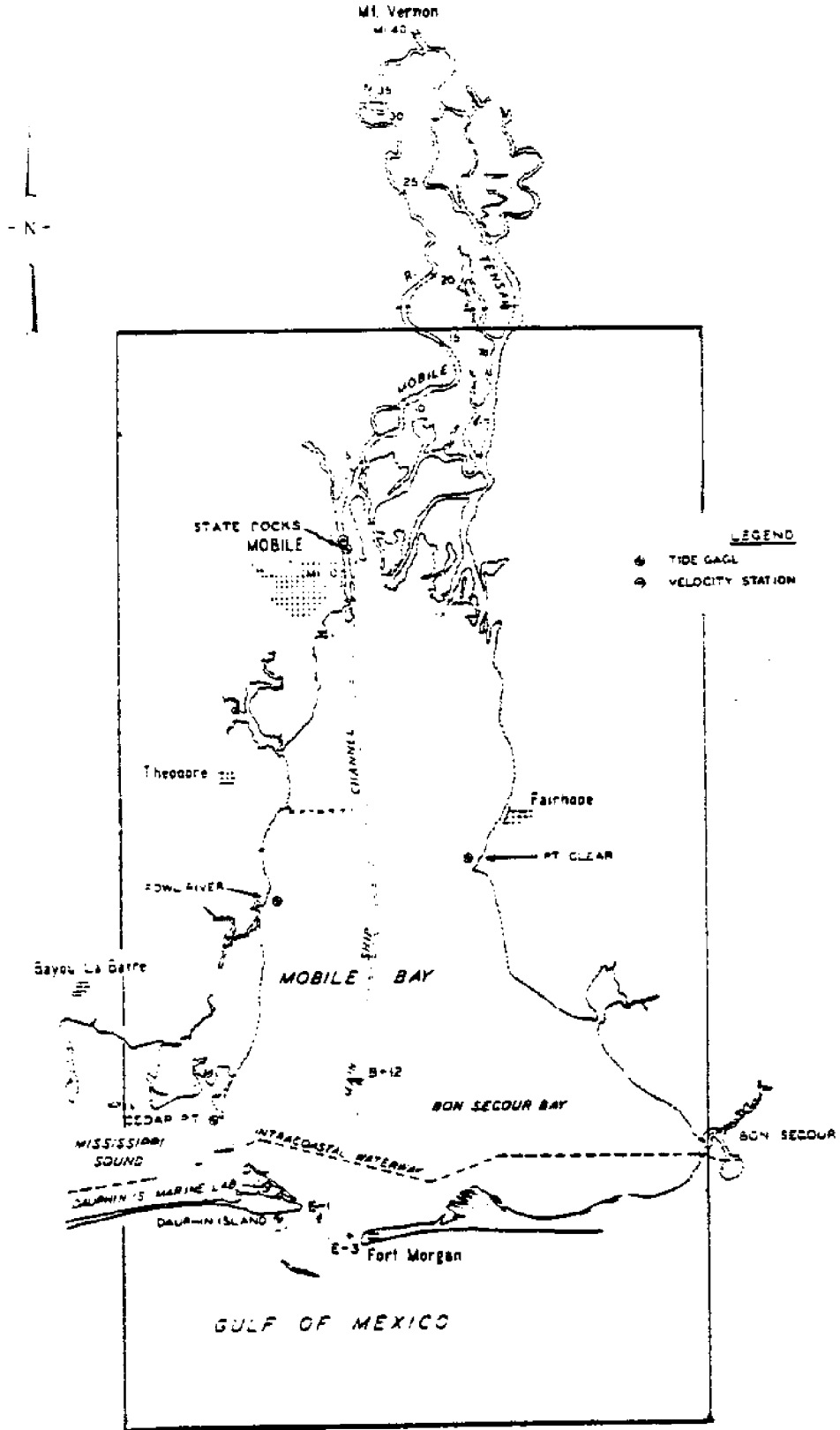


$$v_{\text{mag}} = \left\{ \frac{(0.5(U_1 + U_2))^2 + (0.5(V_1 + V_2))^2}{d(N,M)} \right\}^{\frac{1}{2}}$$

Figure 11. Velocity Calculation for Field Data Station at Grid Cell (N,M)--Four-Point Average.

Figure 12. Location of Field Data Stations  
for May 15-16, 1972 (26).

B-12 = Buoy 12  
Dauphin Island = Dauphin Island Gulf  
E-1 = West Main Pass  
E-3 = East Main Pass



SCALE IN FEET  
0 1000 2000

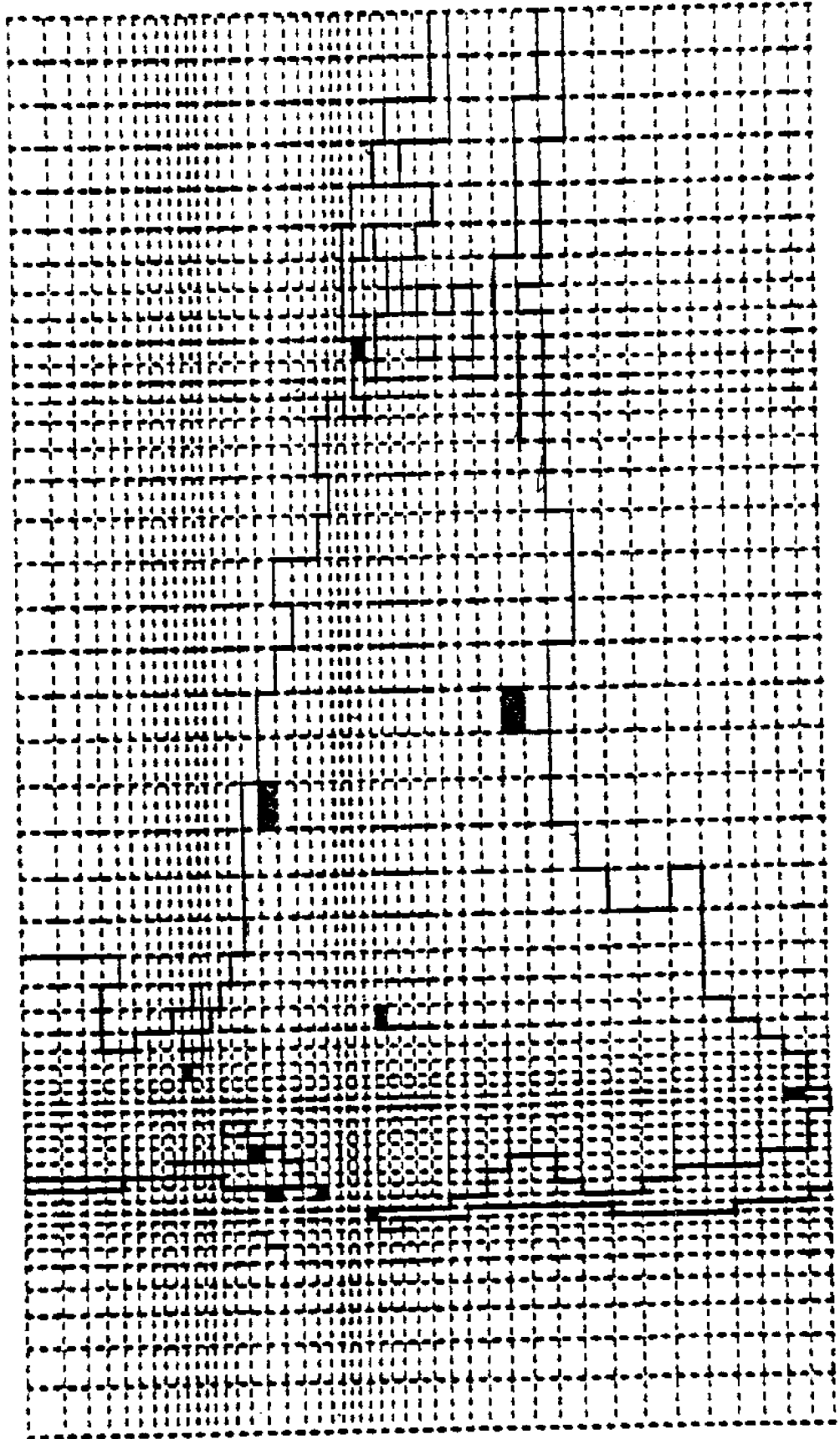


Figure 13. Grid Representation of Field Data Stations for 1972.

The tidal boundary condition at the Gulf of Mexico was specified as the tide record at the Dauphin Island Gulf station obtained from Hill (11). The tide record at Cedar Point was used as the tidal boundary condition for East Mississippi Sound.

In contrast to Hill, a correlation equation for these tides was not necessary as input to the model. The explicit solution format of Hill's model needed an equation approximating a tidal cycle for this data, because the model had to run for several tidal cycles in order to produce a stable solution. Inspection of the tide data for Dauphin Island Gulf showed that over a period of days the tide range changed and was not strictly cyclic. This change in tide range over time is typical of the diurnal tide present in much of the Gulf of Mexico.

For WIFM II the actual tide elevations, rather than values from a correlation equation, were read directly from the tide records and applied to the model as boundary conditions. The record at Dauphin Island Gulf was subsequently backed off to the seaward boundary by the model according to the free-gravity-wave speed. The initial flow condition was set at no flow. The initial elevation was set as the average of the starting elevations at Dauphin Island Gulf and Cedar Point.

The model was run with a time step of 180 seconds over a period of 34 prototype hrs. The run spanned a time

period of 9 hrs before, and continued to the end, of the 25 hr field-data collection period. The tide record from Cedar Point lacked data for the 9 hrs previous to the field-data period. Extrapolated values were used in this case. A lead time of up to 8 hrs (see below) for the model run was necessary for the model calculations of elevation and velocity to stabilize.

A time step of 90 sec was implemented to determine the acceptability of a 180 sec time step. No significant change in velocity or elevation was discovered. A lead time of 23 hrs was also tried with no effect on the model results for the 25 hr data period. No study was done to determine the maximum allowable time step or minimum lead time necessary for a good solution.

#### Results of case study of May 15 and 16, 1972

The comparison of model results with the field data is presented in Figures 14-19.

#### Tide elevation

Dauphin Island Gulf, Dauphin Island Marine Lab, and Cedar Point tide gages showed excellent agreement of model results and field data both in phase of the tide and in magnitude. The State Docks, Bon Secour, and Point Clear stations also gave reasonable agreement between model results and field data. The phases of these gage locations

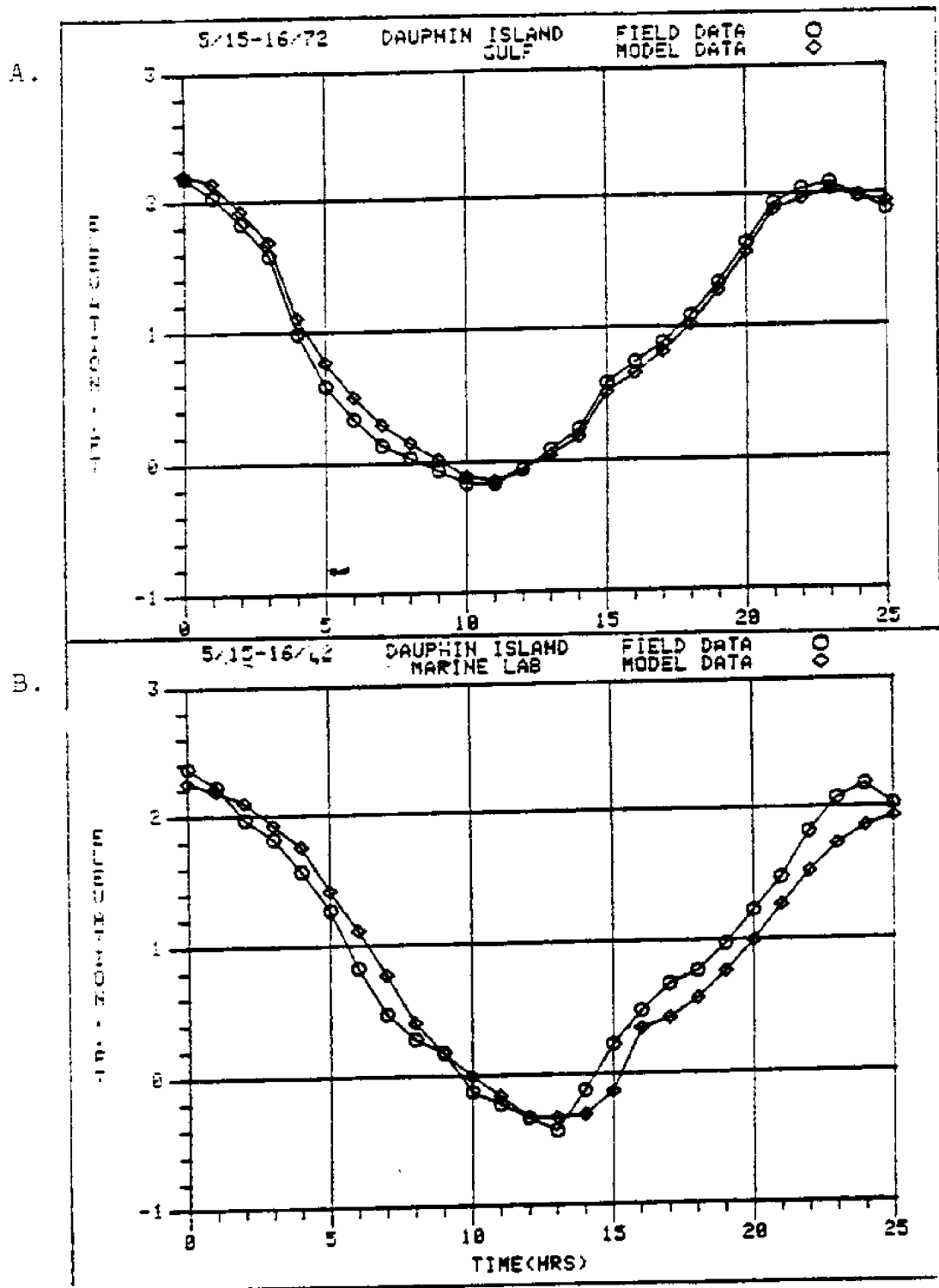


Figure 14. Comparison of Model Results with 1972 Data.  
 A. Dauphin Island Gulf Tide Gage  
 B. Dauphin Island Marine Lab Tide Gage

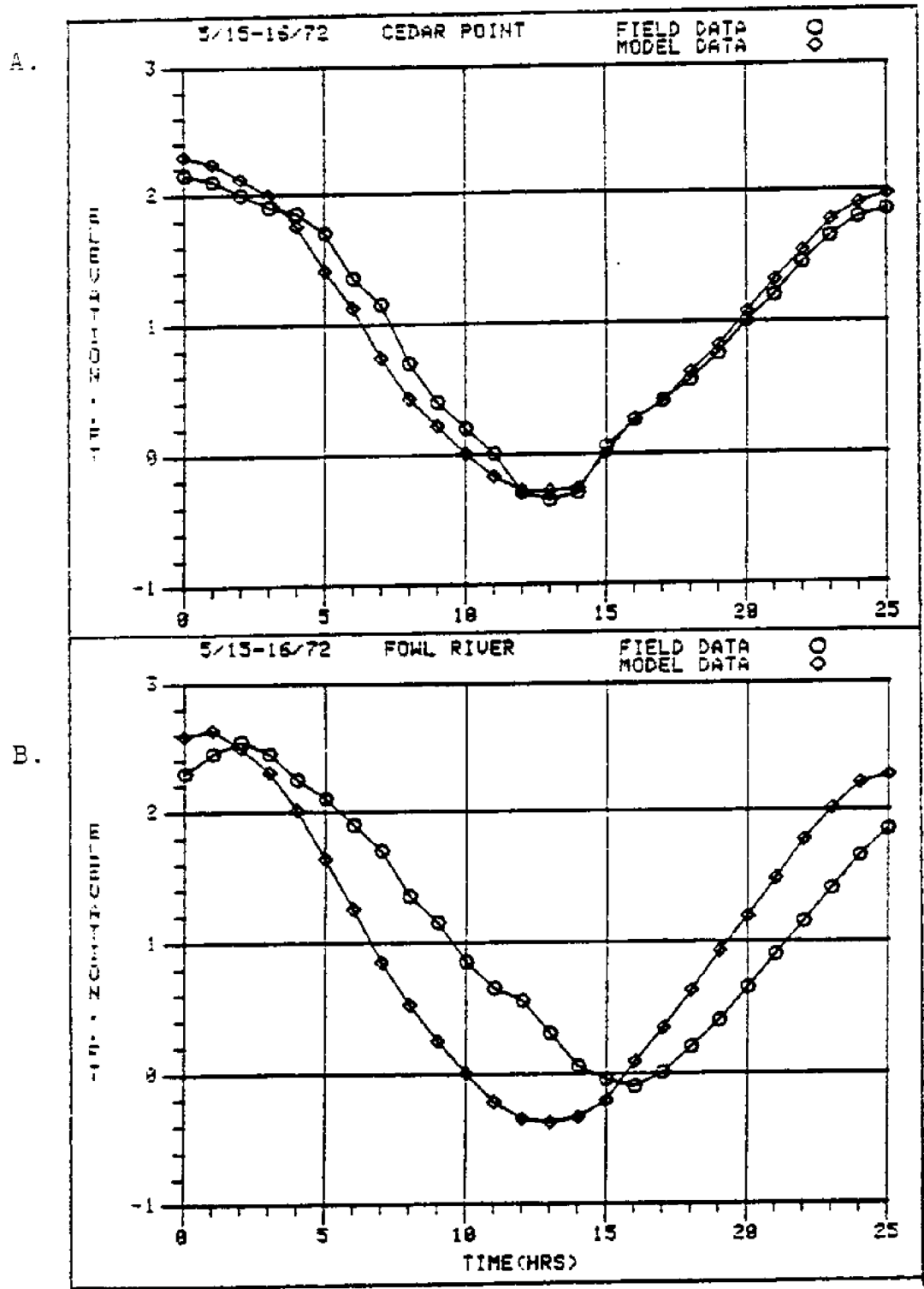


Figure 15. Comparison of Model Results with 1972 Data.  
 A. Cedar Point Tide Gage  
 B. Fowl River Tide Gage

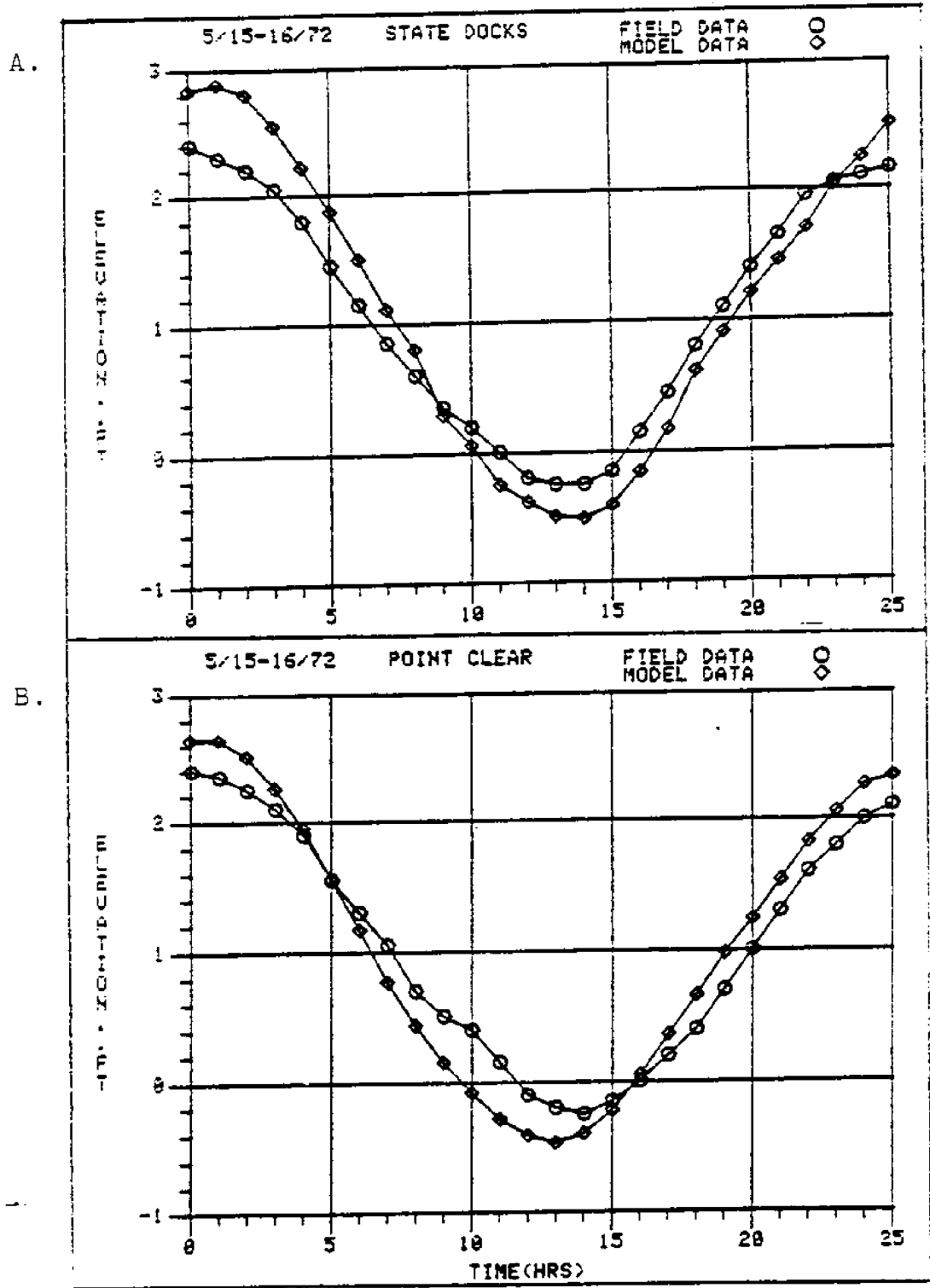


Figure 16. Comparison of Model Results with 1972 Data.  
 A. State Docks Tide Gauge  
 B. Point Clear Tide Gauge

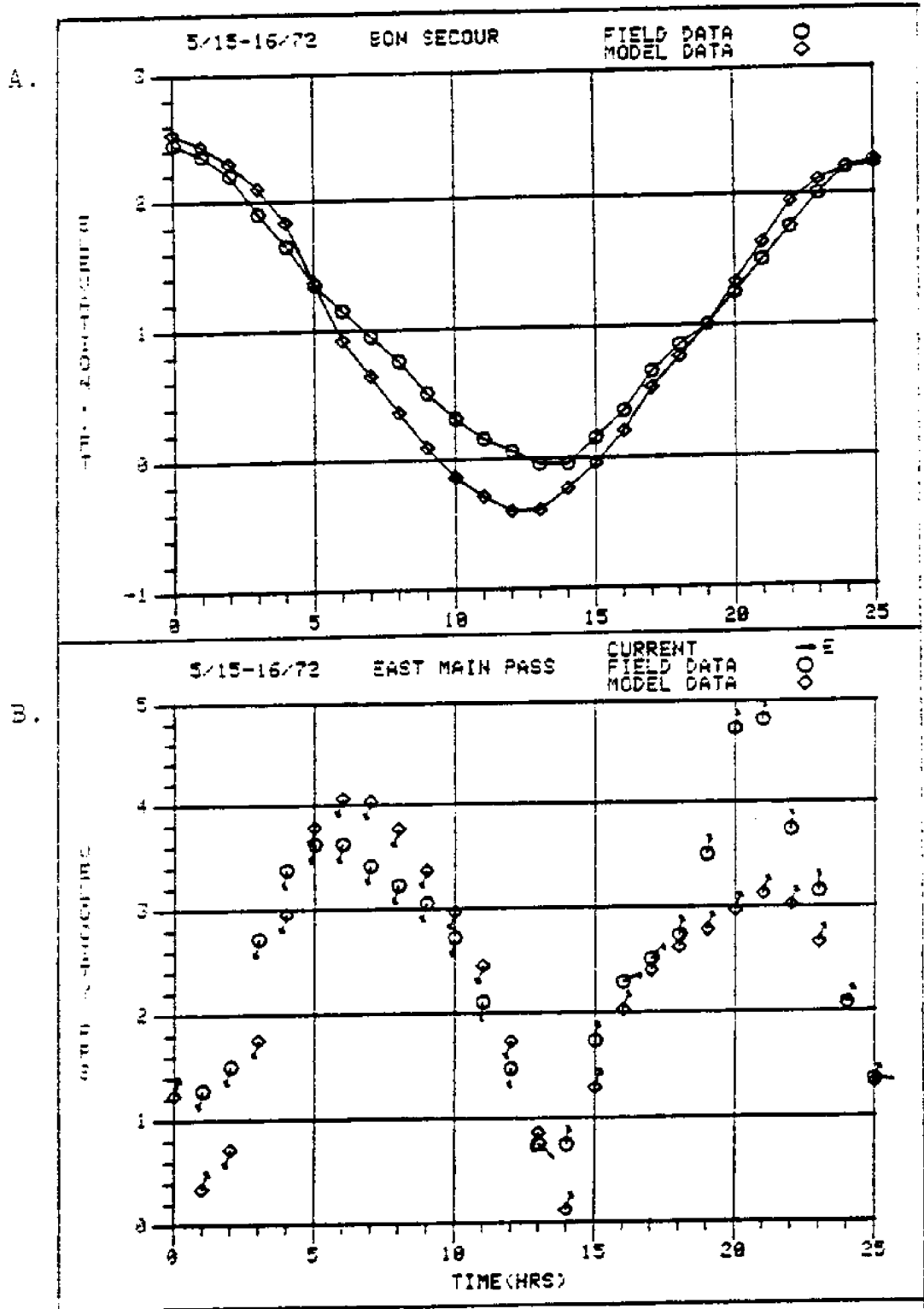


Figure 17. Comparison of Model Results with 1972 Data.  
 A. Bon Secour Tide Gage  
 B. East Main Pass Velocity Station

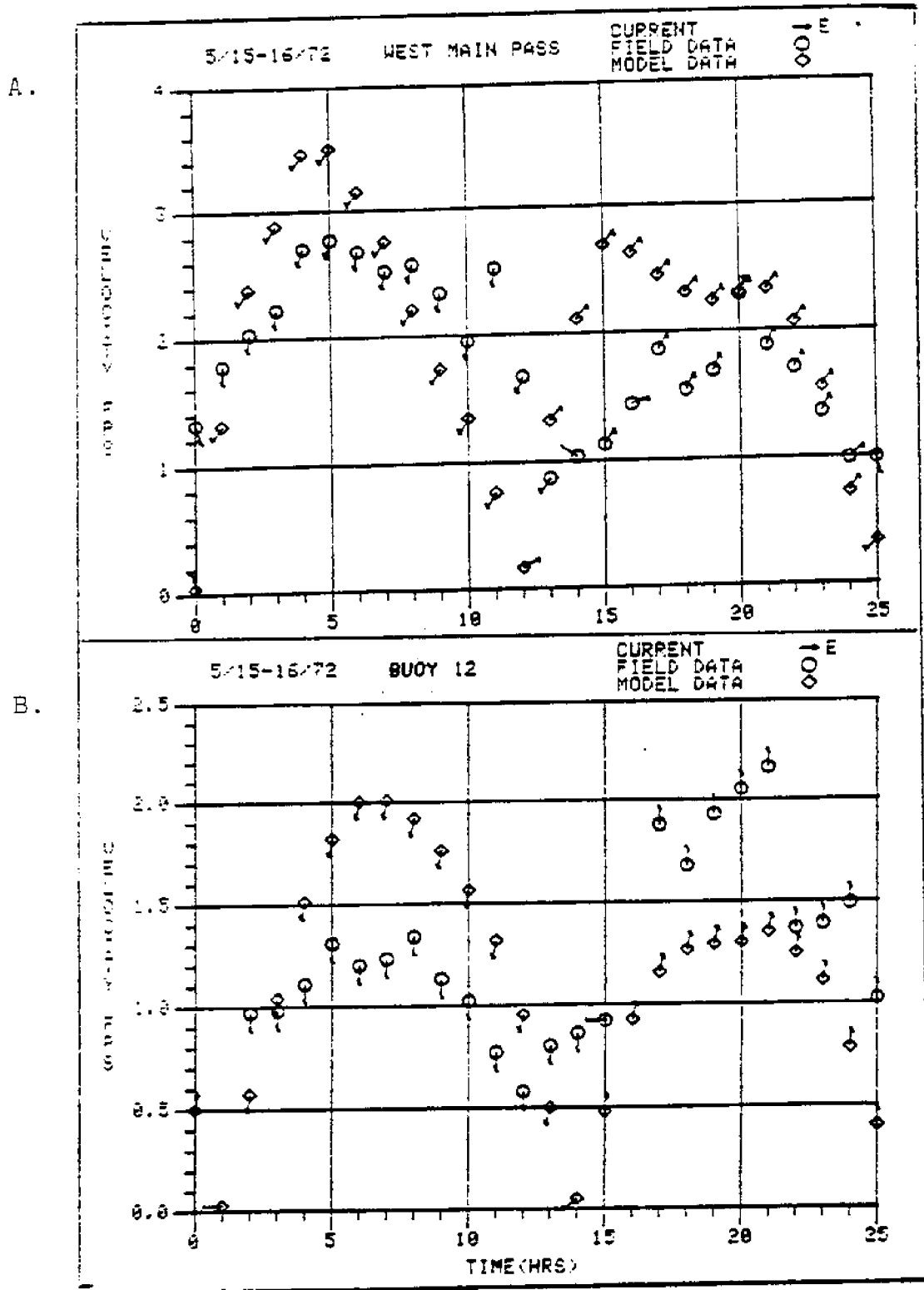


Figure 18. Comparison of Model Results with 1972 Data.  
 A. West Main Pass Velocity Station  
 B. Buoy 12 Velocity Station

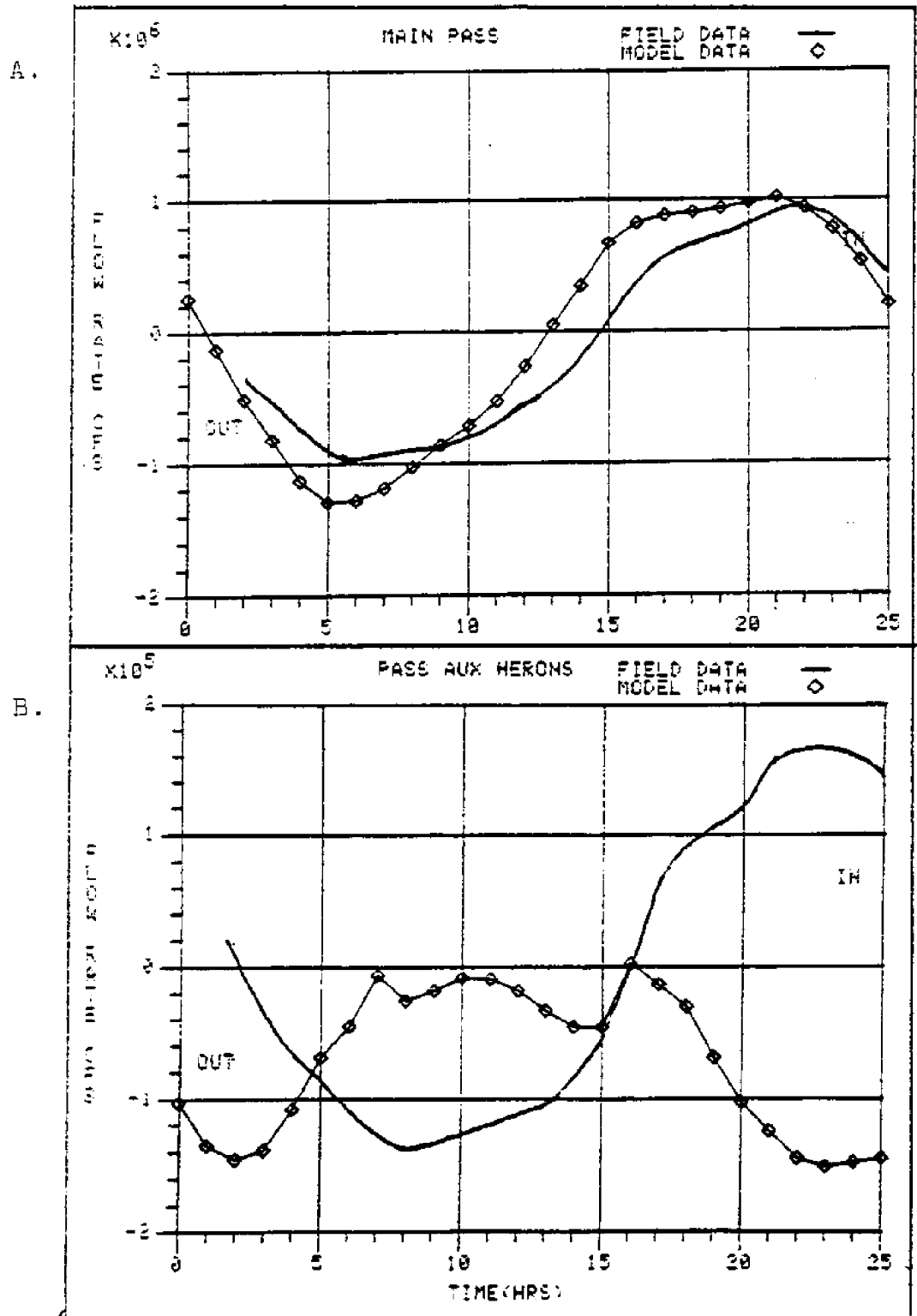


Figure 19. Comparison of Model Results with 1972 Data.  
 A. Main Pass Flow Rate  
 B. Pass aux Herons Flow Rate

did not match as well as the other gages, but were considered to follow the trend of these tide records well. A possible explanation was the relatively large size of the grid cells in these areas. The larger cell size caused the locations of these gage points to be more crude than the others. Fowl River gage results were suspect in terms of phase agreement. Further study (below) revealed problems with the field data that could have caused this result.

#### Velocity magnitude and direction

Both the East Main Pass and the Buoy 12 stations showed good agreement with the velocity trends in both magnitude and direction. West Main Pass model output agreed well with respect to velocity magnitude. However, the model time for the reversal of velocity direction (hrs 12-14) caused by the tide change was 2 hrs early compared to the field data.

#### Pass flow rates

The pass flow-rate records could not be reproduced acceptably for the 1972 field data. The calculated flows in the Main Pass followed the general trend of the field data. The time of the tide change was 2 hrs early relative to the field data, as was also noted above for the West Main Pass results. The flows in Pass aux Herons could not be reproduced at all for this data.

Many changes in model parameters were implemented in attempts to improve the flow-rate results. The parameters that were varied included Manning coefficients, cell depths, and the number and position of flood cells. No improvement was obtainable. The 1973 data set was then analyzed using the same model parameters (depths, boundaries, etc.) as for the 1972 data set.

Case study of field data  
From June 13 and 14, 1973

The field data were collected over the 25 hr period from 0900 CST June 13 through 1000 CST June 14, 1973. Notes on the raw velocity-data sheets indicated low wind conditions. The data consisted of tide-elevation and velocity stations only. No pass flow-rate calculations were available. The locations of the gages are shown in Figure 20 with the grid locations following in Figure 21.

A constant total river flow of 116,000 cfs was used as in Lawing (26). The flow was divided equally between the Mobile and Tensaw Rivers.

A tide-elevation record for Dauphin Island Gulf was not available in the 1973 field data for the specification of the Gulf of Mexico boundary condition. The only alternative for setting any reasonable boundary condition at the Gulf was the use of the predicted or astronomical tide for this time period. The Tide Tables (31) provided the predictions of the elevations and times of the high and

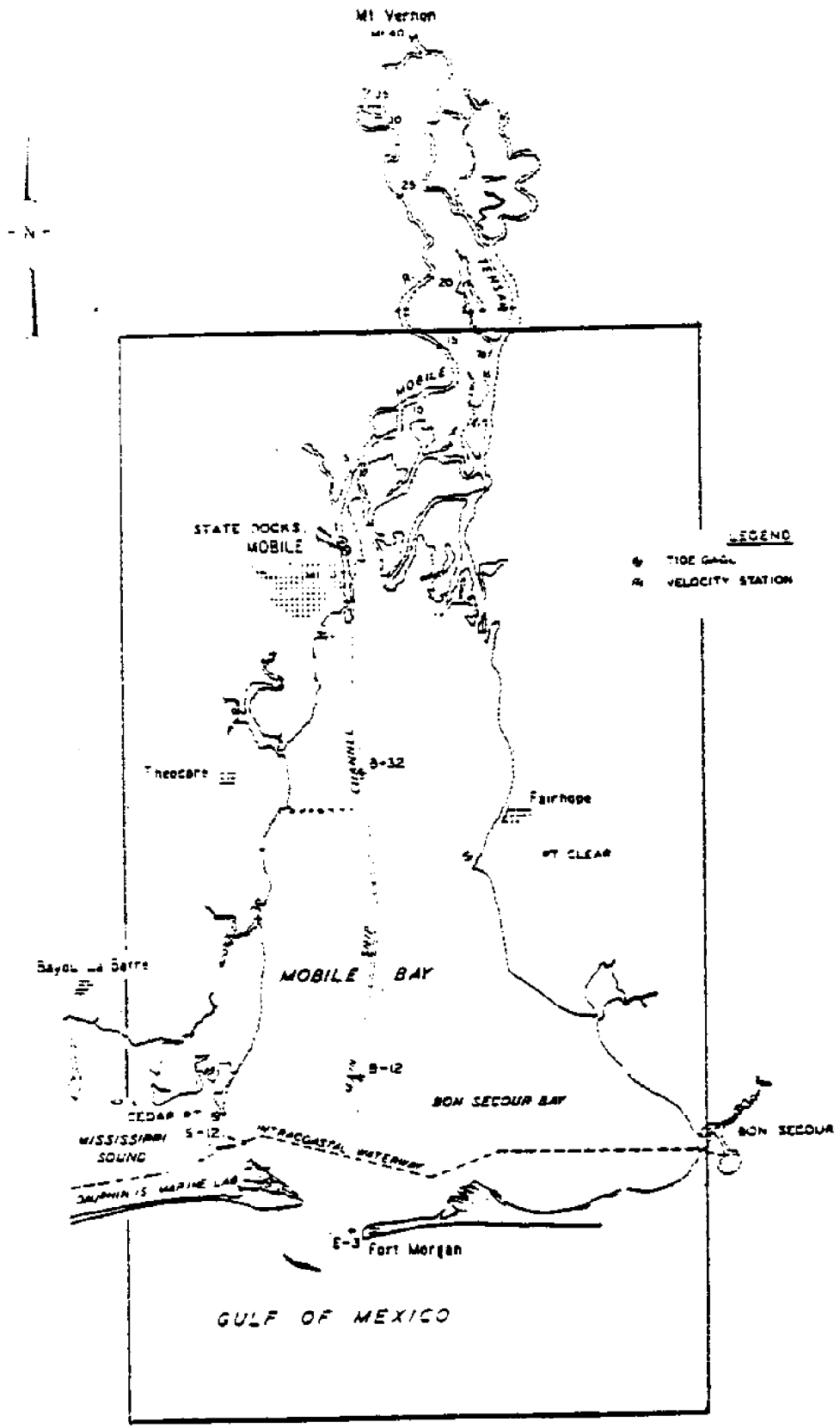
Figure 20. Location of Field Data Stations  
for June 13-14, 1973 (26).

B-12 = Buoy 12

B-32 = Buoy 32

E-3 = East Main Pass

S-12 = Dauphin Island Bridge



SCALE IN FEET  
 0 100 200 400

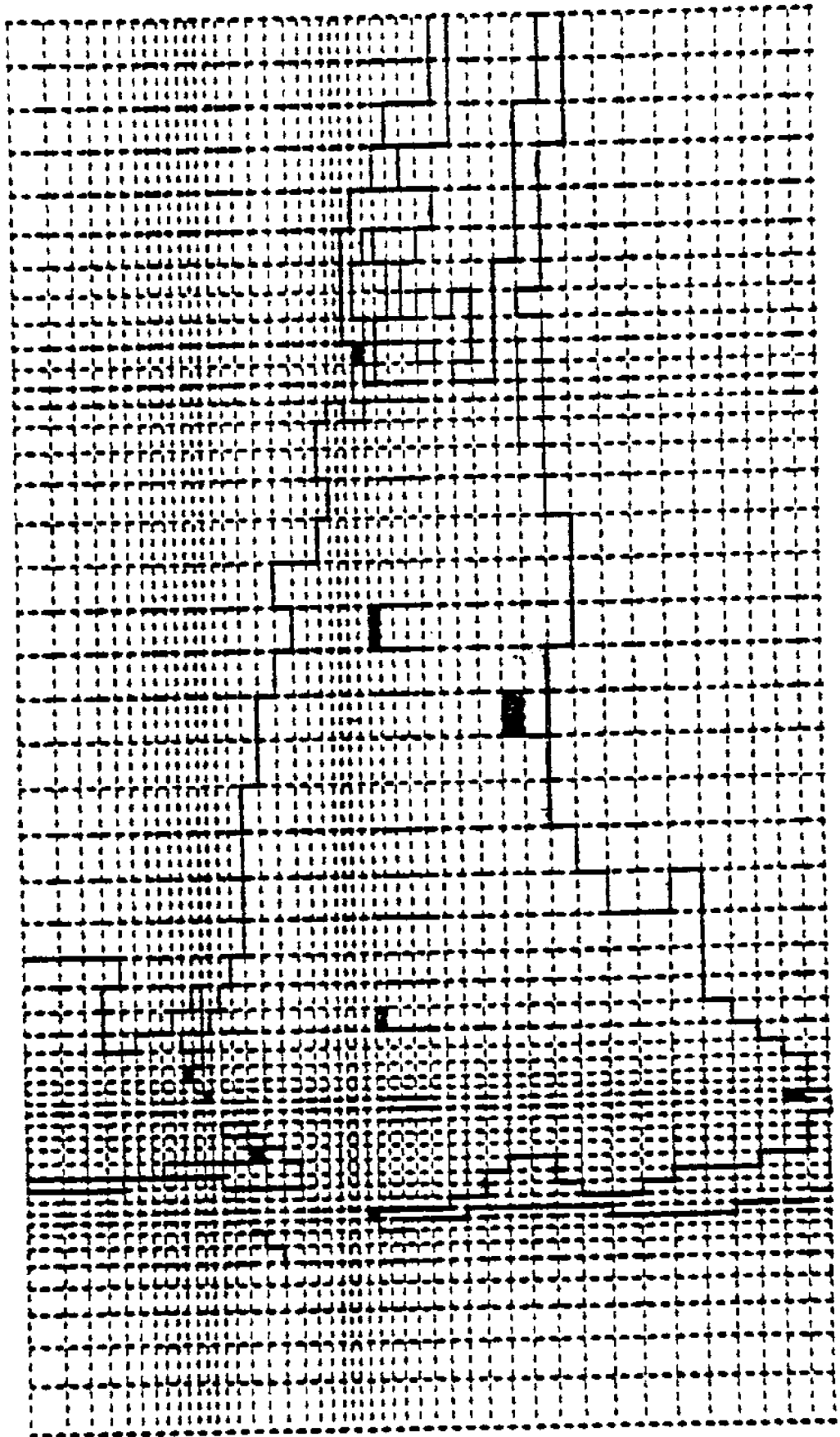


Figure 21. Grid Representation of Field Data Stations for 1973.

low tides at the MLW datum. By interpolation of the tide elevations between these times, an approximation of the predicted tide elevation as a function time was obtained. The data were obtained for June 13 and 14, 1973 at Bayou La Batre, Alabama and Dauphin Island (Fort Gaines), Figure 1. These tide-elevation curves were corrected to MSL and used as the boundary conditions for East Mississippi Sound and the Gulf of Mexico, respectively.

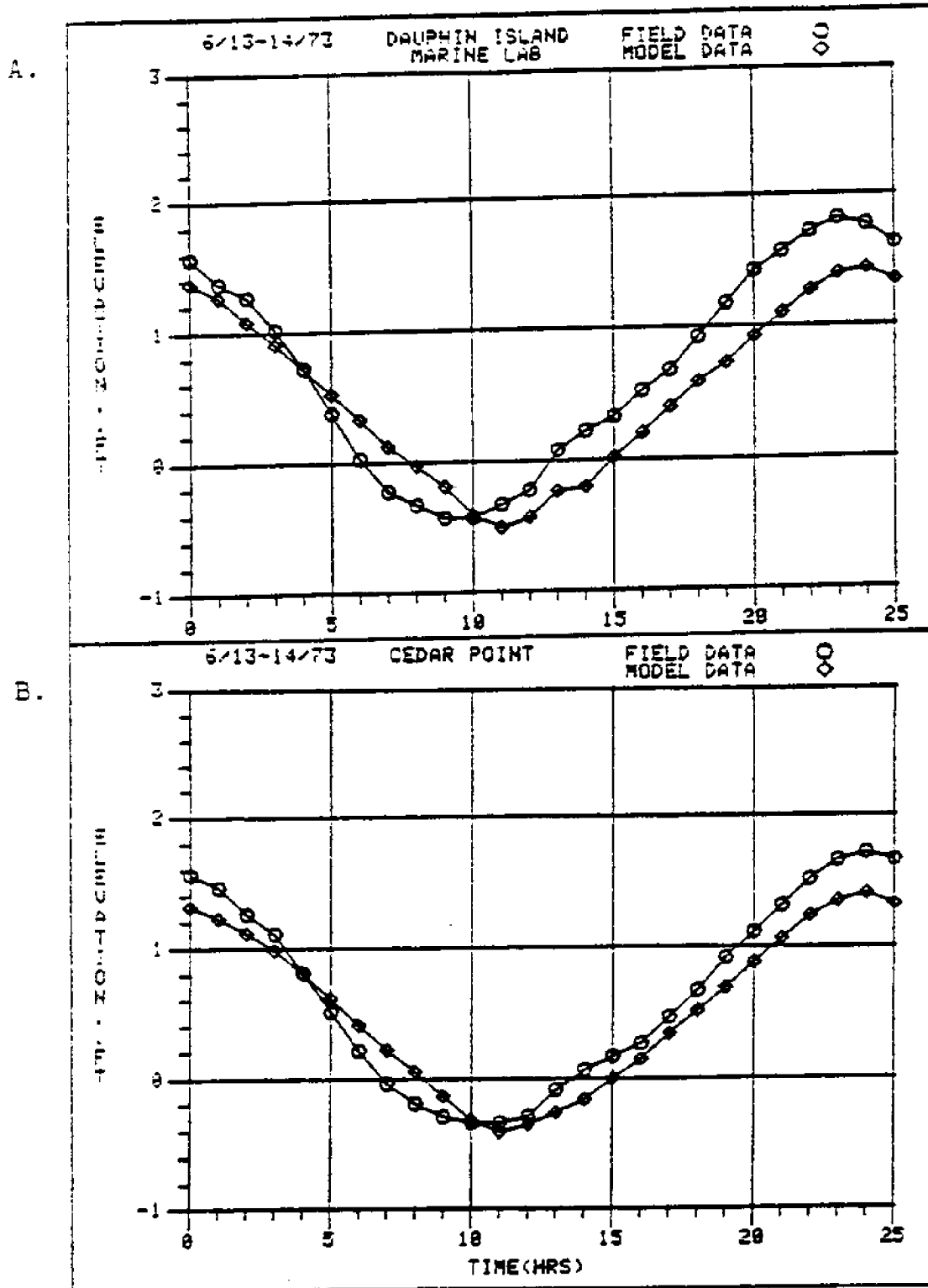
All other model inputs were the same as that for 1972 with one exception. The model run was begun at 8 hrs before the data collection period and continued to 1 hr afterward. As stated above, runs beginning 23 hrs prior to the data collection period produced no significant changes in tide elevation or velocity.

#### Results of case study of June 13 and 14, 1973

The comparison of the model results with the field data is presented in Figures 22-26.

#### Tide elevation

Considering the approximate nature of the tidal boundary conditions, the model tide elevations were considered to be good in terms of reproducing the trends of the tidal data. The Cedar Point gage results showed excellent agreement with the field data, both in magnitude and in phase. All the other tidal gage stations in Mobile



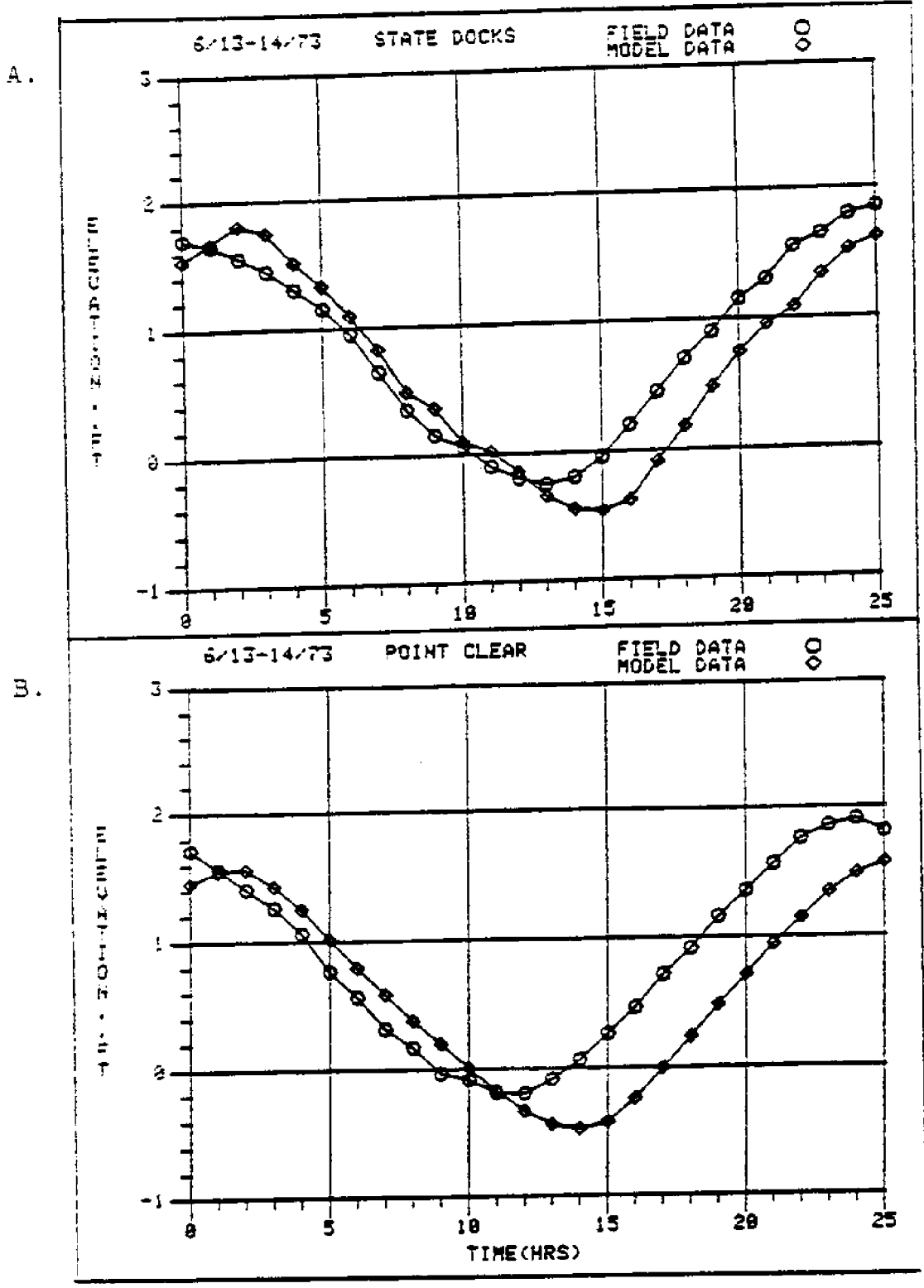


Figure 23. Comparison of Model Results with 1973 Data.  
A. State Docks Tide Gage  
B. Point Clear Tide Gage

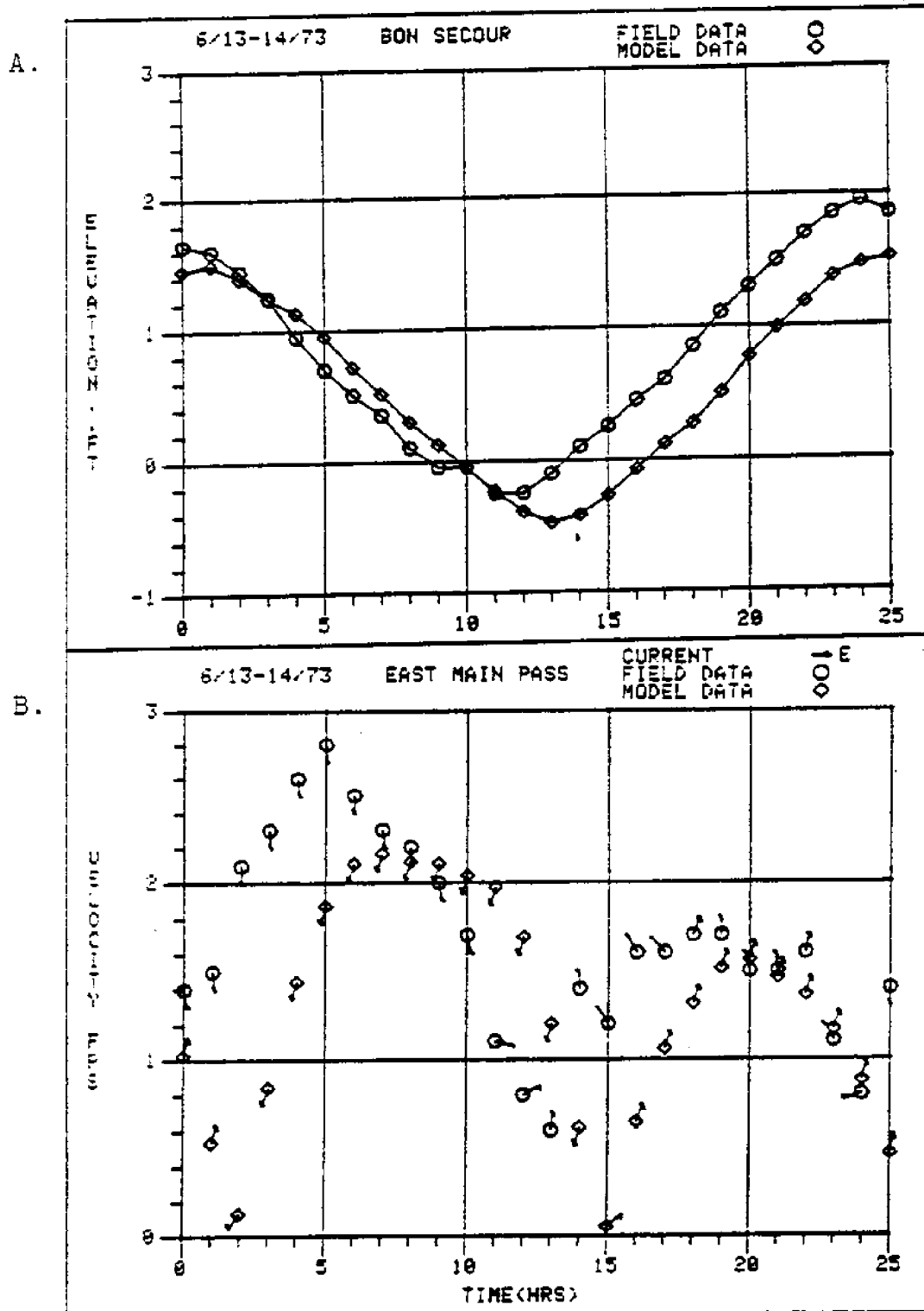


Figure 24. Comparison of Model Results with 1973 Data.  
 A. Bon Secour Tide Gage  
 B. East Main Pass Velocity Station

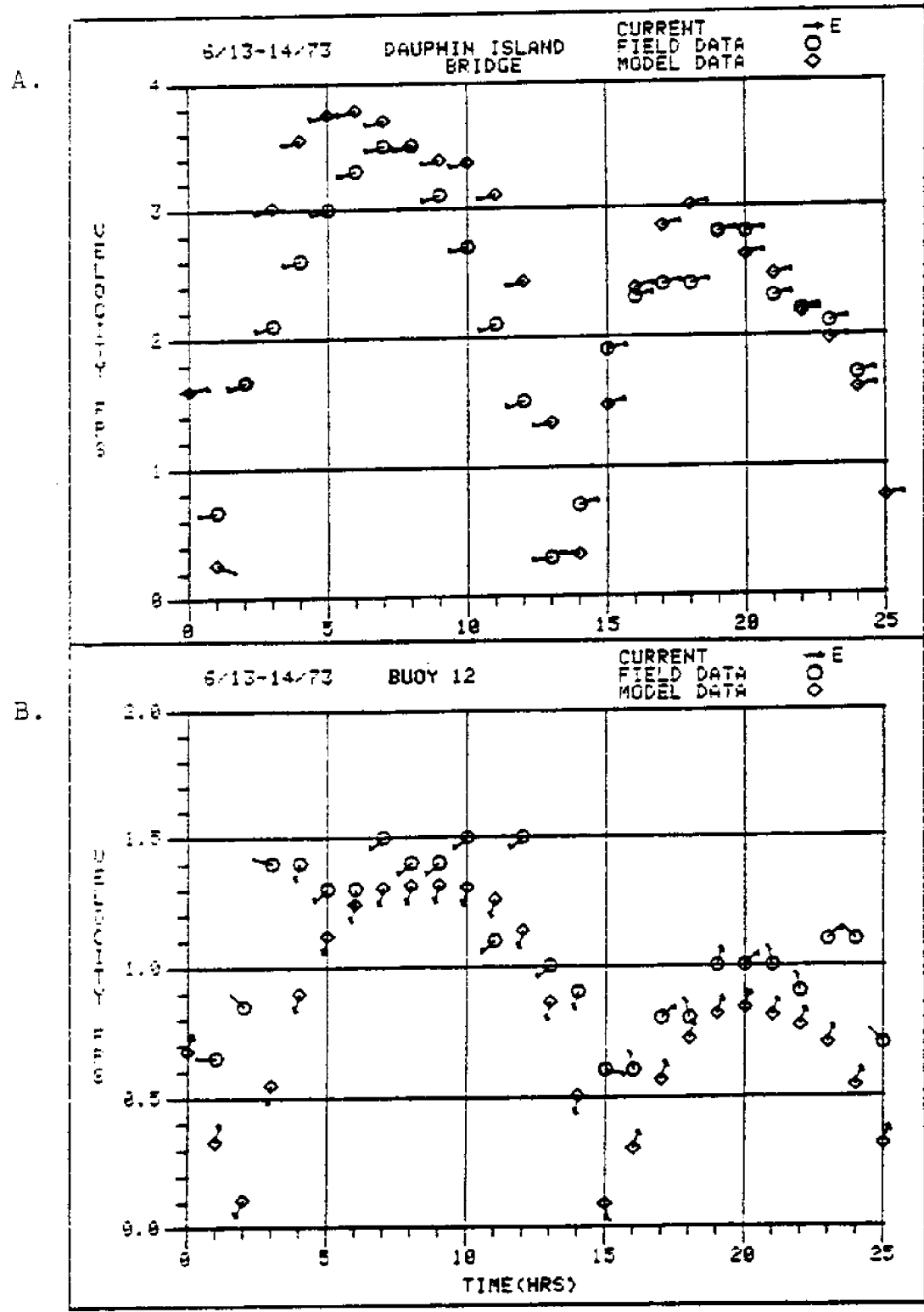
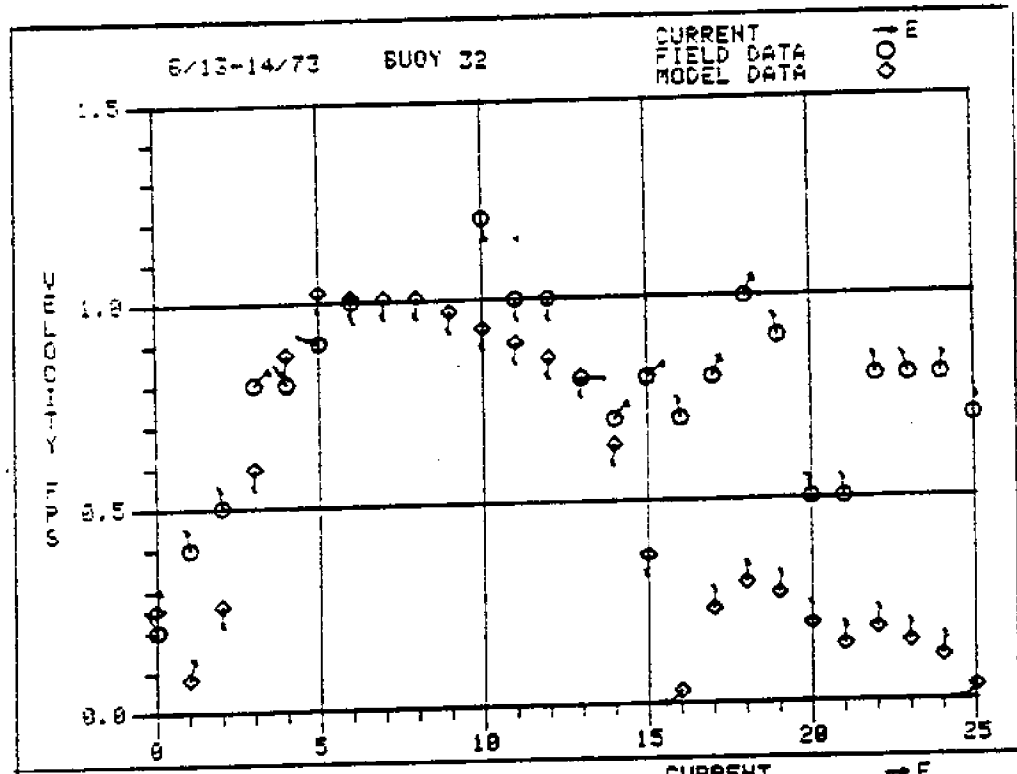


Figure 25. Comparison of Model Results with 1973 Data.  
A. Dauphin Island Bridge Velocity Station  
B. Buoy 12 Velocity Station

A.



B.

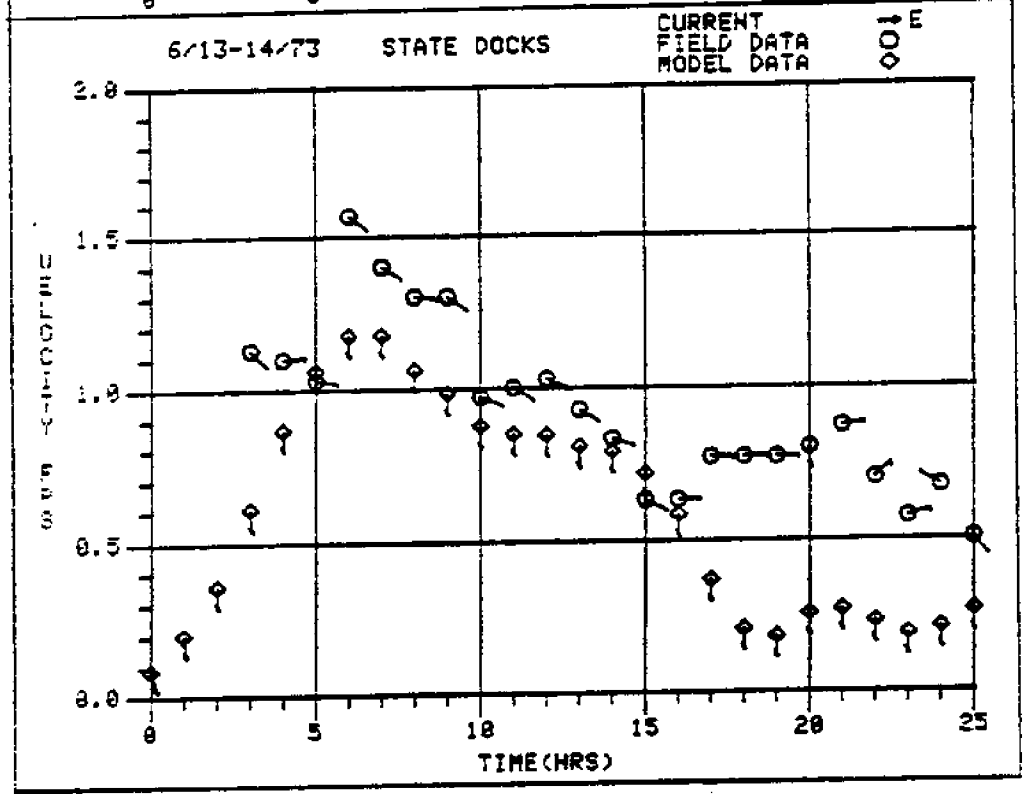


Figure 26. Comparison of Model Results with 1973 Data.  
 A. Buoy 32 Velocity Station  
 B. State Docks Velocity Station

Bay proper were somewhat out of phase. In studying the effects of the model input parameters on the results calculated from the model, it was observed that the variation of the Gulf boundary condition produced the strongest effect upon the calculated values of the elevation. Re-evaluation of the 1972 field data (below) led to the assumption that a Gulf boundary based on reliable field data could improve results.

#### Velocity magnitude and direction

All the current-velocity results from the model run reproduced the trend of the field data. Particularly important was the excellent comparison of the field data with the results of the Dauphin Island Bridge velocity station. The model reproduced both the magnitude and the direction of the field data well.

The calculations for East Main Pass agreed well with the field data, considering the approximate nature of the Gulf boundary condition. The magnitude and phase at this station were greatly dependent on this boundary condition.

The model velocity stations at Buoy 12, Buoy 13, and the State Docks also reproduced the trends of the field data well. These stations were all located in the ship channel. It is well documented in MacPhearson (32), Hill (11), and others that some stratification of the water column occurs in the channel, with fresh water from the

rivers lying on top of the more saline water from the Gulf. The stratification causes a variation in velocity at different depths which was noticed in the evaluation of the field data. During tide changes, water near the surface in some cases flows in one direction, while water near the bottom flows in the other. Recognizing that depth-averaged values of the velocity magnitude and direction were used at these stations, it was apparent that the actual magnitudes and directions of the current could not be reproduced by the two-dimensional model. This was especially true at the change of the tide and during the incoming tide (hrs 13-25). In addition, the grid size of the model at the State Docks did not permit an accurate depiction of the area. This accounted for the discrepancy in the current direction noticed between the model and the field data.

#### Re-evaluation of the 1972 case study

The good results obtained in the case study of the 1973 data set led to the re-evaluation of the 1972 data. Upon referring to Hill (11) and Lawing (26), it was noted that difficulty was experienced in reproducing the field data from 1972. Lawing (26), in fact, stated that the 1973 field-data survey was motivated by this difficulty.

Figure 27A compares the tide record at Cedar Point with the astronomical tide for Bayou La Batre from the Tide

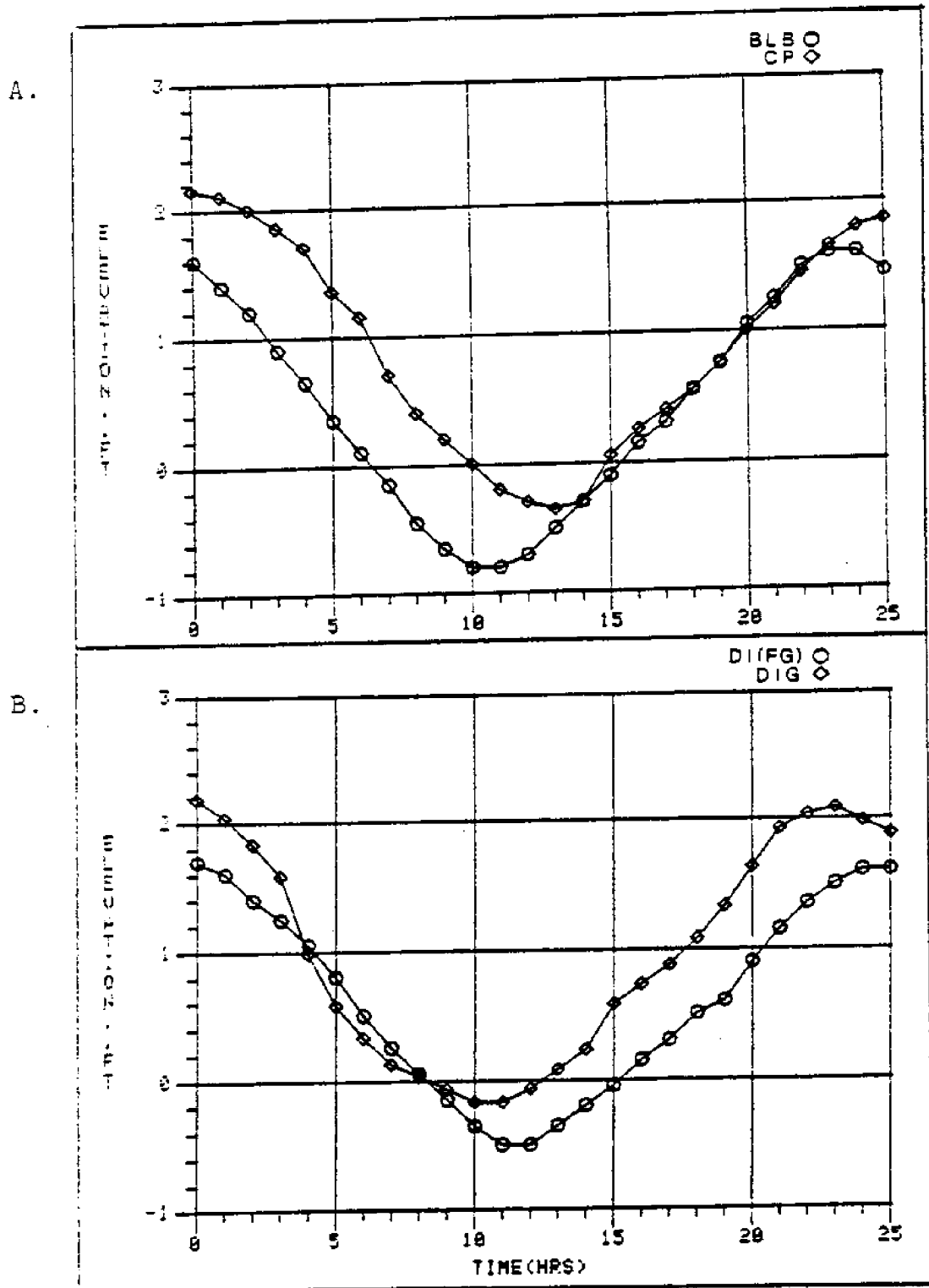


Figure 27. Comparison of Astronomical Tide with Tide Record.

- A. Bayou La Batre (BLB)-Cedar Point (CP)  
 B. Dauphin Island (Fort Gaines) (DI(FG))-  
 Dauphin Island Gulf (DIG)

Tables (31). Figure 27B compares the record of Dauphin Island Gulf with the astronomical tide for Dauphin Island (Fort Gaines). The phase of the Dauphin Island Gulf gage was 2 hrs behind that predicted by the astronomical-tide data. The large discrepancy suggested the possibility that the time axis of the Dauphin Island Gulf gage could be inaccurate. It was also recognized that the strong, variable winds indicated on the velocity field-data sheets could alter the tidal elevations significantly from what they would be under calm conditions. See Tide Tables (31).

Model runs were then executed using the 1972 data to test the plausibility of an inaccurate gage at Dauphin Island Gulf. The first run used the astronomical tides at Bayou La Batre and Dauphin Island (Fort Gaines) as the tidal boundary conditions. The second used the tide records as tidal boundary conditions. The Dauphin Island Gulf gage was delayed 2 hrs to come closer to the relation of the tidal phases as shown in the astronomical tides.

Results of model run using  
astronomical tides from  
May 15 and 16, 1972

The comparison of model results with the field data is shown in Figures 28-33.

Tide elevation

In all cases, the model tide elevations did not agree well with the tide elevations from the field data. The

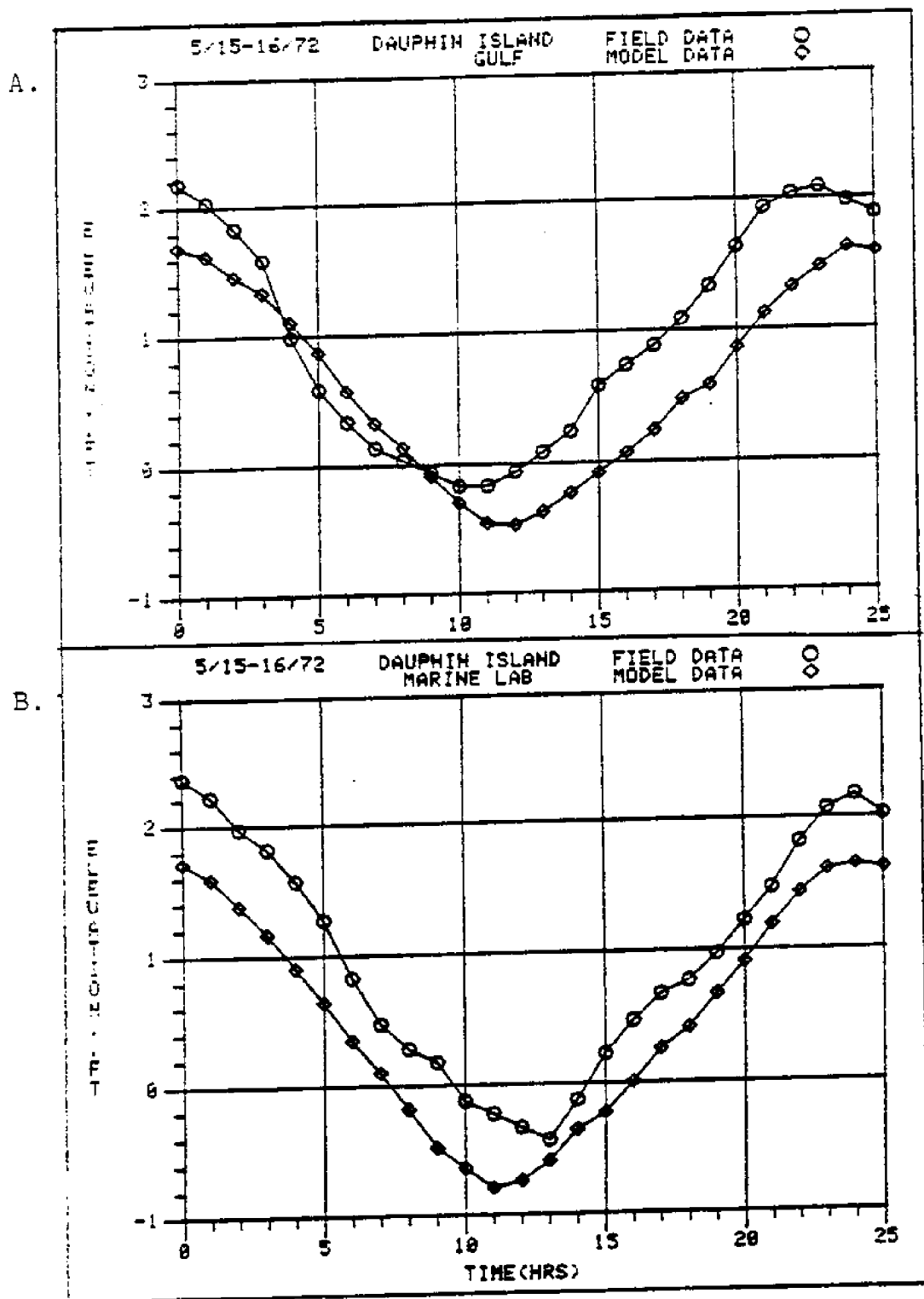


Figure 28. Comparison of Astronomical-tide Model Results with 1972 Data.

A. Dauphin Island Gulf Tide Gage

B. Dauphin Island Marine Lab Tide Gage

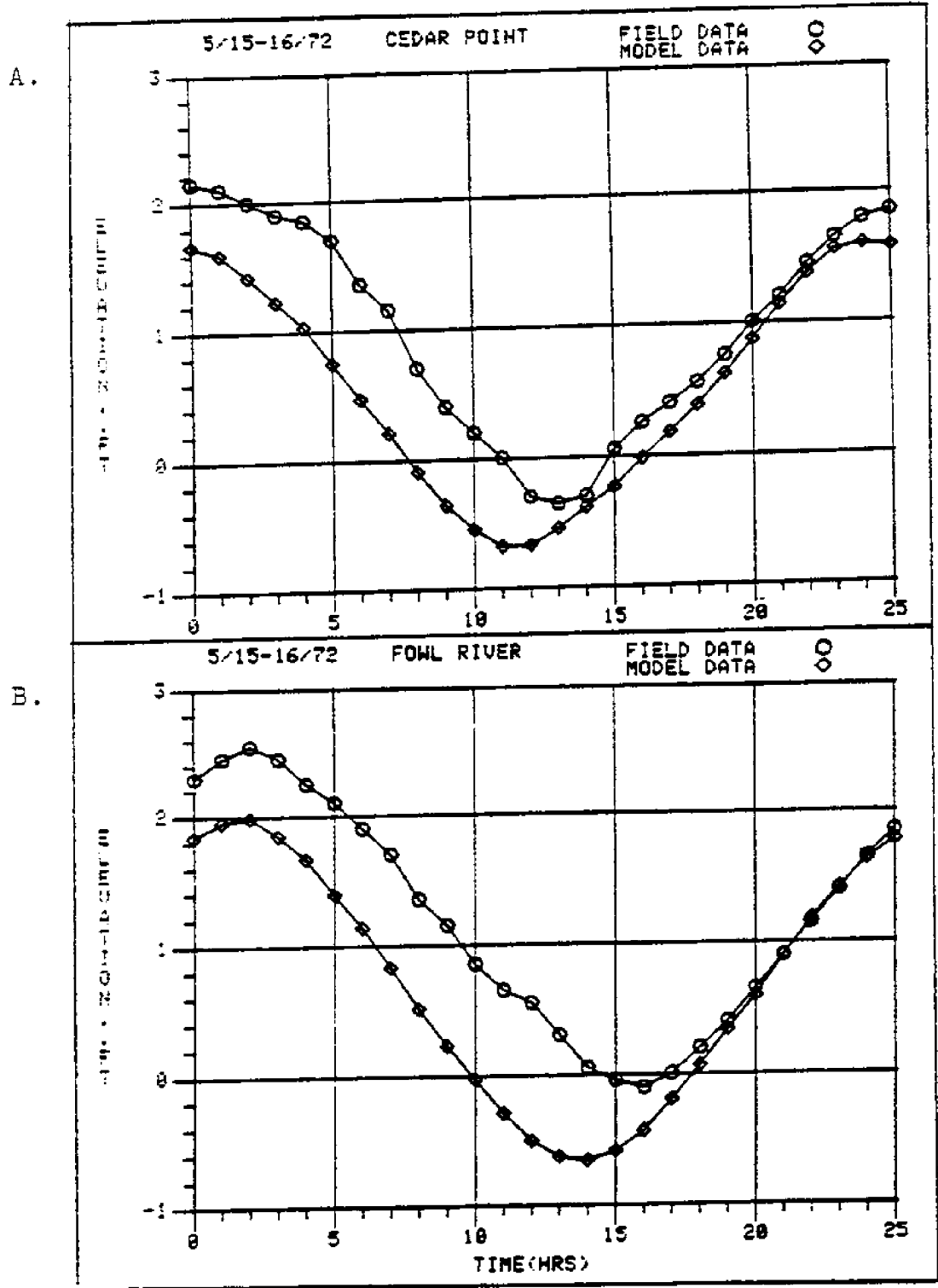


Figure 29. Comparison of Astronomical-tide Model Results with 1972 Data.  
A. Cedar Point Tide Gage  
B. Fowl River Tide Gage

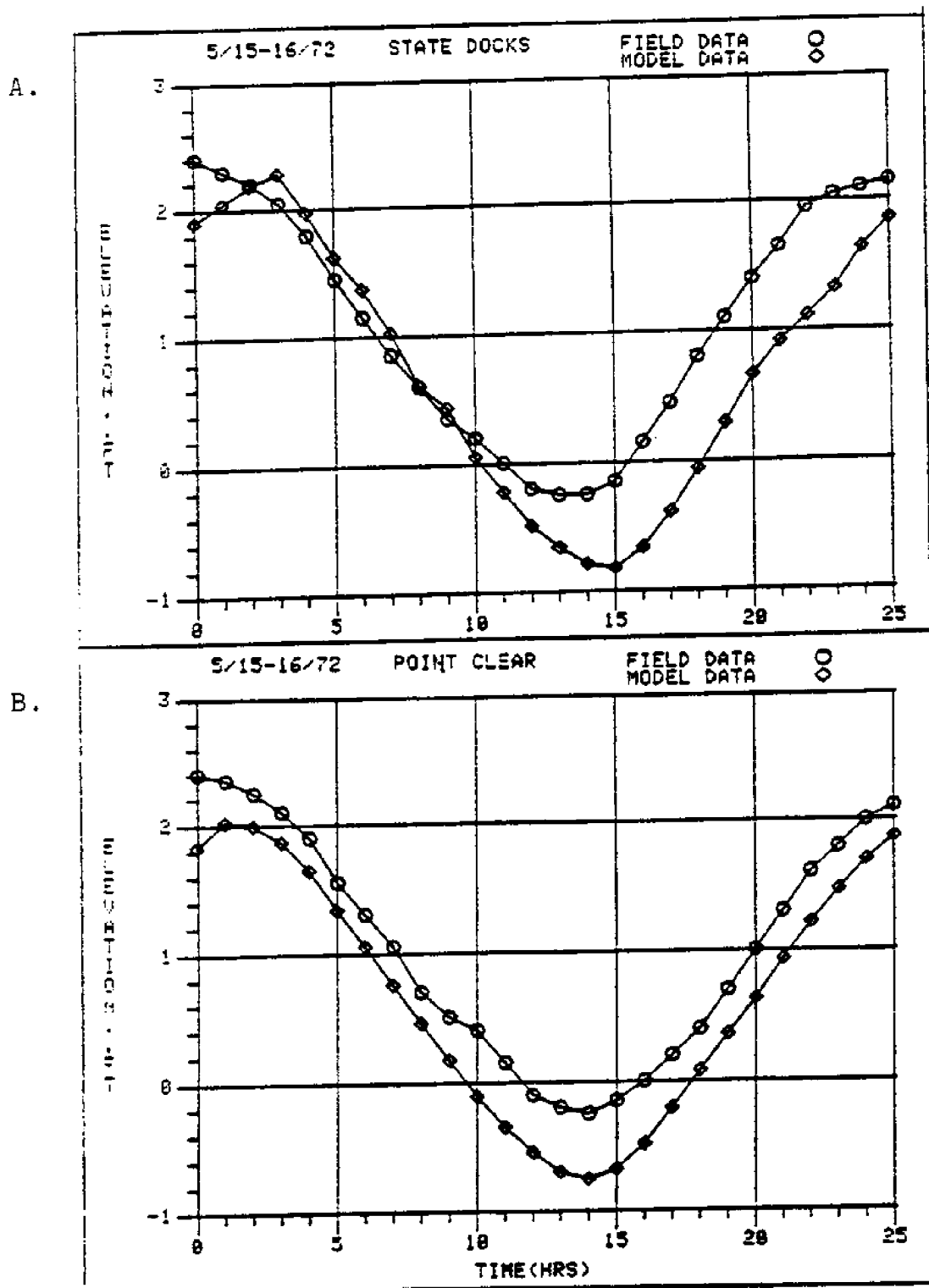


Figure 30. Comparison of Astronomical-tide Model Results with 1972 Data.

- A. State Docks Tide Gage  
 B. Point Clear Tide Gage

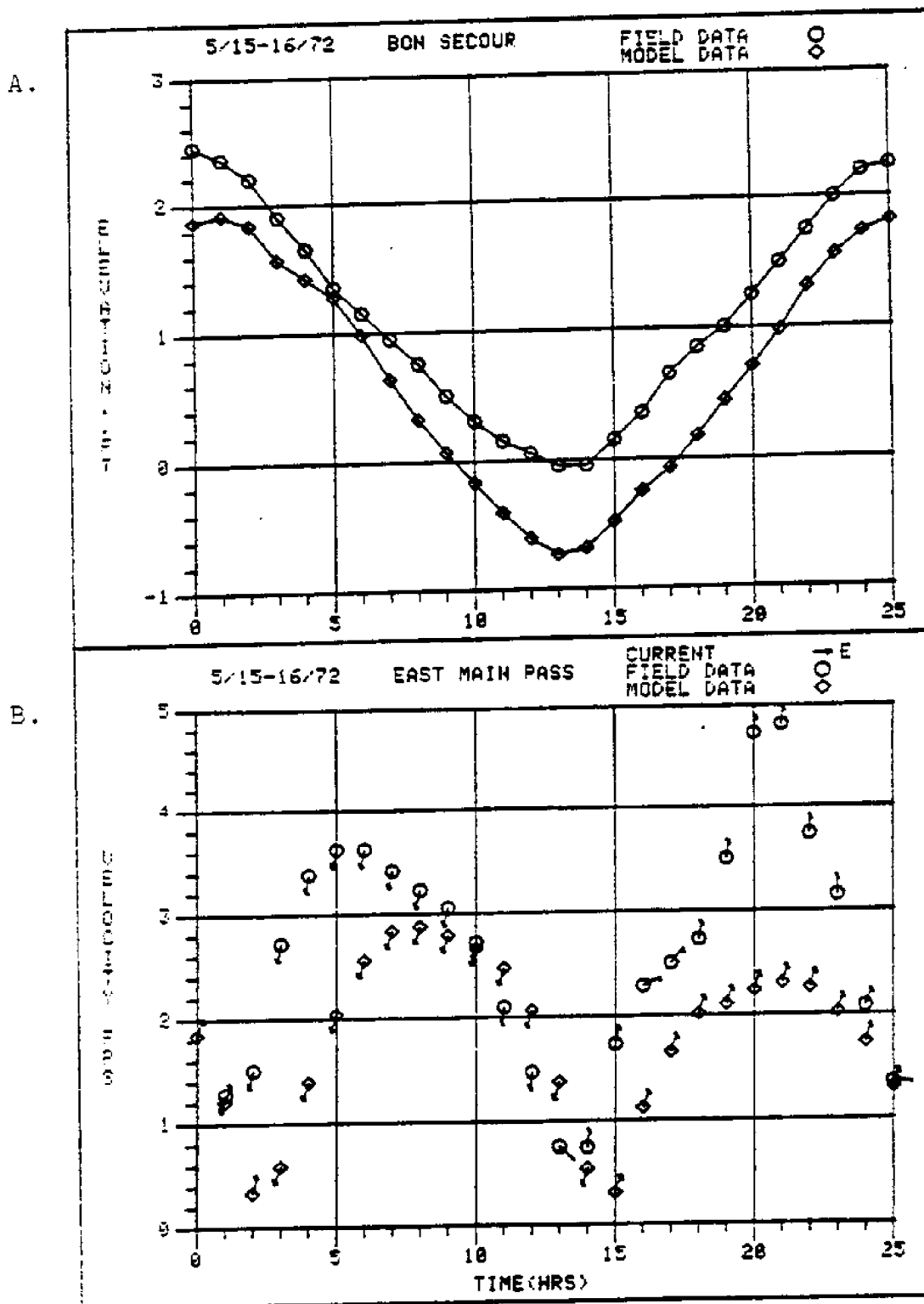
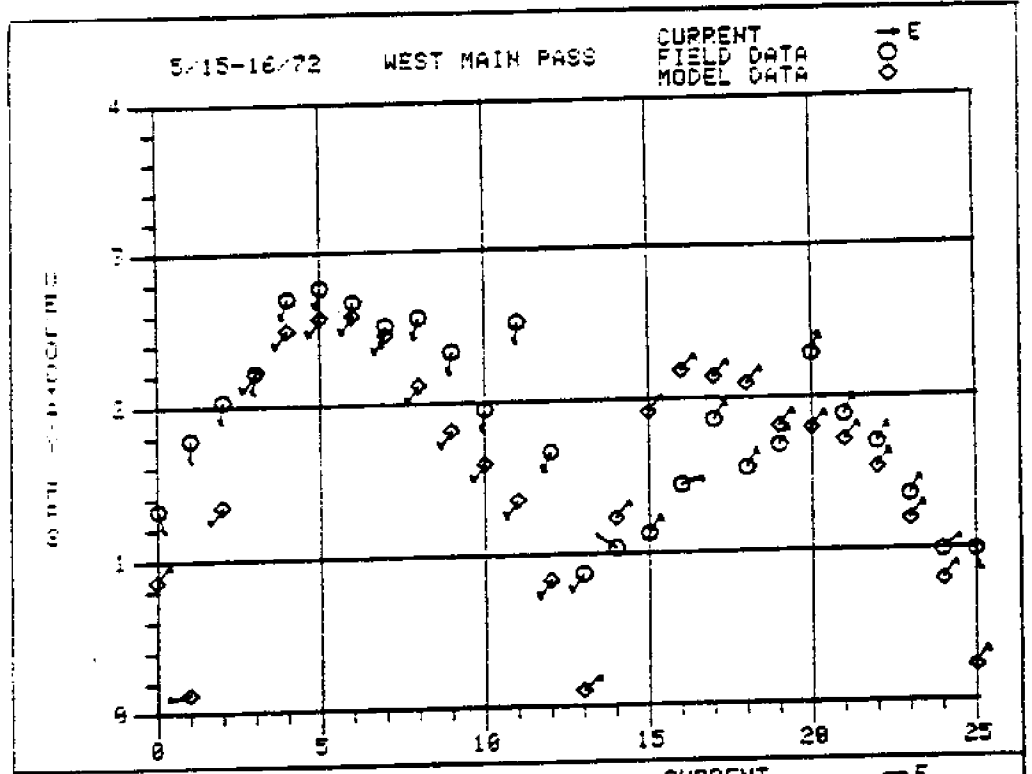


Figure 31. Comparison of Astronomical-tide Model Results with 1972 Data.

A. Bon Secour Tide Gage

B. East Main Pass Velocity Station

A.



B.

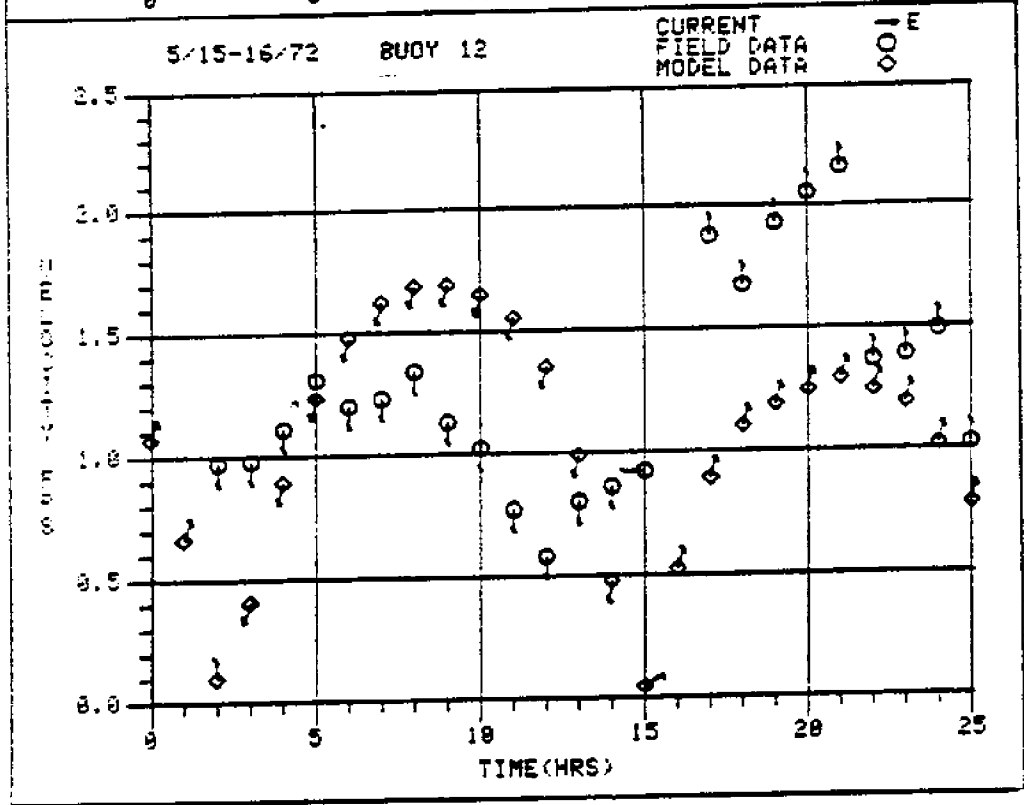


Figure 32. Comparison of Astronomical-tide Model Results with 1972 Data.  
 A. West Main Pass Velocity Station  
 B. Buoy 12 Velocity Station

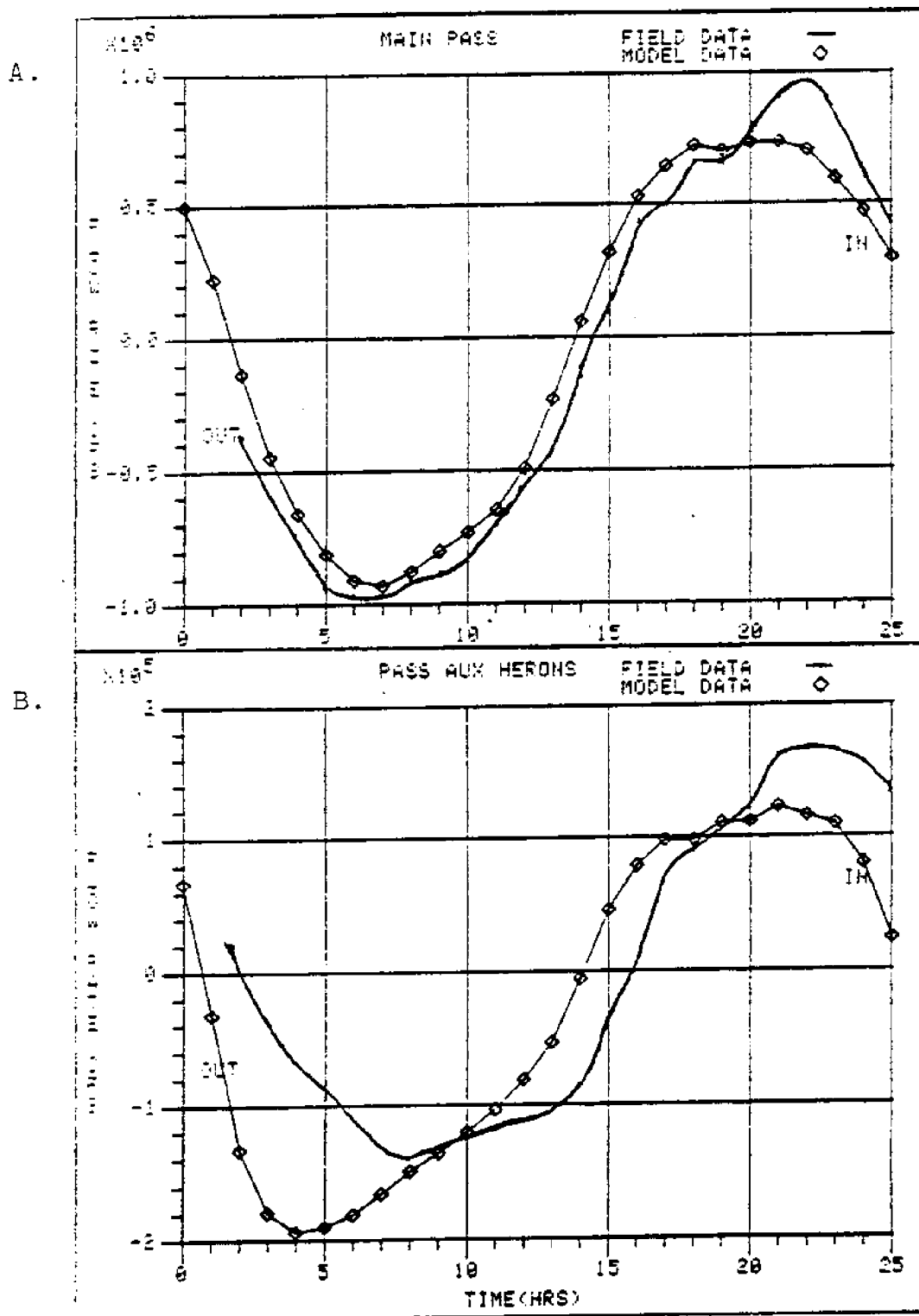


Figure 33. Comparison of Astronomical-tide Model Results with 1972 Data.

- A. Main Pass Flow Rate
- B. Pass aux Herons Flow Rate

difference in tidal height and range between the astronomical tide and tide records caused this discrepancy.

Velocity magnitude  
and direction

The velocity stations at Buoy 12 and West Main Pass showed improvement in terms of both magnitude and direction over the previous model run. At West Main Pass, the reproduction of the time of the tide change (hrs 13-15) was better. Similar improvement was noted for Buoy 12 at hrs 14-16. The East Main Pass station did not improve for this run. The trends of the velocities were reproduced within the uncertainty caused by the stratification of the deep water (see above).

Pass flow rates

Significant improvement in the magnitude and phase of the flow-rate curves produced by the model was noted for both Main Pass and Pass aux Herons. While the actual flow-rate curve at Pass aux Herons was not well reproduced, the trend of the incoming and outgoing flow rates was much better.

Results of model run using  
Dauphin Island Gulf gage  
from May 15 and 16, 1972  
delayed 2 hrs

The comparison of model results with the field data is shown in Figures 34-39.

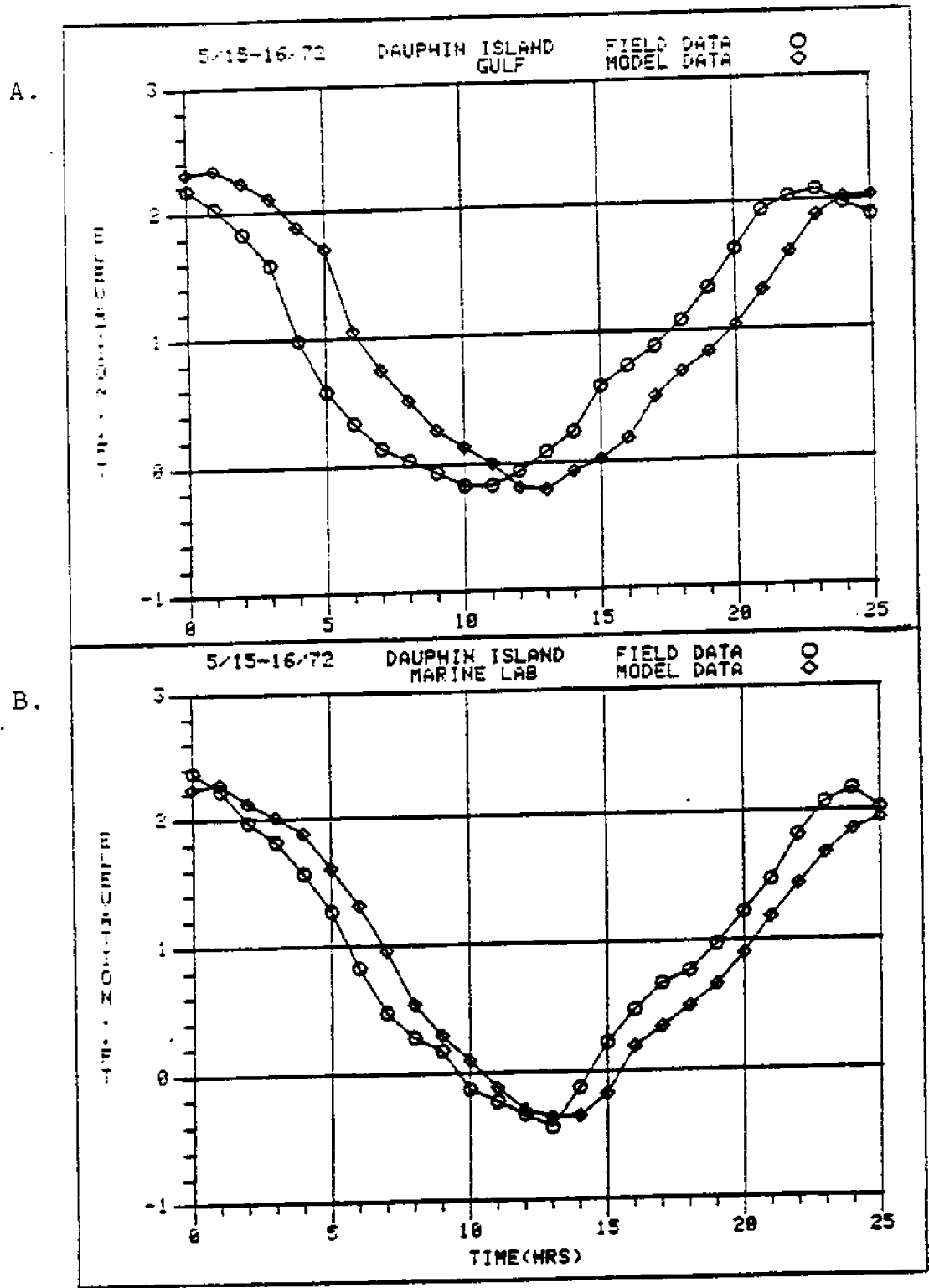


Figure 34. Comparison of Dauphin Island Gulf Record Delayed 2 hrs with 1972 Data.  
 A. Dauphin Island Gulf Tide Gage  
 B. Dauphin Island Marine Lab Tide Gage

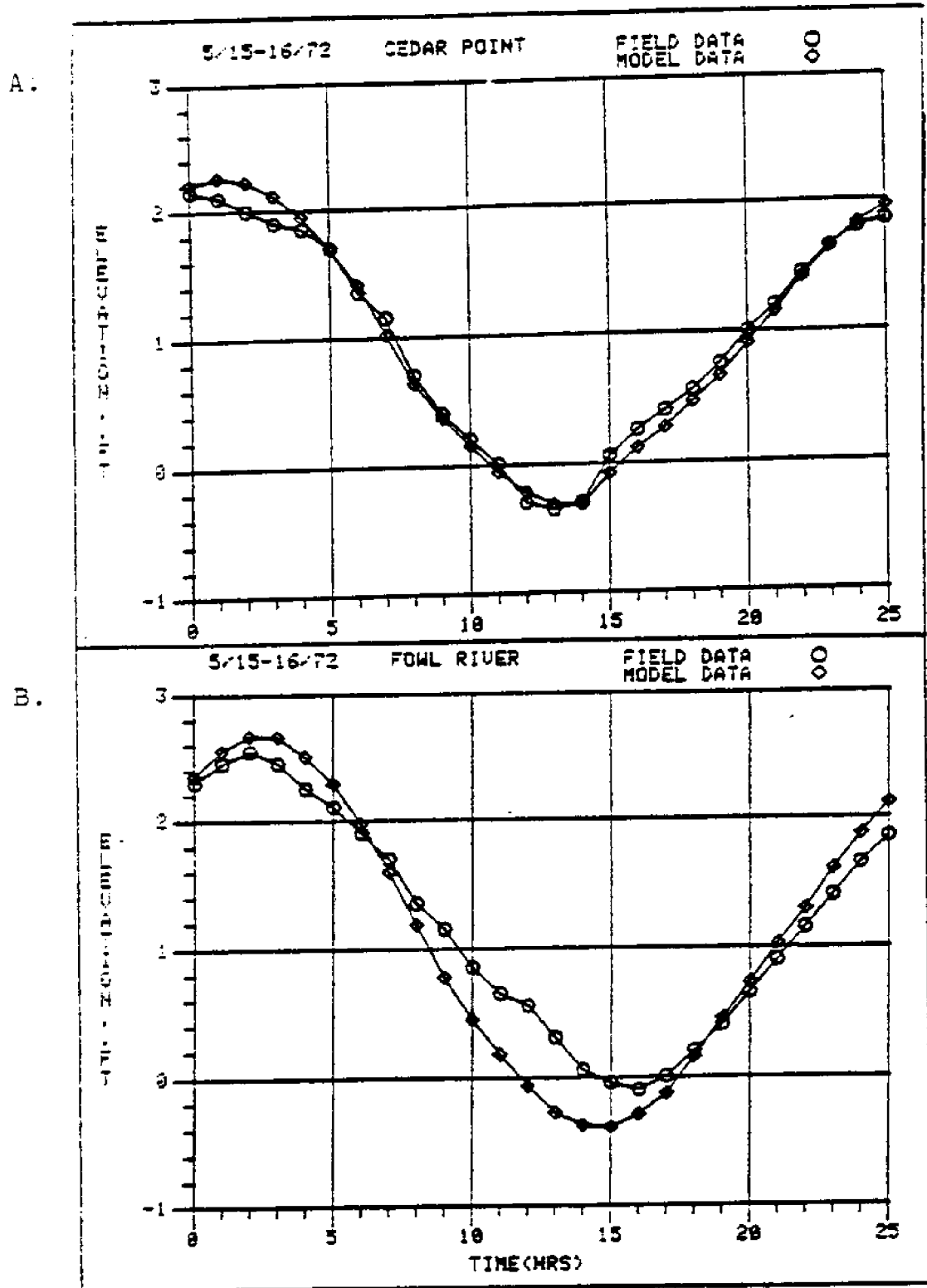


Figure 35. Comparison of Dauphin Island Gulf Record Delayed 2 hrs with 1972 Data.  
 A. Cedar Point Tide Gage  
 B. Fowl River Tide Gage

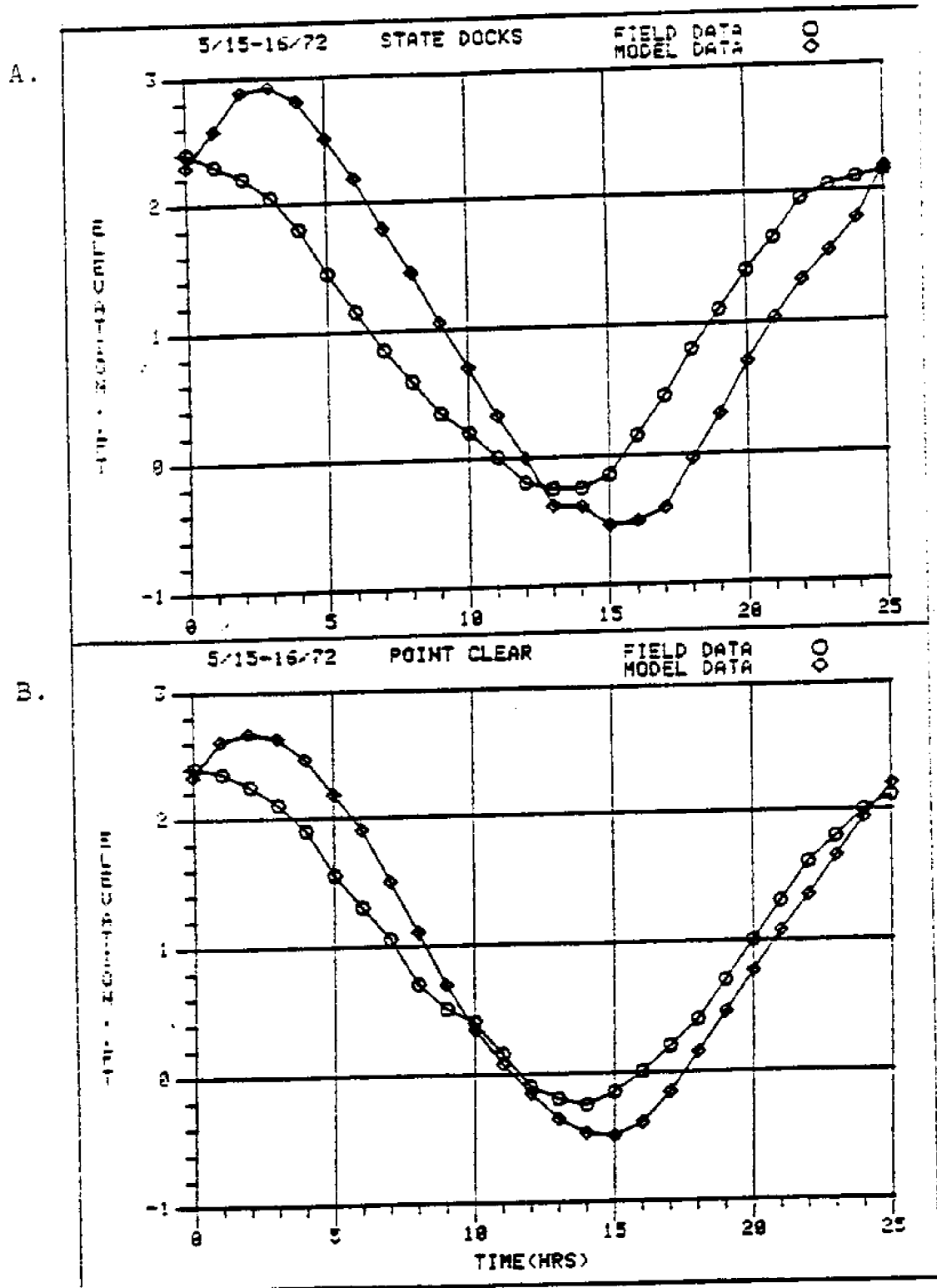


Figure 36. Comparison of Dauphin Island Gulf Record Delayed 2 hrs with 1972 Data.  
 A. State Docks Tide Gage  
 B. Point Clear Tide Gage

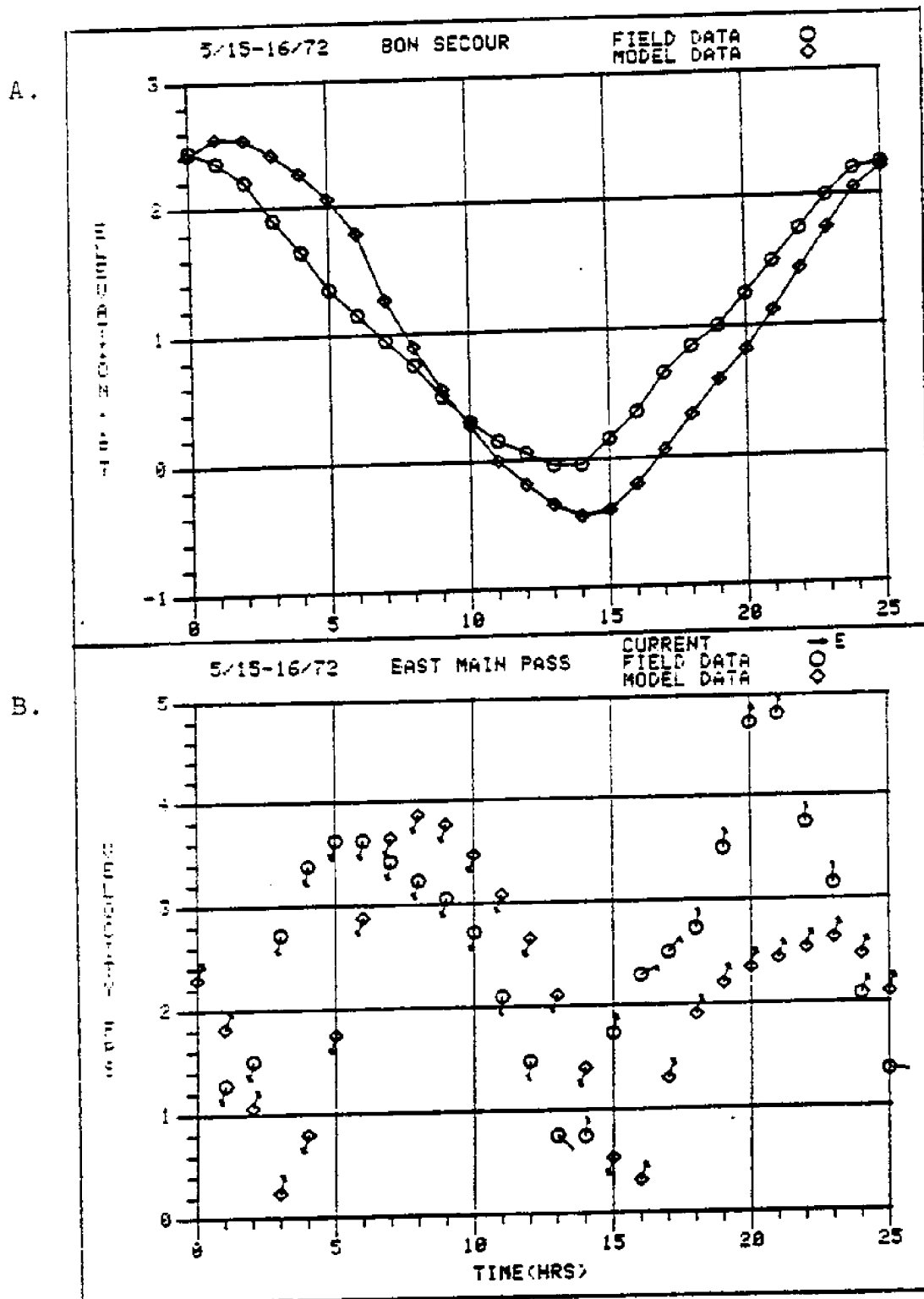


Figure 37. Comparison of Dauphin Island Gulf Record Delayed 2 hrs with 1972 Data.  
 A. Bon Secour Tide Gage  
 B. East Main Pass Velocity Station

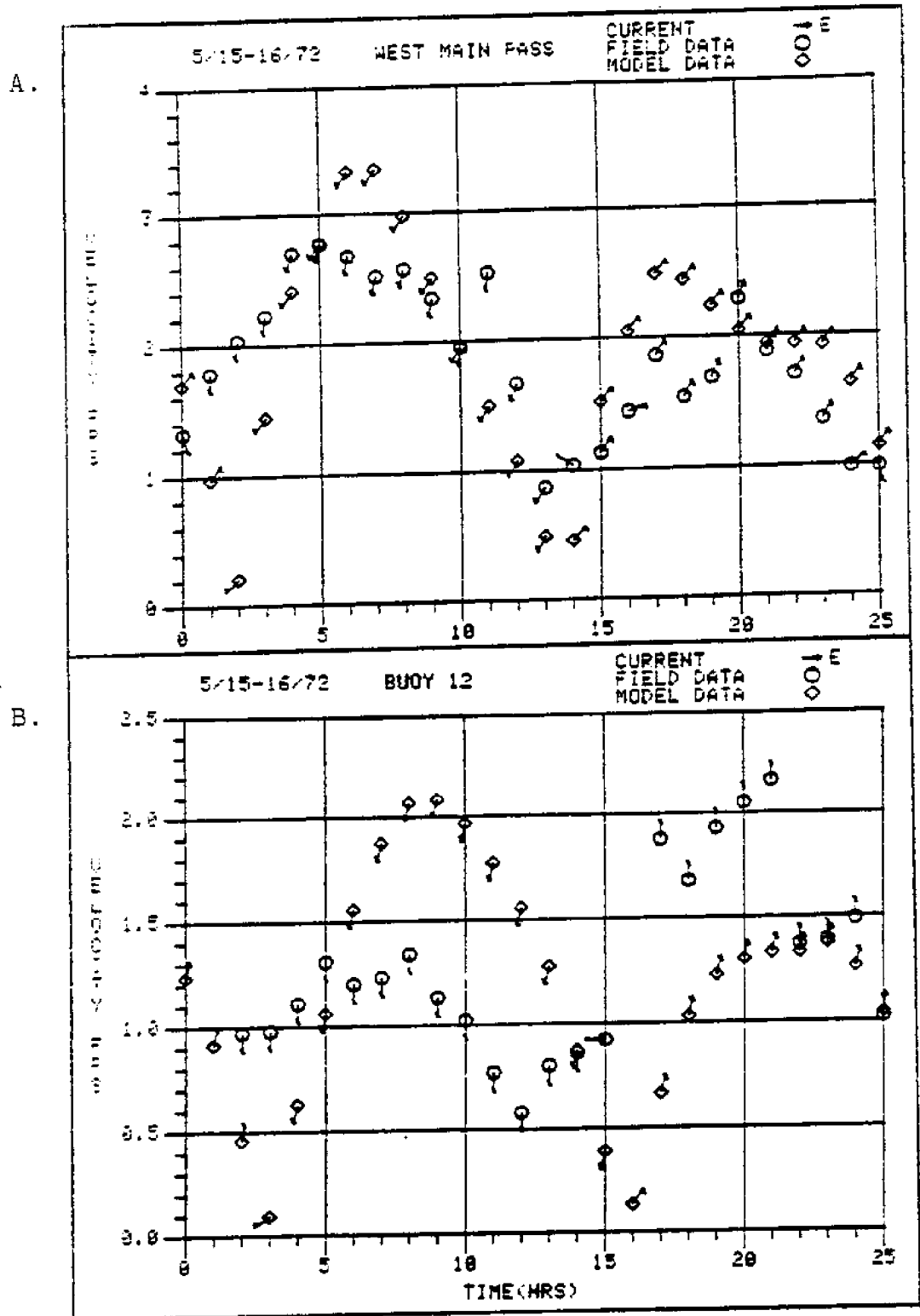


Figure 38. Comparison of Dauphin Island Gulf Record Delayed 2 hrs with 1972 Data.  
A. West Main Pass Velocity Station  
B. Buoy 12 Velocity Station

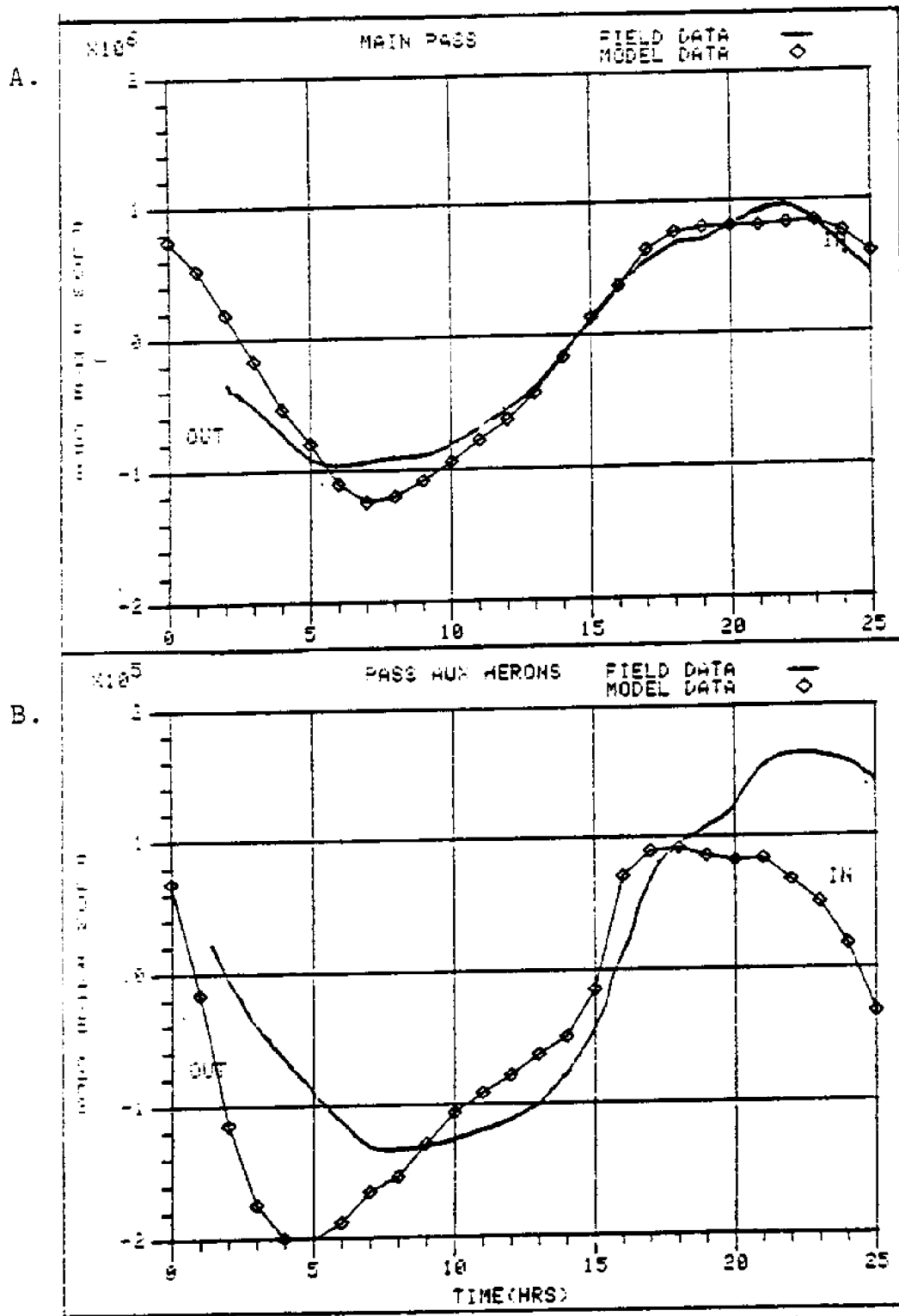


Figure 39. Comparison of Dauphin Island Gulf Record  
 Delayed 2 hrs with 1972 Data.  
 A. Main Pass Flow Rate  
 B. Pass aux Herons Flow Rate

### Tide elevation

The tide elevations calculated by the model for Dauphin Island Marine Lab and Cedar Point reproduced the field data well in this run. The Point Clear and Fowl River gages showed improvement over the first model run, the results of which were discussed previously. The remaining tide gages showed a shift in phase corresponding to the 2 hr phase shift of the Dauphin Island Gulf tidal boundary condition.

### Velocity magnitude and direction

All the velocity stations showed a shift in the time of the change in current direction effected by the tide change. Though no real improvement relative to the first model run was realized, the trends of the velocity magnitudes and directions were close to that of the field data.

### Pass flow rates

The Main Pass flow-rate curve for this run represented the best correlation between model results and field data. The Pass aux Herons flow-rate curve again showed an improvement in the pattern of the outgoing and incoming flows, but did not reproduce the magnitude of the curve well.

Conclusion of  
calibration/verification study

Good comparisons between the model results and field data were obtained from the case study of the 1973 data. This occurred in spite of the fact that no field data were available for the specification of the Gulf of Mexico boundary condition. The predicted tides for Dauphin Island (Fort Gaines) and Bayou La Batre, Alabama were used as boundary conditions instead.

Difficulty was encountered in reproducing the field data in the 1972 case study, especially with regard to pass flow rates. The positive results from the 1973 case study and the difficulty of other researchers (10,26) in modeling the 1972 data motivated the re-evaluation of the 1972 data. Comparison of the predicted tide at Dauphin Island (Fort Gaines) and Bayou La Batre with the tide records at Dauphin Island Gulf and Cedar Point showed a significant difference in the relative phases of these tides. Model runs using the astronomical tide and the Dauphin Island Gulf gage with a 2 hr delay were made. These runs showed improved results in terms of pass flow rates and velocity correlations. The improvement suggested that the tide gages were either incorrect or influenced by strong, variable winds. Lack of suitable wind data prevented the investigation of the wind effect.

Before the model can be evaluated on a quantitative basis, improved field-data studies are essential. The field data should include accurate tide records for the specification of boundary conditions. The data should be collected at low wind conditions if possible. In the event of windy conditions, accurate wind records for each tide or velocity station should be kept to provide the input for a variable wind field to the model.

On the basis of the above study, it was concluded that the present version of the WIFM II model could be successfully used to elucidate the relative trend effects, but not the quantitative effects of changing inputs to Mobile Bay-East Mississippi Sound. These inputs include river flow, wind, and tide range. The exceptionally good results obtained in the Pass aux Herons area for the 1973 data supported the use of this model to study the trends of the water transport in the area.

## CHAPTER V

### PARAMETRIC STUDY

#### Tide Range, River Flow, and Wind

The model was exercised 6 times to investigate the effects of tide range, river flow, and wind on the flows in the passes, Table 1. The tide ranges were chosen from the Tide Tables (31) predictions for 1973. Plots of the tide elevations used as boundary conditions are shown in Figure 40. Low, intermediate, and high tide ranges were chosen. The tide elevations were plotted so that the times of the high and low tides for each tide range would nearly coincide to facilitate evaluation of the results. The river flows were chosen to correspond to the 90 percentile, average, and 10 percentile (low, medium, and high, respectively) river flows as reported by Schroeder (15). The wind condition was chosen to correspond to the average wind direction as reported by Hill (11). The initial run was made using the medium tide range and river flow with no wind. All subsequent runs were compared to the initial run.

#### Effects on Flows through Passes

The total incoming and outgoing flows through Pass aux Herons and Main Pass for each model run are shown in

Table 1. Tide Range, River Flow, and Wind for Each Model Run.

	Run 1	Run 2	Run 3	Run 4	Run 5	Run 6
River Flow Rate (cfs)	61,790	13,070	150,070	61,790	61,790	61,790
Tide Range (ft) at Dauphin Island . . .	1.7	1.7	1.7	0.5	2.5	1.7
Tide Range (ft) at Bayou La Batre . . .	2.0	2.0	2.0	0.7	2.7	2.0
Wind Speed (k) . . .	0	0	0	0	0	15
Wind Direction* . . .	-	-	-	-	-	225°

\* Direction is that from which wind blows.

- A. Low Tide Range
- B. Medium Tide Range
- C. High Tide Range

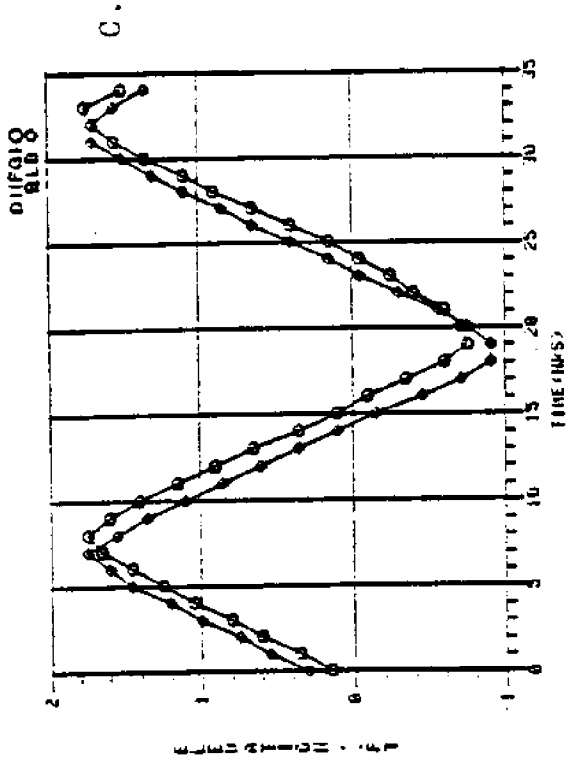
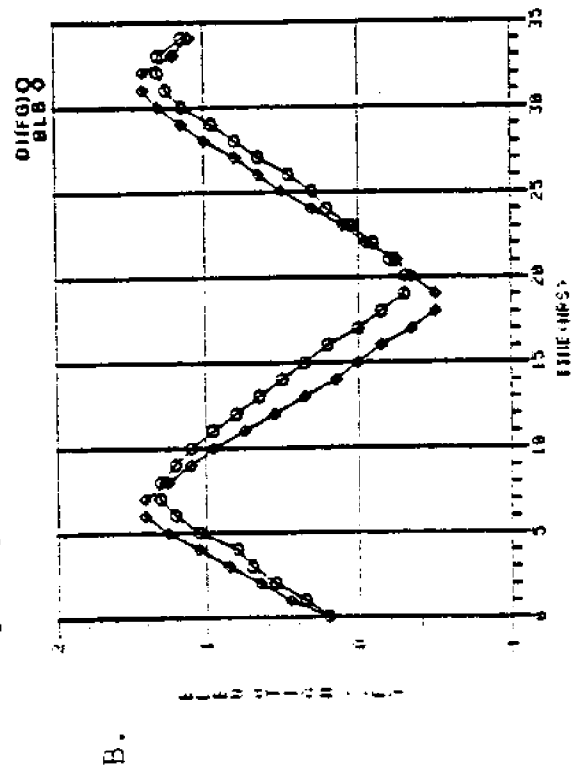
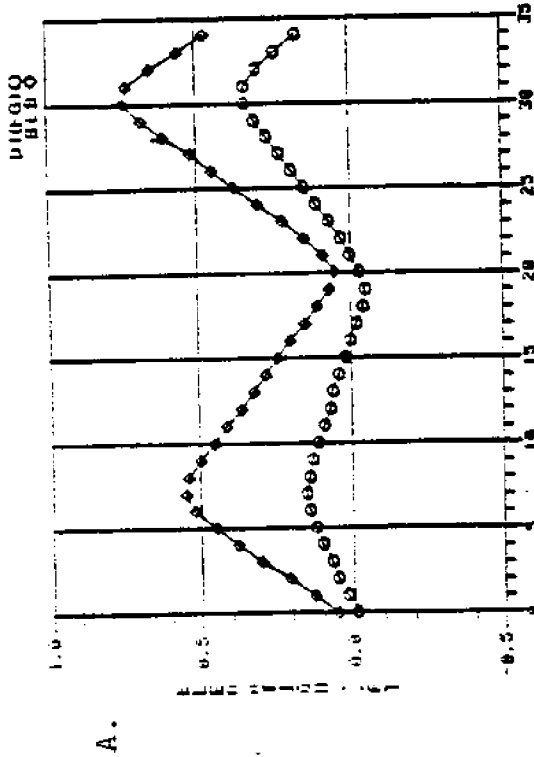


Figure 40. Tide Elevations Used as Boundary Conditions for Parametric Studies.

Table 2. The model calculated the total flows from a material balance involving the area under the flow-rate curves, Figures 41-43, for hrs 8-33.

Comparison of runs 2 and 3 with run 1 showed the effect of river flow in determining the amount of water which passed into and out of the Bay over a tidal period. At low river flow, run 2, more water flowed into the Bay on flood tide than for the medium river flow, run 1. Less water flowed out of the Bay. The reverse effect was obtained for the high river flow, run 3. The high river flow was a 143% change from the medium river flow while the low river flow was a 79% change. The greater effect of the high river flow on the passes was attributed to this fact.

Runs 4 and 5 illustrated the large effect of tide range on the model results. In run 4 it was noted that the tide flowed into the Bay through Pass aux Herons over the entire run. In Figure 40A it was observed that the tide elevation at Bayou La Batre was higher than for Dauphin Island at all times. The elevation difference caused the water to flow from East Mississippi Sound to Mobile Bay. In the Alabama Gulf Coast area, an approximately monthly interval of nearly constant tide elevation, lasting up to 48 hrs, was noted (31). The tide range for run 4 was at the end of one of these intervals, as the tide was returning to the generally observed diurnal period. No field data were found to compare with these results.

Table 2. Total Incoming and Outgoing Pass Flows for Each Model Run.

	MP ft <sup>3</sup> x 10 <sup>9</sup>	PaH ft <sup>3</sup> x 10 <sup>9</sup>	MP* Percentage	PaH Percentage	MP** Percentage Change from Run 1	PaH Percentage Change from Run 1
<u>Run 1</u>						
Incoming	19.20	3.908	83.1%	16.9%	--	--
Outgoing	21.93	4.907	81.7%	18.3%	--	--
<u>Run 2</u>						
Incoming	21.40	4.155	83.7%	16.3%	+11.5%	+ 5.9%
Outgoing	20.37	4.727	81.2%	18.8%	- 7.1%	- 3.8%
<u>Run 3</u>						
Incoming	15.09	3.457	81.4%	18.6%	-21.4%	-11.5%
Outgoing	24.90	5.251	82.6%	17.4%	+13.5%	+ 7.0%
<u>Run 4</u>						
Incoming	1.821	7.647	19.2%	80.8%	-90.5%	+95.7%
Outgoing	1.821	7.647	19.2%	80.8%	-90.5%	+95.7%
	12.05	0.000	100%	0.0%	-45.1%	--
<u>Run 5</u>						
Incoming	28.49	4.995	85.1%	14.9%	+48.5%	+27.8%
Outgoing	30.54	5.727	84.2%	15.8%	+39.3%	+16.7%
<u>Run 6</u>						
Incoming	17.25	6.365	73.0%	27.0%	-10.2%	+62.9%
Outgoing	24.13	2.719	89.9%	10.1%	+10.0%	-44.6%

$$\begin{aligned} * & \quad \frac{\text{MP Flow}}{\text{MP Flow} + \text{Pah Flow}} \times 100 \\ ** & \quad \frac{\text{MP Flow (Run 1)} - \text{MP Flow (Run X)}}{\text{MP Flow (Run 1)}} \times 100 \end{aligned}$$

X = 2 through 6

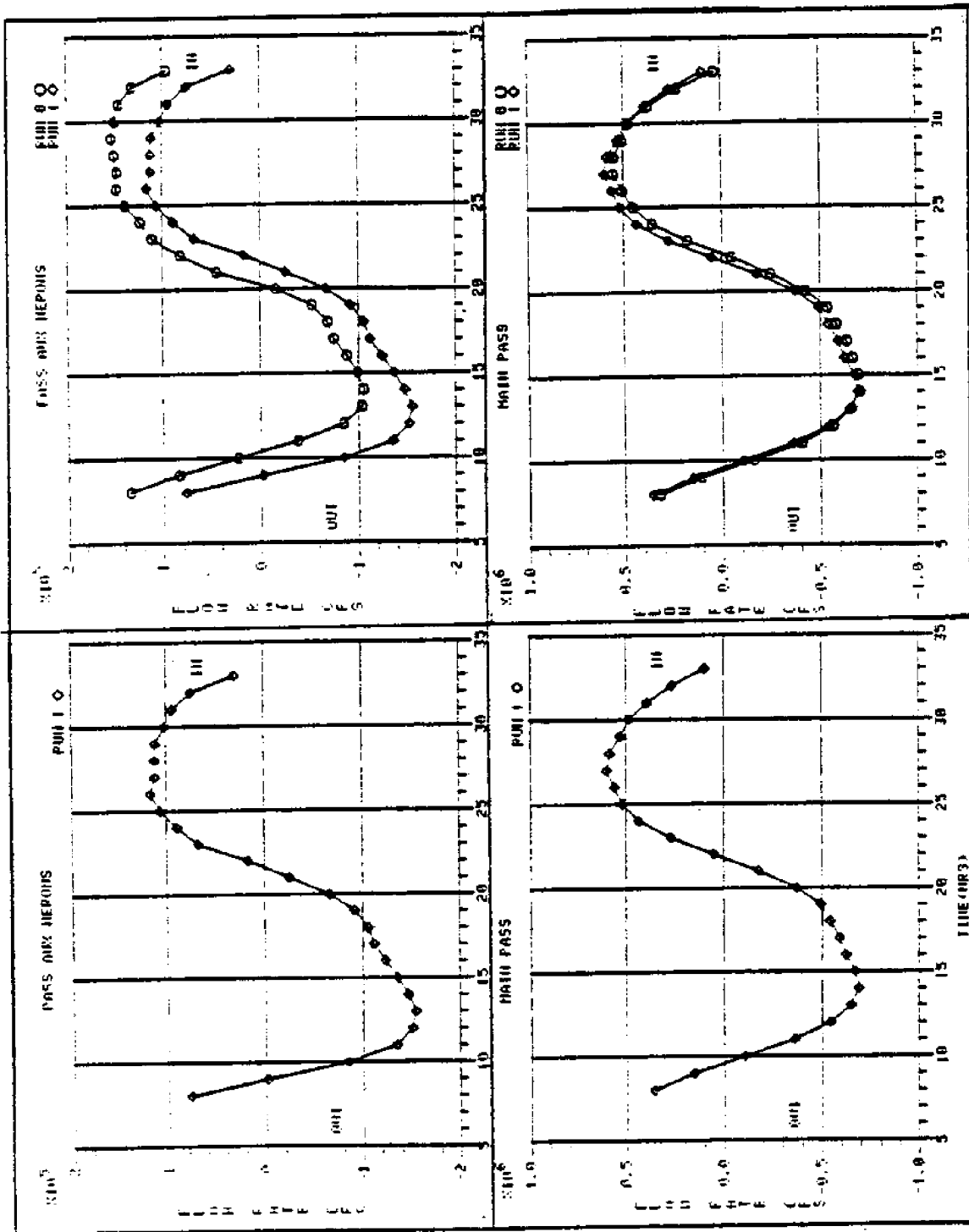


Figure 41. Comparison of Pass Flow Rates of Run 6 with Run 1.

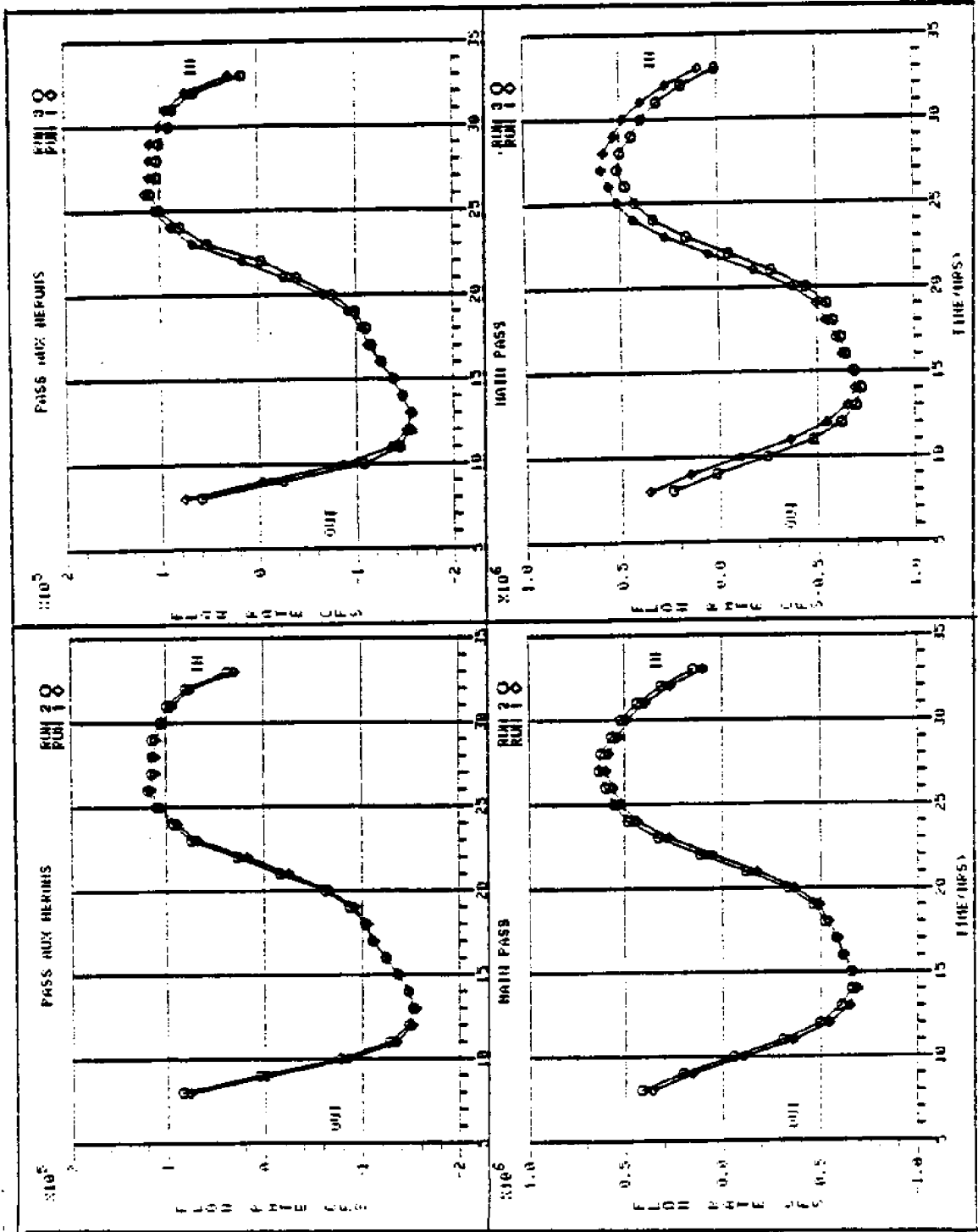


Figure 42. Comparison of Pass Flow Rates of Run 2 and Run 3 with Run 1.

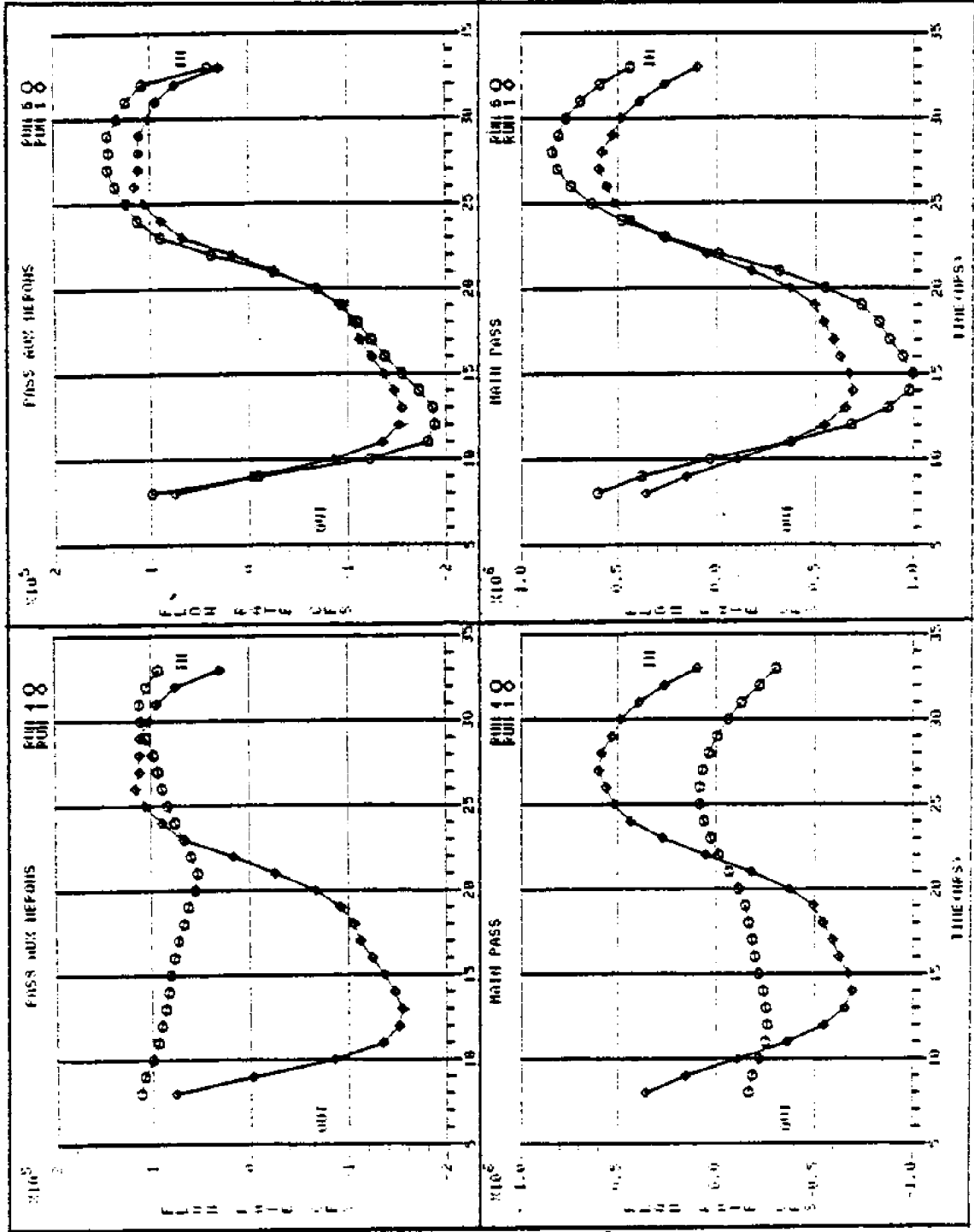


Figure 43. Comparison of Pass Flow Rates of Run 4 and Run 5 with Run 1.

The effect of a constant 15 k wind from the southwest ( $225^{\circ}$ ) was shown in run 6. The direction and speed were chosen to correspond to the average direction and intermediate wind speed as used by Hill (11). A marked shift in the flow-rate curve, Figure 41, for Pass aux Herons was noticed. The large influence of wind on the shallow water in the pass and in East Mississippi Sound caused the water to be pushed from East Mississippi Sound to Mobile Bay. The wind delayed the change from outgoing flow to incoming flow at hrs 21-23 for Main Pass. The delay reduced the incoming flow and increased the outgoing flow. More field data must be obtained to determine how well the model reproduces wind effects in the Mobile Bay-East Mississippi Sound area.

#### Effects on Current Velocities in the Passes

Figures 44-47 show vector plots for the entire Bay from run 1 at ebb, low, flood, and high tides. Comparing the time of the vector plot with Figure 41 shows the state of the tide at the corresponding time. The maximum current speed and the cell at which it occurred were given. The alternate flooding (hrs 14 and 34) and drying (hrs 22 and 28) of the Mobile River delta is shown in Figures 44-47. The high velocities at some of the inundated land cells in the upper Bay at hr 14 were caused by the small water elevations at these flood cells. The depth-averaged model

VELOCITY FIELD AT T(HR) = 14.00    TIME STEP (SEC) = 180.0  
MAX (FPS) = 7.05    CELL(H,M) = 25, 8    SCALE = .250  
BASIC GRID SIZE (FT) -- DN X DM -- 1666.70    X 1666.70

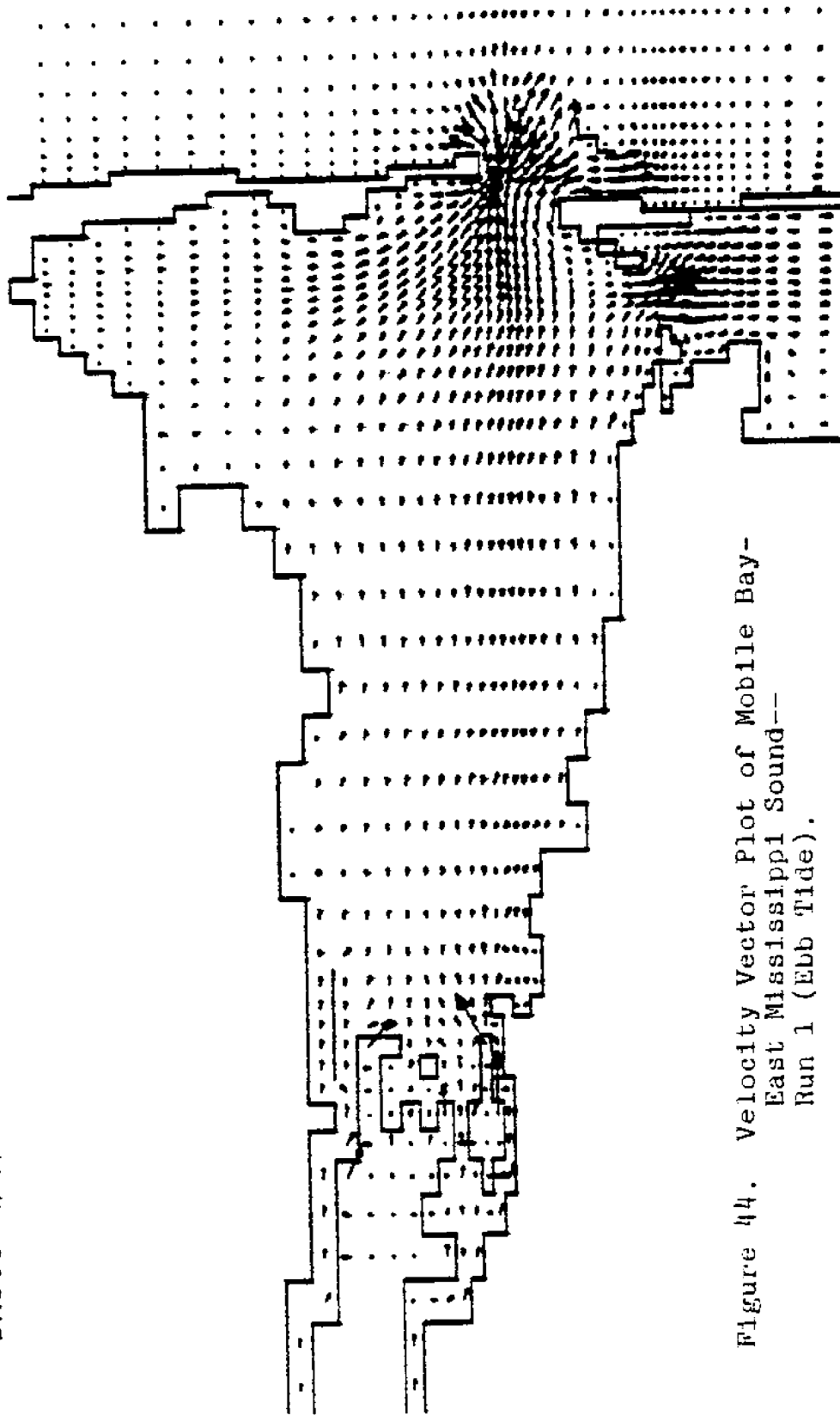


Figure 44. Velocity Vector Plot of Mobile Bay--  
East Mississippi Sound--  
Run 1 (Ebb Tide).

VELOCITY FIELD AT T(HR) = 22.00    TIME STEP (SEC) = 180.0  
MAX (FPS) = 1.76    CELL(N,M) = 22, 44    SCALE = .250  
BASIC GRID SIZE (FT) -- DN X DM -- 1666.70 X 1666.70

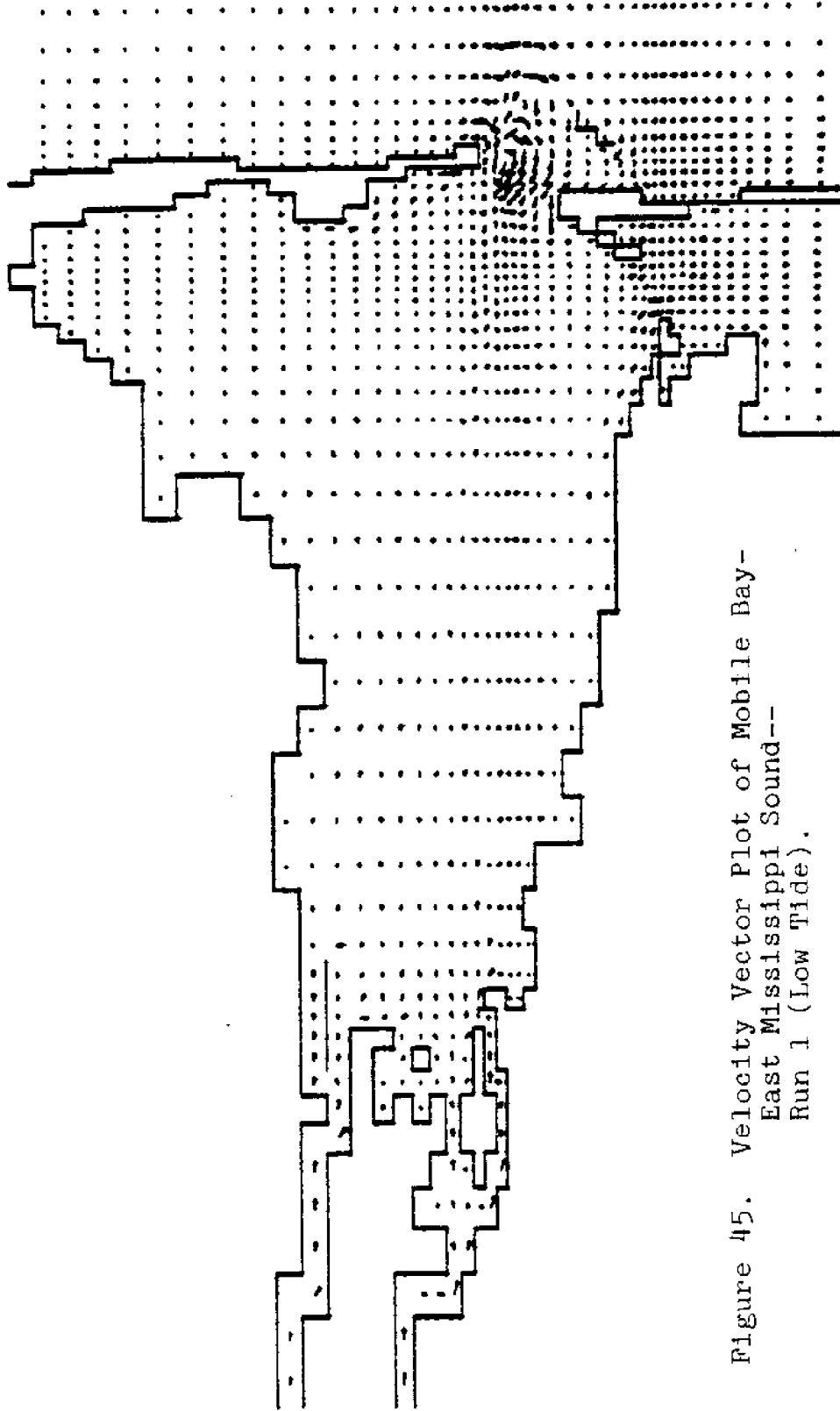


Figure 45. Velocity Vector Plot of Mobile Bay--  
East Mississippi Sound--  
Run 1 (Low Tide).

VELOCITY FIELD AT T(HR) = 29.00 TIME STEP (SEC) = 180.0  
MAX (FPS) = 3.88 CELL(H,M) = 23, 45 SCALE = .250  
BASIC GRID SIZE (FT) -- DN X DM -- 1666.70 X 1666.70

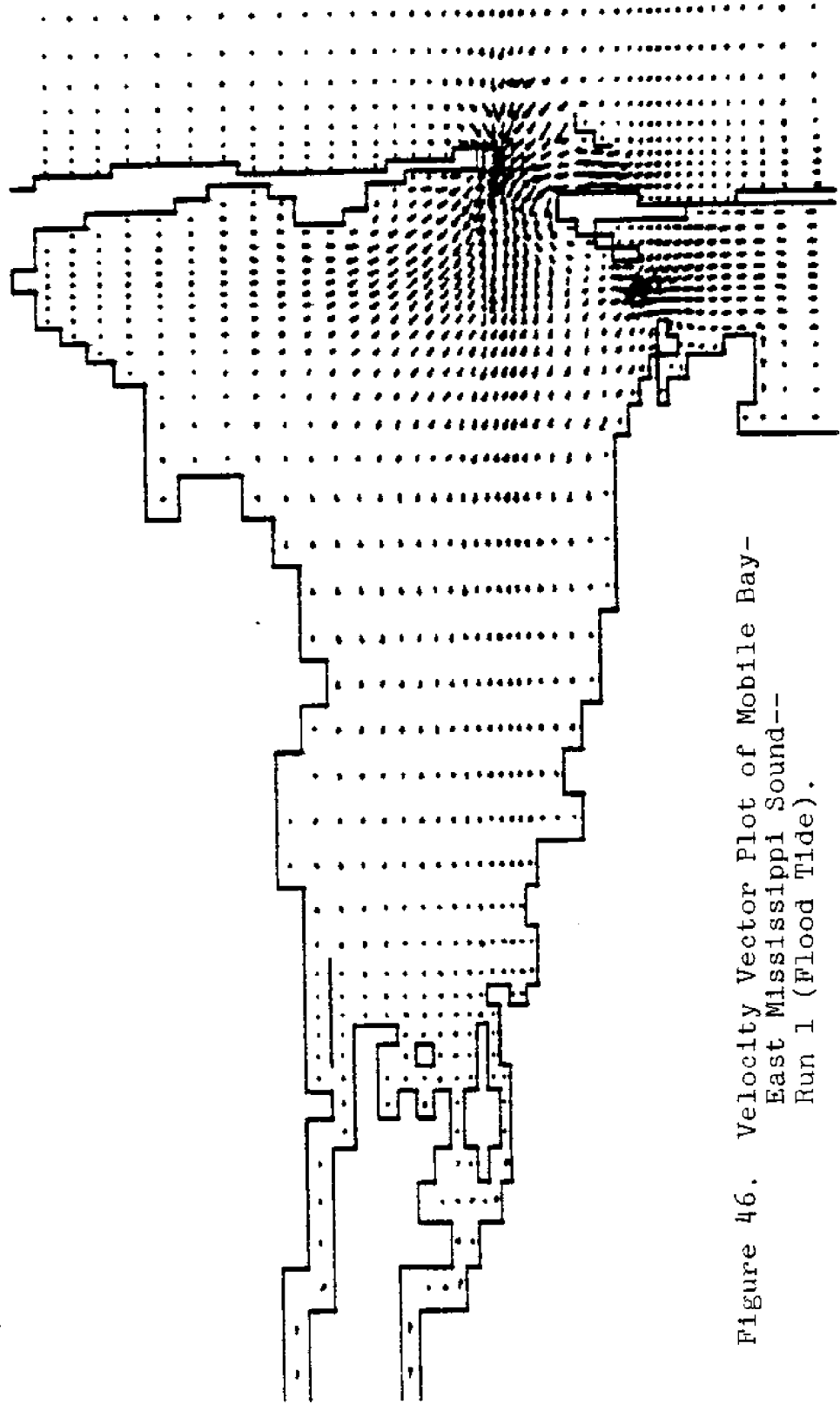


Figure 46. Velocity Vector Plot of Mobile Bay--  
East Mississippi Sound--  
Run 1 (Flood Tide).

VELOCITY FIELD AT T(HR) = 34.00    TIME STEP (SEC) = 180.0  
MAX (FPS) = 1.81    CELL(H,M) = 22, 45    SCALE = .250  
BASIC GRID SIZE (FT) -- DN X DM --    1666.70    X    1666.70

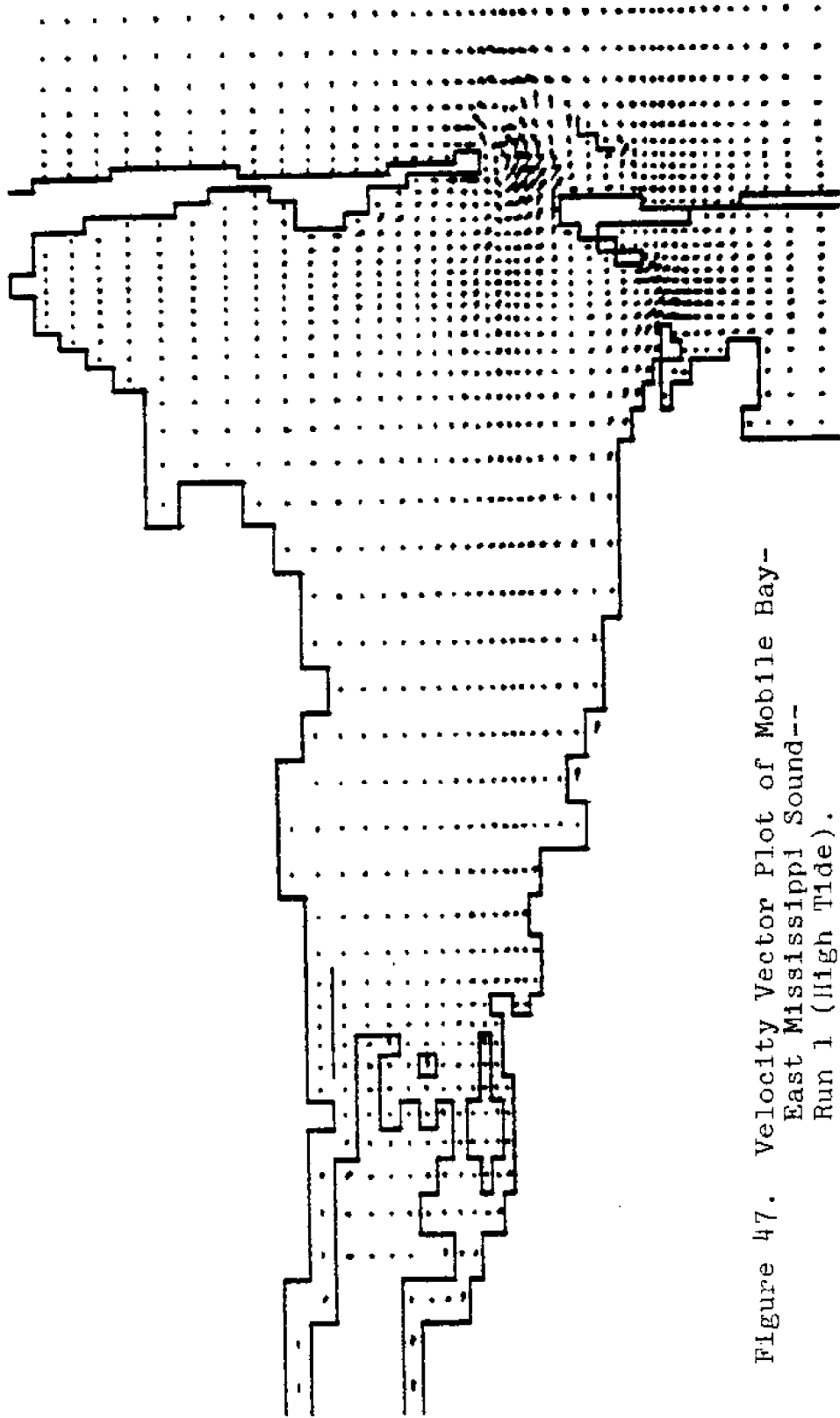


Figure 47. Velocity Vector Plot of Mobile Bay--  
East Mississippi Sound--  
Run 1 (High Tide).

solved the two-dimensional equations of change in terms of flow per unit width ( $\text{ft}^2/\text{sec}$ ). The velocities were obtained by dividing the flow per unit width by the water depth at each cell. As a flood cell began to dry, the water depth at the cell became very small. Division of the flow per unit width by this small water depth resulted in a high velocity for the cell.

In Figures 48-51 the velocity vector plots were compared to the flow-rate vector plots for both passes at corresponding times from run 1. From this comparison, it was observed that while the velocities in the two passes were comparable, significantly more flow occurred in the Main Pass. The greatest flows were noted in the deep waters of the Main Channel. It should be noted that the flow-rate plot for Pass aux Herons at hr 22 was scaled larger than the others by a factor of 4. Since the same relationship of velocity to flow rate held for each model run, only the velocity plots were included for runs 2-6. See Figures 52-61.

Little change relative to run 1 in the velocities for Pass aux Herons was noted for run 2 at ebb and flood tide (hrs 14 and 28, respectively) in Figures 52-53. Main Pass showed a 4.2% decrease in maximum velocity on ebb tide and a 5.4% increase on flood tide. The current directions did not change significantly. The low-tide and high-tide plots (hrs 22 and 34) showed decreased outflow and increased

inflow at both passes. These trends reflected the decreased momentum of the water from the upper Bay due to a smaller river flow.

The outgoing velocities for run 3 in Pass aux Herons (hr 14) were not affected by the increased river flow relative to run 1, Figures 54-55. However, the velocities at flood tide showed an 8.3% decrease from run 1 due to the action of the high river impeding the incoming tide. Main Pass showed an 8.5% increase and a 12.1% decrease in ebb and flood maximum velocities, respectively. At low tide, the high river flow caused the velocities in Pass aux Herons to still be predominantly outgoing in contrast to run 1. At high tide, cell [11,31] reflected flooding caused by the excess water from the river. The abnormally high velocity was caused by the small water elevation at this flood cell as explained above. The high-tide and low-tide plots of Main Pass followed the same trend of increased outflow from the Bay.

The effect of the low tide range and elevation difference between Bayou La Batre and Dauphin Island, Figure 40, was elucidated in Figures 56-57 for run 4. As noted in the total-flow calculations (Table 2), water continually flowed into Mobile Bay from East Mississippi Sound. Significantly decreased velocities in Main Pass for all plots were observed due to the small tide range of 0.5 ft which was used for the Gulf of Mexico boundary condition.

Large increases in ebb-tide and flood-tide velocities for run 5, Figures 58-59, were observed in both passes. The greatest increase in maximum velocity was found to be 46.9% for the flood tide (hr 28) in Main Pass. The velocities in Pass aux Herons at low tide were directed more strongly into Mobile Bay than for run 1 and showed a 64.6% increase in maximum velocity. The high-tide velocities in Pass aux Herons changed little, except for the occurrence of flooding at cell [11,31]. The velocities in West Main Pass at low and high tides were similar. A significant increase in velocities in East Main Pass was observed.

The 15 k southwest wind of run 6, Figures 60-61, caused large decreases in outgoing velocities and large increases in incoming velocities in Pass aux Herons as noted in the total flow calculations above. This effect was due to the momentum of the wind being transferred to the shallow water of Pass aux Herons. The prevailing direction of the current was opposed to the wind on ebb tide and concurrent with the wind on flood tide. The wind did not significantly alter the maximum velocities for ebb and flood tides. The direction of the current was affected to a greater degree. At flood tide, the velocities in West Main Pass were deflected eastward. At ebb tide, they were deflected in a southerly direction. In Pass aux Herons, the action of the wind pushing water into the Bay from the

Sound was again observed at both low and high tides. The strong effect of the wind on the relatively shallow water of West Main Pass was also noted. The wind had much less effect on the deeper East Main Pass.

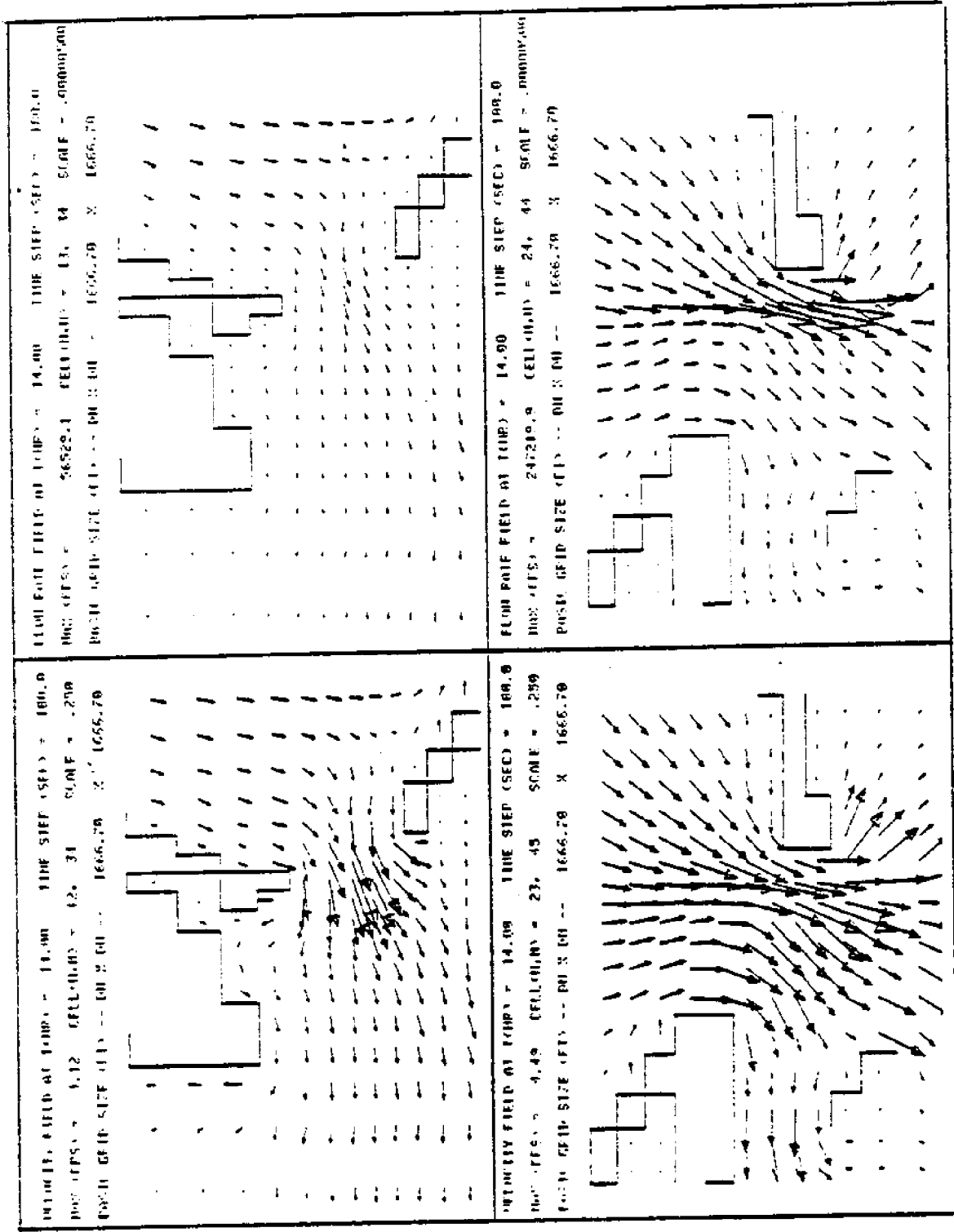


Figure 48. Velocity and Flow-rate Vector Plots--Run 1 (Ebb Tide).

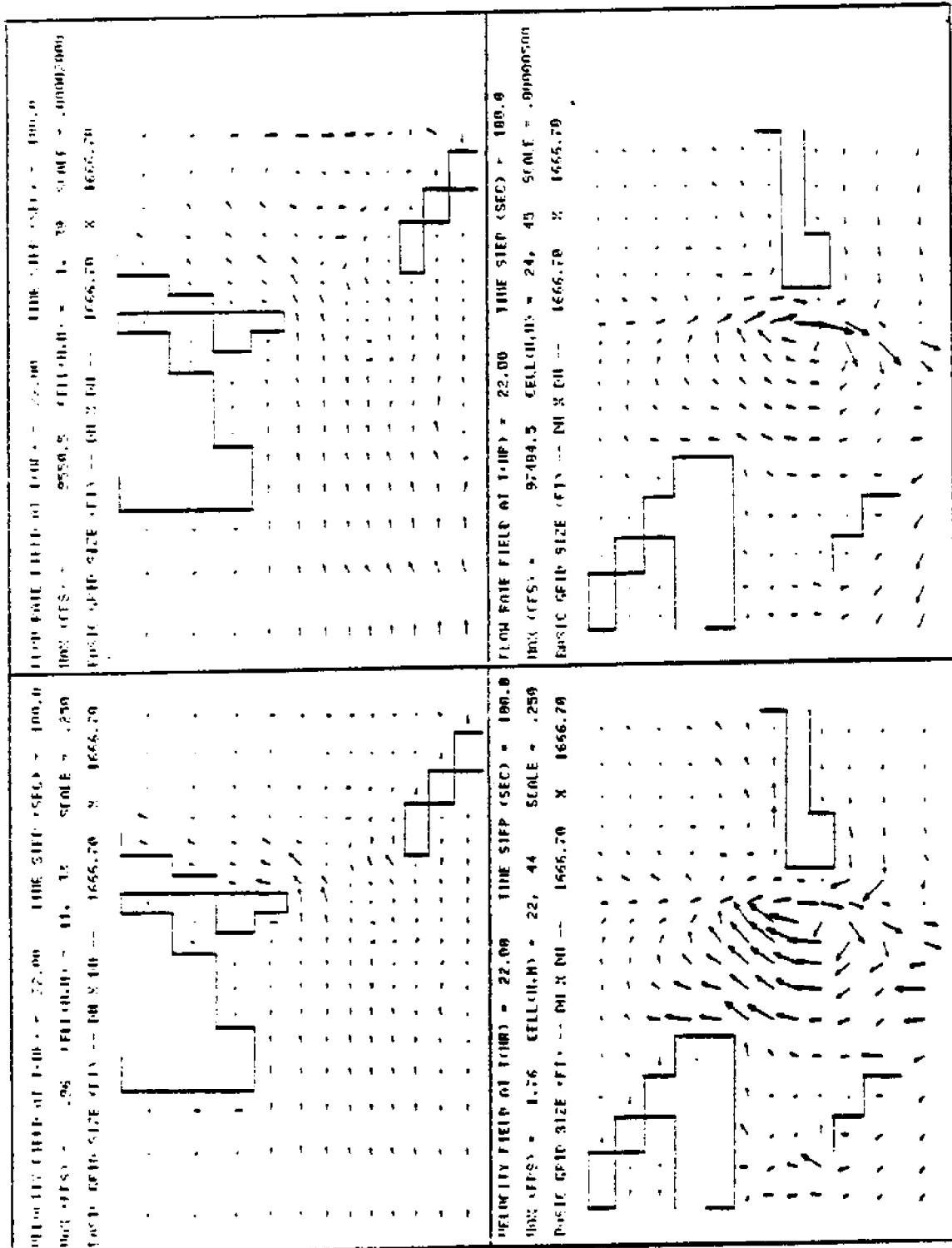


Figure 49. Velocity and Flow-rate Vector Plots--Run 1 (Low Tide).

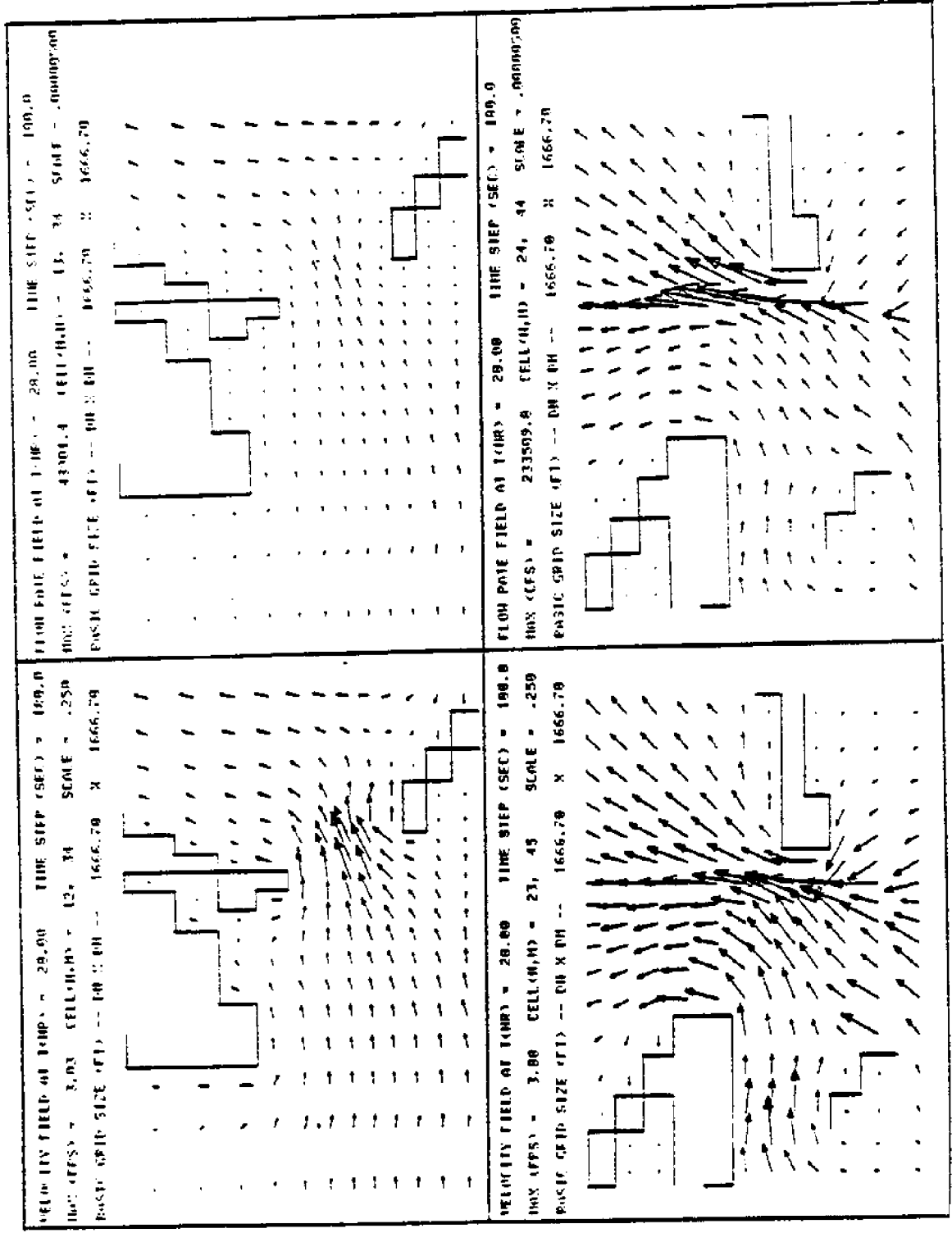


Figure 50. Velocity and Flow-rate Vector Plots--Run 1 (Flood Tide).

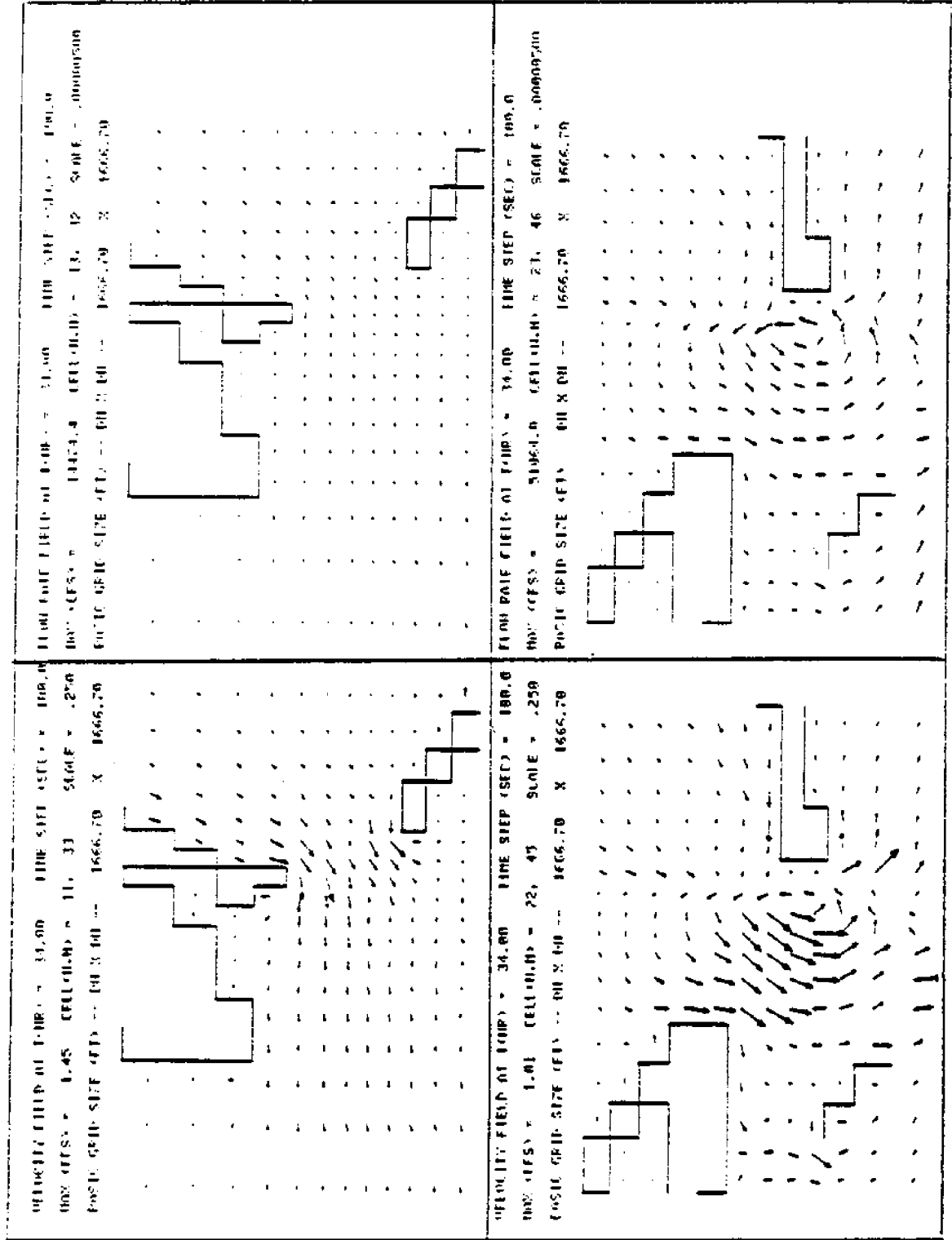
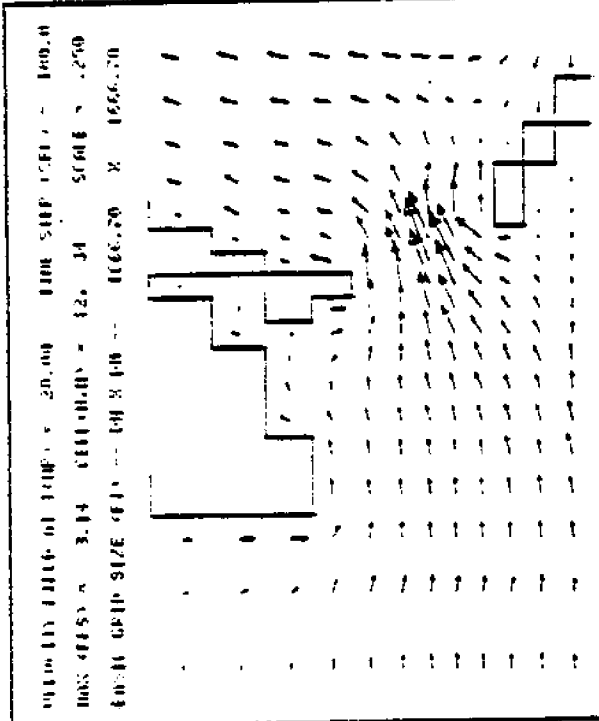


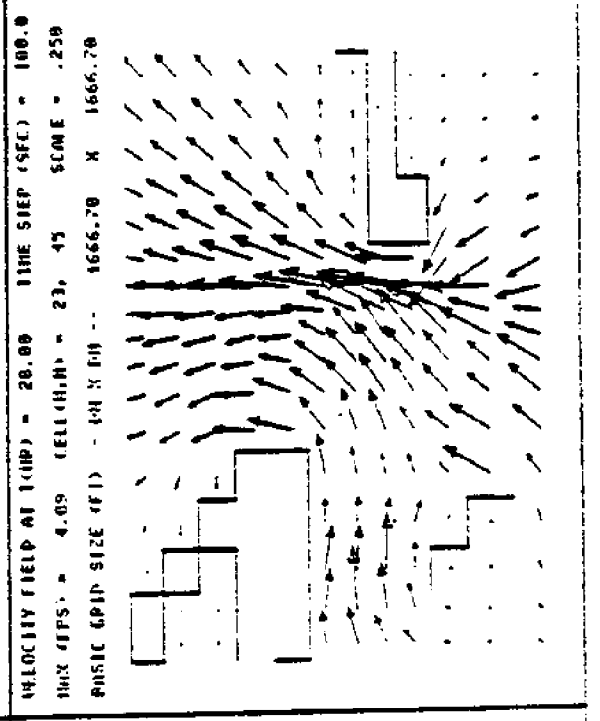
Figure 51. Velocity and Flow-rate Vector Plots--Run 1 (High Tide).

Figure 52. Velocity Vector Plots--Run 2  
(Medium Tide Range, Low River, No Wind)  
Ebb Tide--A. Pass aux Herons B. Main Pass  
Flood Tide--C. Pass aux Herons D. Main Pass

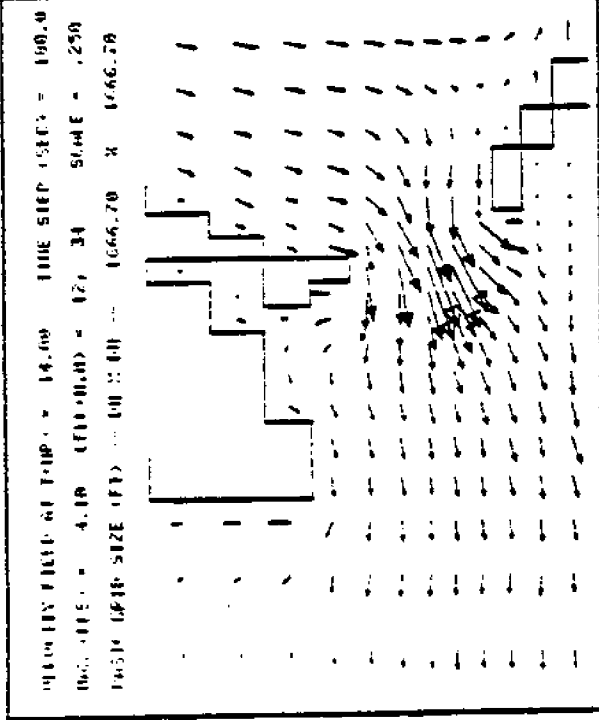
C.



D.



A.



B.

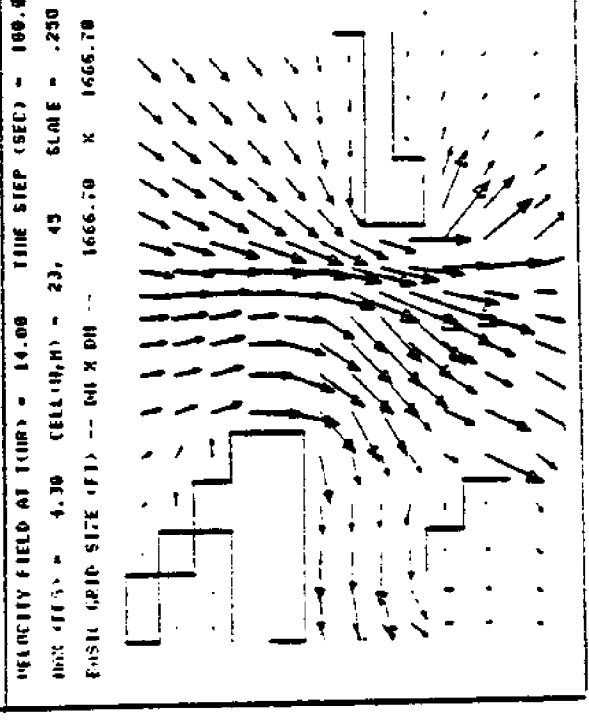
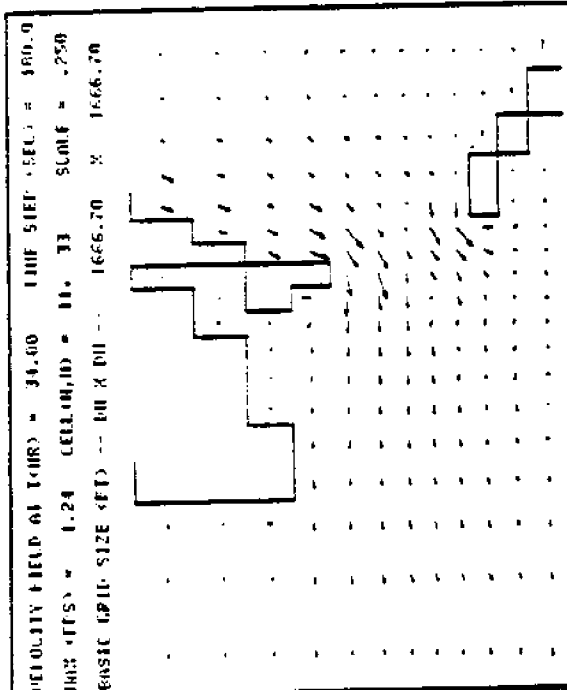
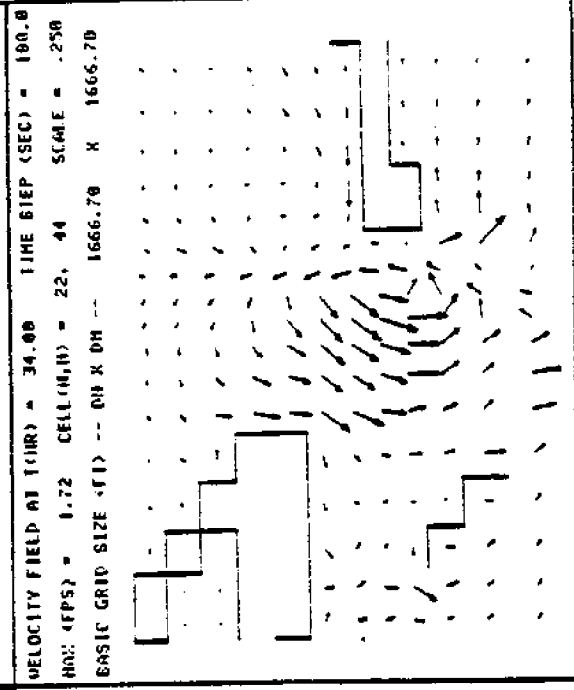


Figure 53. Velocity Vector Plots--Run 2  
(Medium Tide Range, Low River, No Wind)  
Low Tide--A. Pass aux Herons B. Main Pass  
High Tide--C. Pass aux Herons D. Main Pass

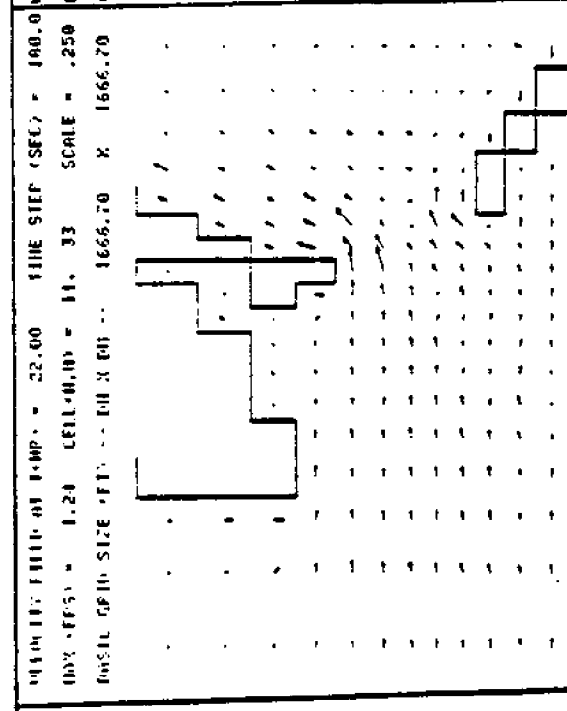
C.



D.



A.



B.

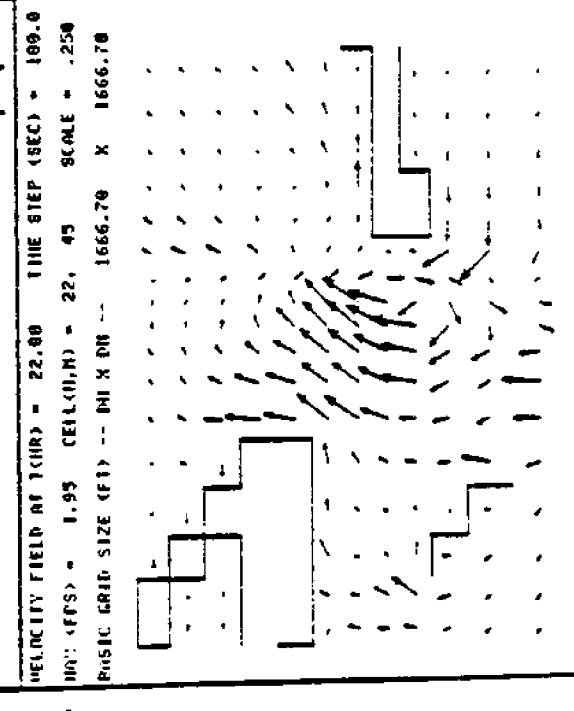
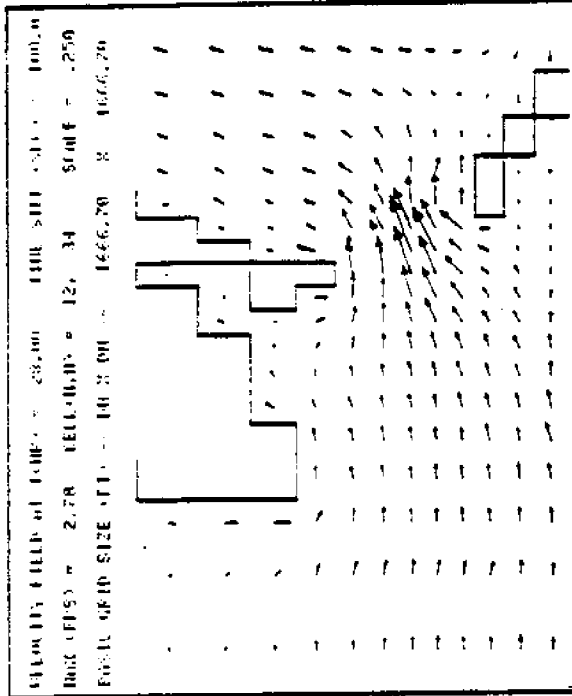
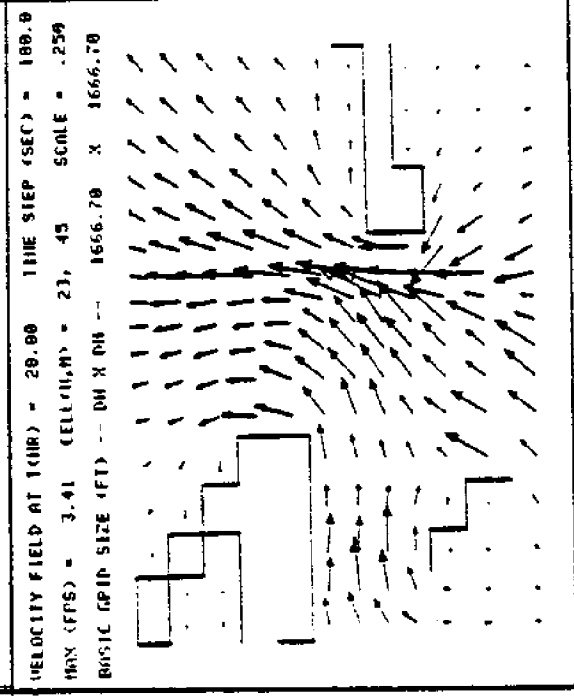


Figure 54. Velocity Vector Plots--Run 3  
(Medium Tide Range, High River, No Wind)  
Ebb Tide--A. Pass aux Herons B. Main Pass  
Flood Tide--C. Pass aux Herons D. Main Pass

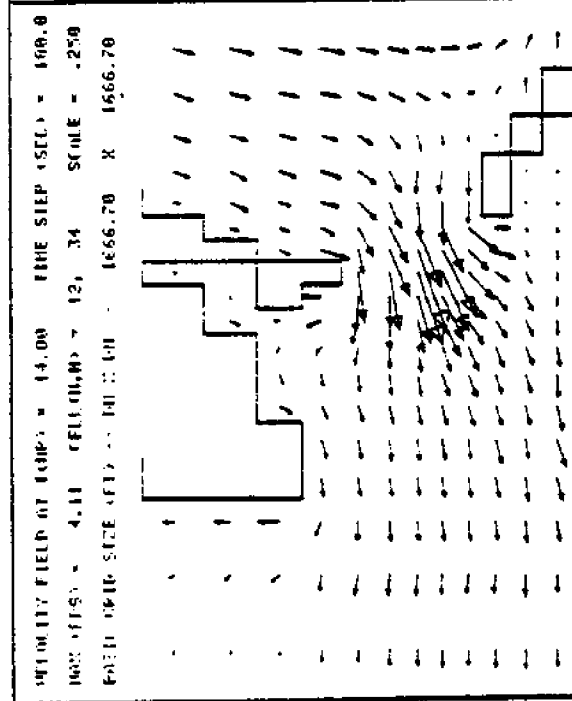
C.



D.



A.



B.

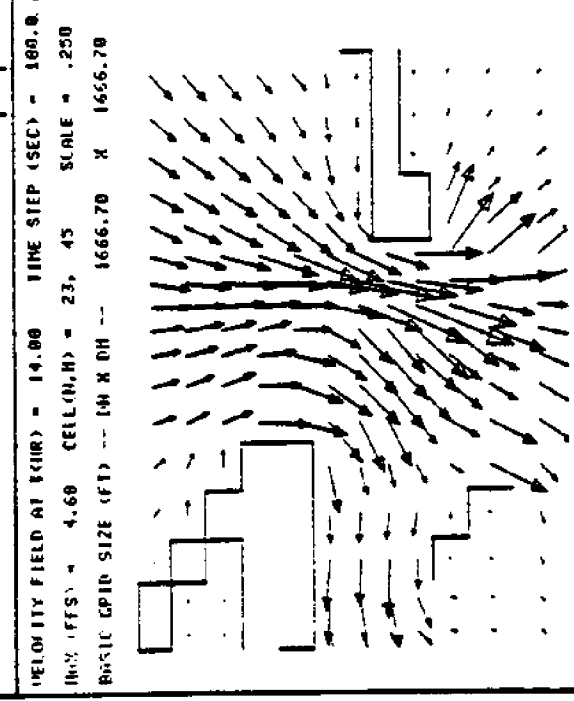
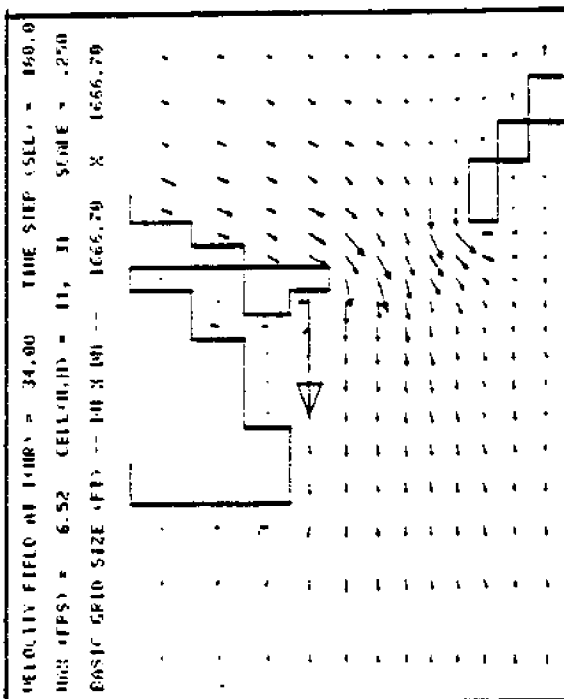
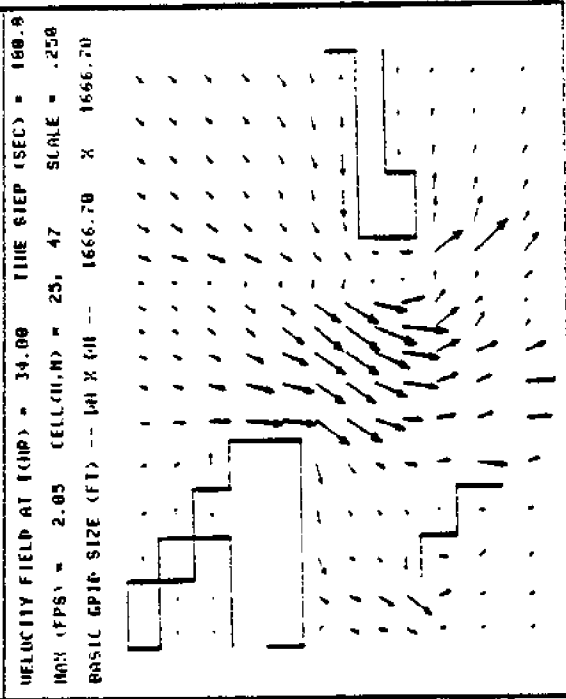


Figure 55. Velocity Vector Plots--Run 3  
(Medium Tide Range, High River, No Wind)  
Low Tide--A. Pass aux Herons B. Main Pass  
High Tide--C. Pass aux Herons D. Main Pass

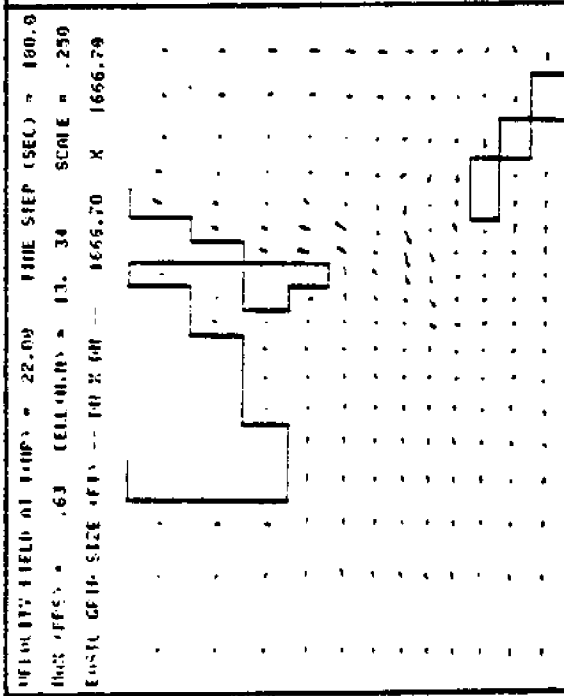
C.



D.



A.



B.

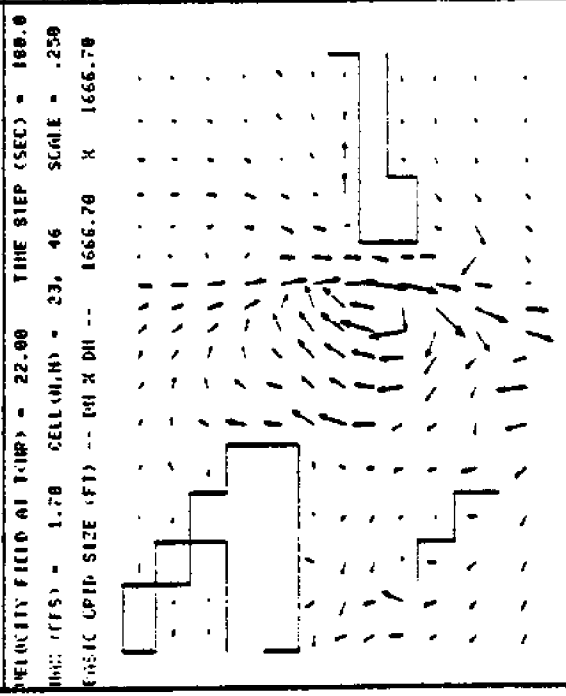
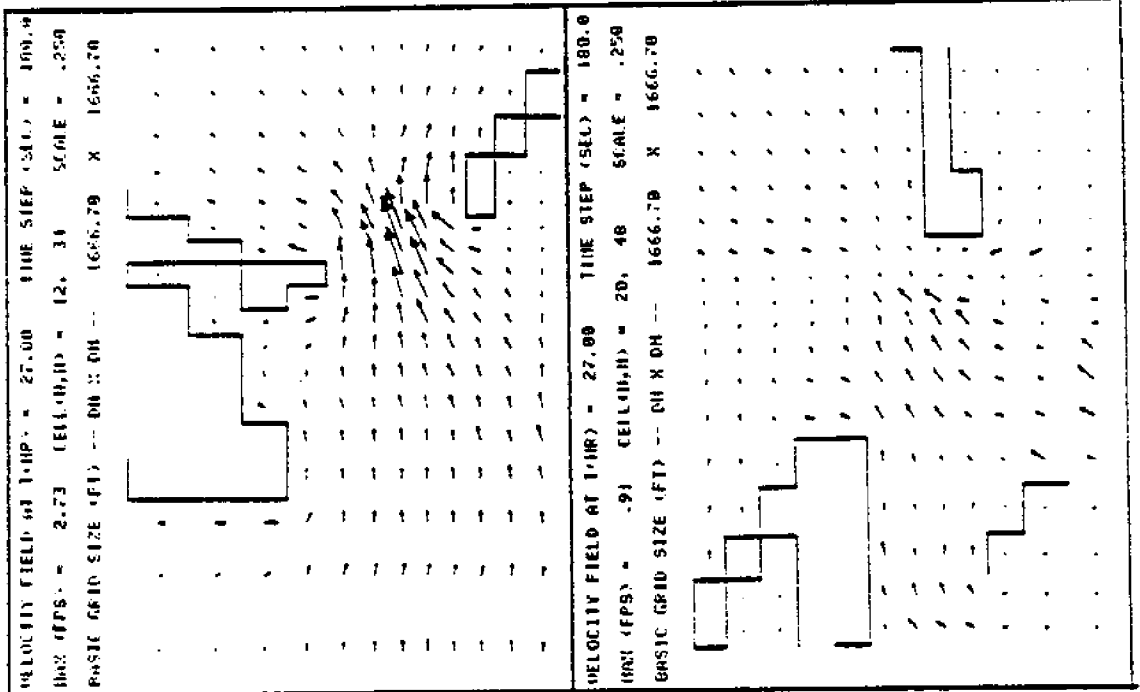


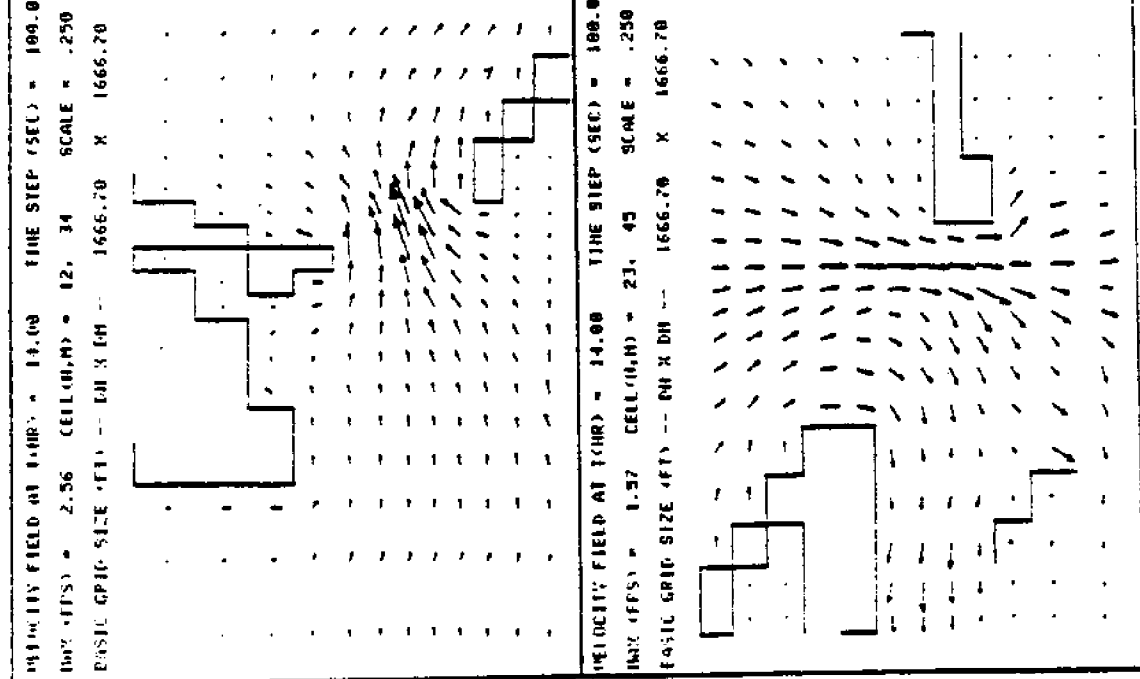
Figure 56. Velocity Vector Plots--Run 4  
(Low Tide Range, Medium River, No Wind)  
Ebb Tide--A. Pass aux Herons B. Main Pass  
Flood Tide--C. Pass aux Herons D. Main Pass

C.



D.

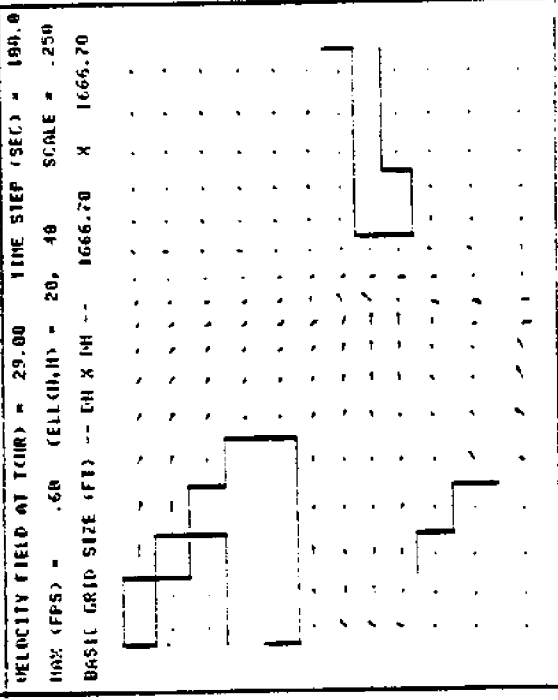
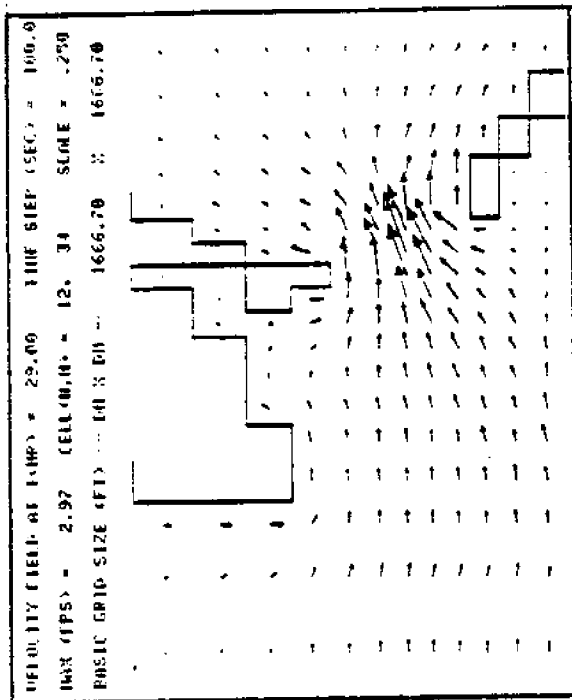
A.



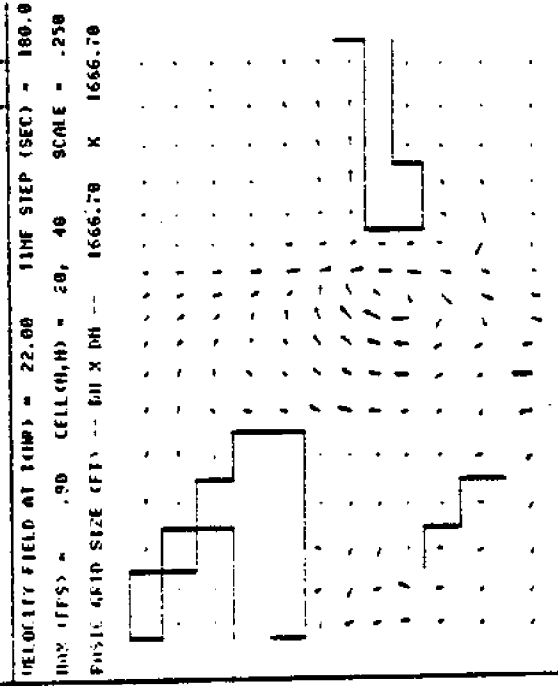
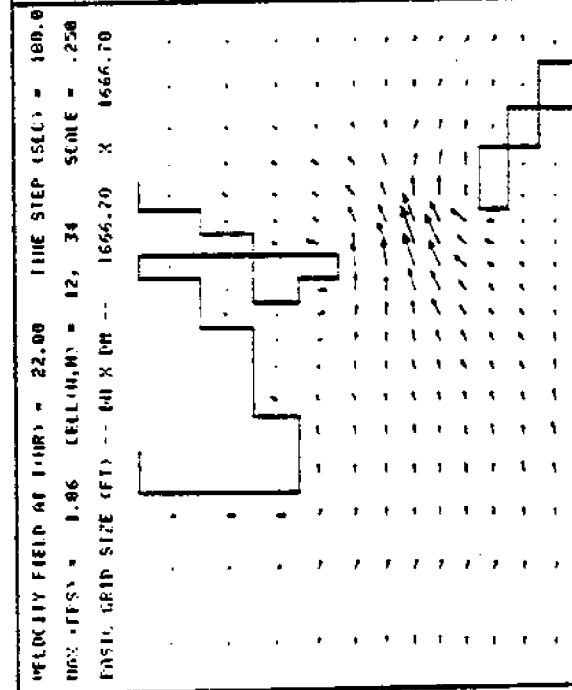
B.

Figure 57. Velocity Vector Plots--Run 4  
(Low Tide Range, Medium River, No Wind)  
Low Tide--A. Pass aux Herons B. Main Pass  
High Tide--C. Pass aux Herons D. Main Pass

C.



D.

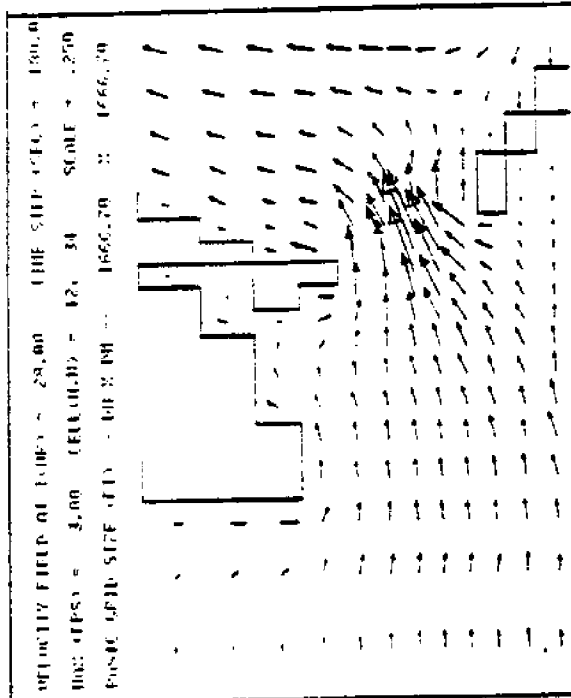


A.

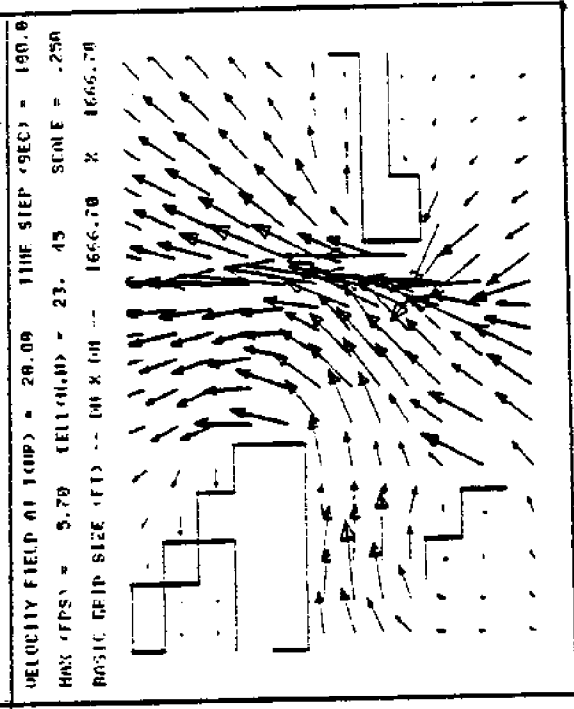
B.

Figure 58. Velocity Vector Plots--Run 5  
(High Tide Range, Medium River, No Wind)  
Ebb Tide--A. Pass aux Herons B. Main Pass  
Flood Tide--C. Pass aux Herons D. Main Pass

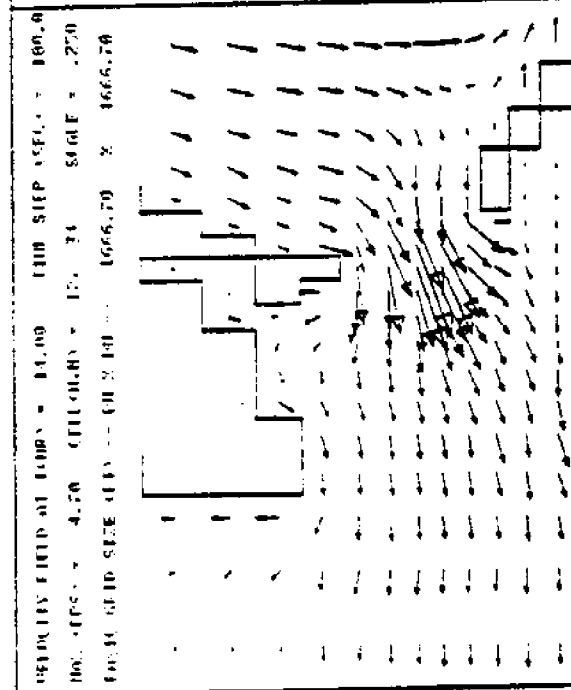
C.



D.



A.



B.

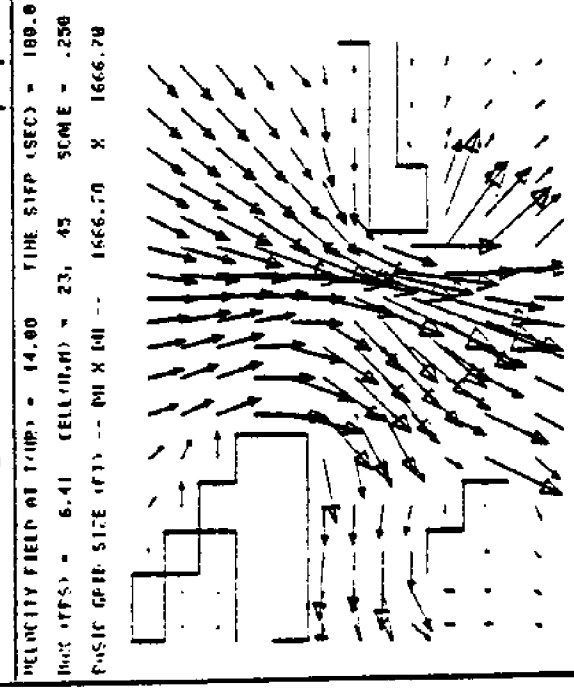
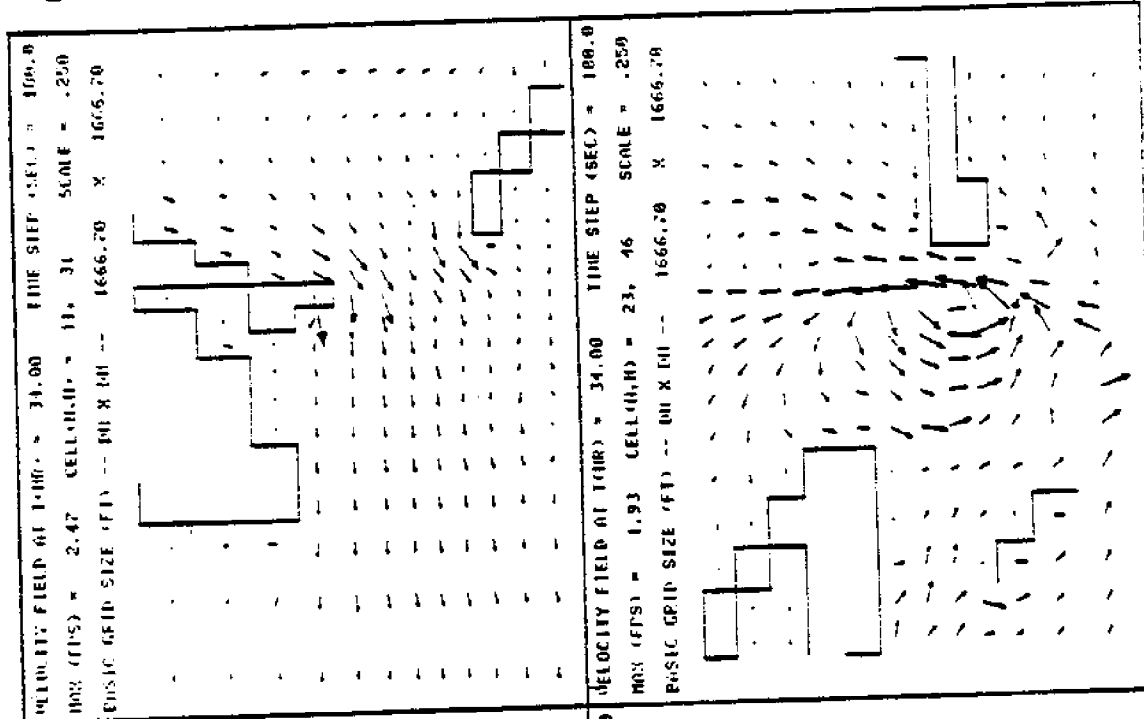
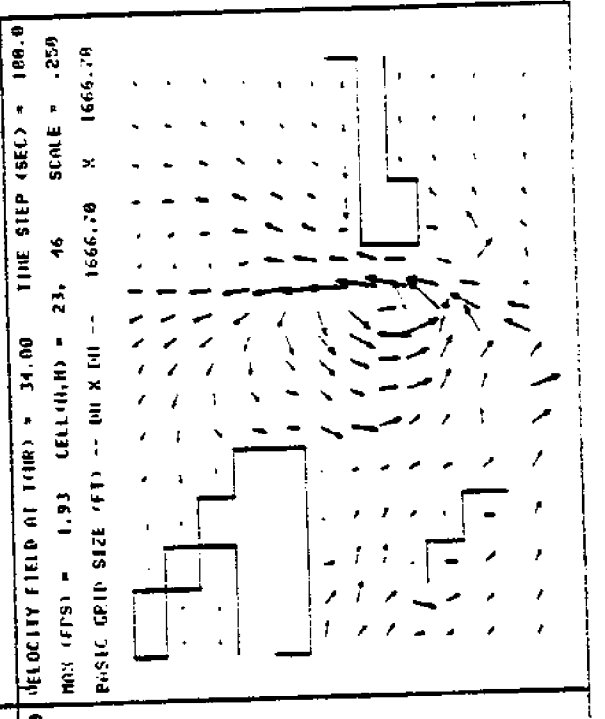


Figure 59. Velocity Vector Plots--Run 5  
(High Tide Range, Medium River, No Wind)  
Low Tide--A. Pass aux Herons B. Main Pass  
High Tide--C. Pass aux Herons D. Main Pass

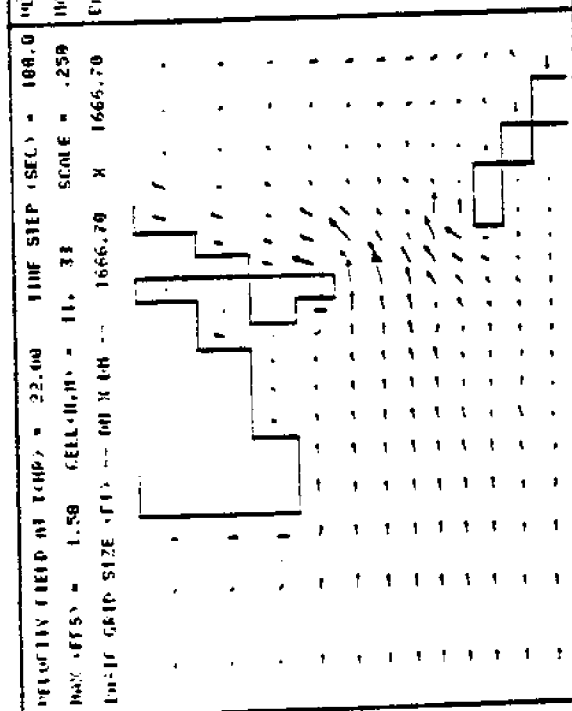
C.



D.



A.



B.

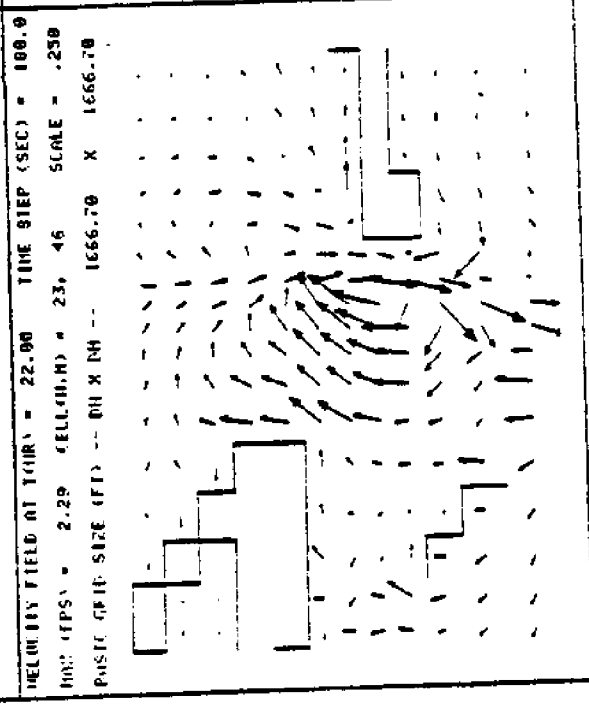
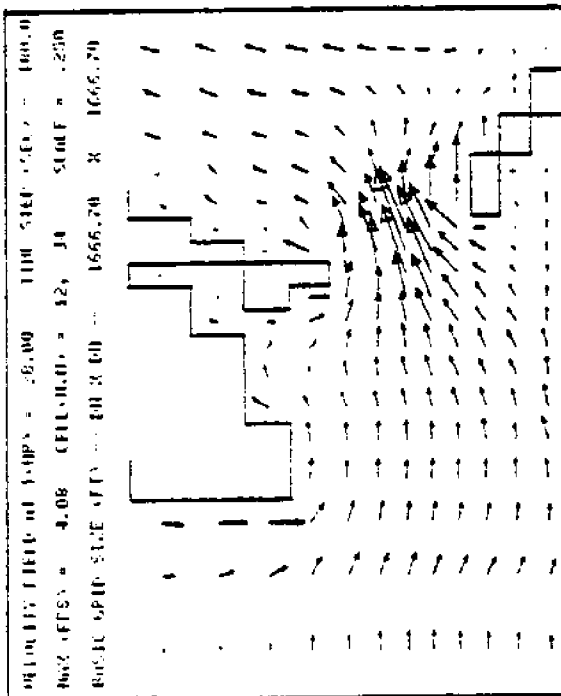
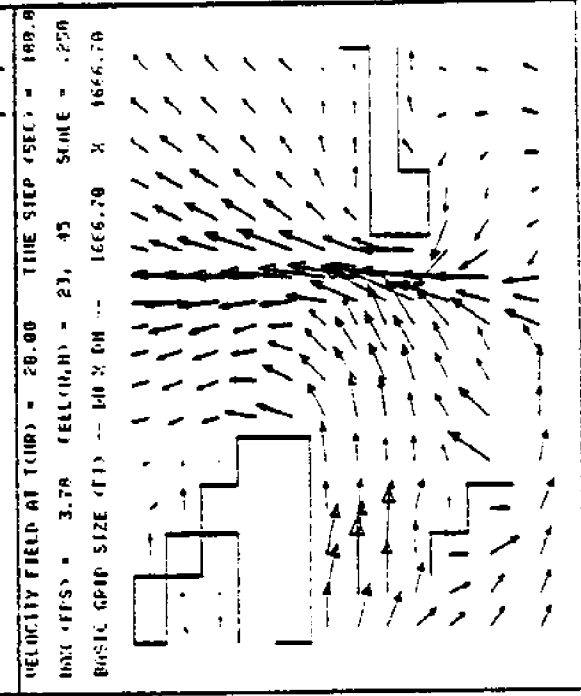


Figure 60. Velocity Vector Plots--Run 6  
(Medium Tide Range, Medium River,  
15 k Wind from Southwest)  
Ebb Tide--A. Pass aux Herons B. Main Pass  
Flood Tide--C. Pass aux Herons D. Main Pass

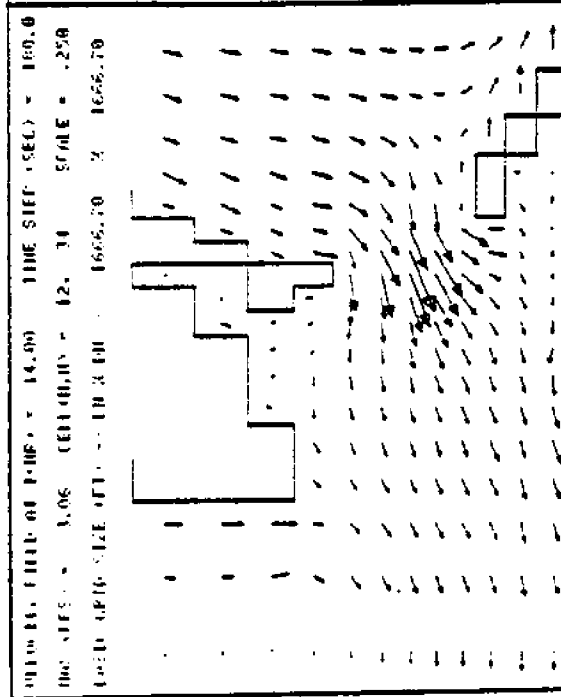
C.



D.



A.



B.

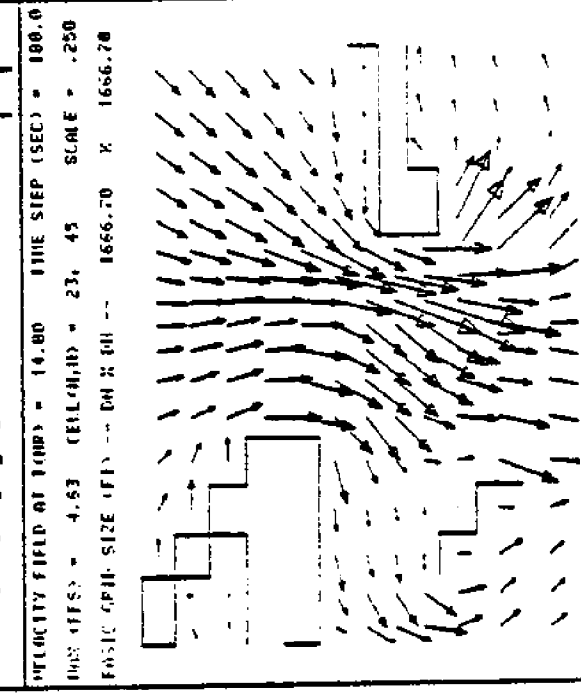
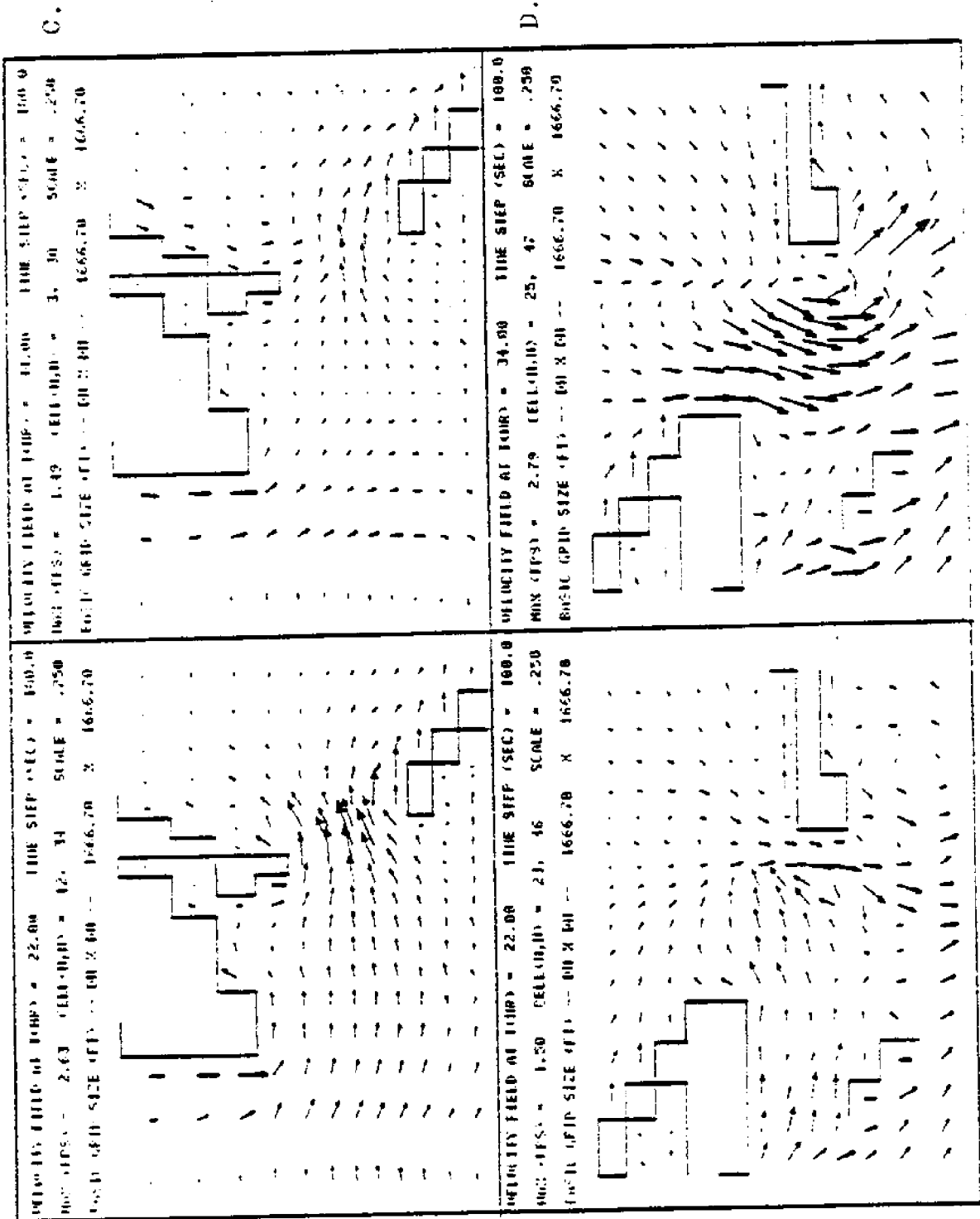


Figure 61. Velocity Vector Plots--Run 6  
(Medium Tide Range, Medium River,  
15 k Wind from Southwest)  
Low Tide--A. Pass aux Herons B. Main Pass  
High Tide--C. Pass aux Herons D. Main Pass



## CHAPTER VI

### CONCLUSIONS AND RECOMMENDATIONS

Chapters IV and V presented the results of the application of a recently developed, implicit, finite-difference numerical model, WIFM II, to Mobile Bay-East Mississippi Sound. The specific interest was the investigation of the interacting hydrodynamics in Pass aux Herons and Main Pass under a variety of input conditions. The water transport in the passes was studied because of its importance to the environment of the area.

The modeling effort was undertaken to expand the existing modeling capabilities in Mobile Bay to include the East Mississippi Sound. The existing Mobile Bay models were unsuitable for the detailed study of the small areas of Pass aux Herons and Main Pass. WIFM II had features, including variable grid size and implicit solution format, which made it applicable to pass-exchange study.

#### Concluding Observations

The results of the Calibration/Verification section showed the model to be applicable to the study of the relative trends of the water transport in the passes. The response of the trend behavior of the water transport to

changing input parameters was investigated. The quantitative effects of the input conditions could not be assessed because of the uncertainty and incompleteness of the field data.

The input parameters studied were tide range, river flow from the Mobile River system, and a constant wind field. Comparisons of the pass flow rates and pass velocity profiles were made for 3 tide ranges, 3 river flows, and 1 wind condition. The largest effects on the pass hydrodynamics were caused by the variation of the tide range. A high tide range caused significantly more water to flow into and out of the Bay, while a low tide range had the reverse effect. The river flow affected the amount of water entering the Bay through each pass over the tidal period. High river flows restricted the incoming flows through the passes. The 15 k wind from the southwest had a strong effect on the shallow water of Pass aux Herons and West Main Pass. The momentum of the wind increased the flow into the Bay through Pass aux Herons due to the coinciding wind and prevailing current directions. The direction of the current in Main Pass was altered by the wind field. The investigation of the constant wind field was included to provide a basis for further study of variable wind fields. Such a study was not made here due to the lack of field data.

### Recommendations for Further Study

The limiting factor in this study was the quantity and quality of the available field data. In order to further evaluate the applicability of this or other models to pass-exchange study, better field data are necessary. The data should include:

1. Accurate tide records at the Gulf of Mexico side of Dauphin Island under low wind conditions for the specification of the Gulf of Mexico tidal boundary
2. Accurate tide records at the east end of Petit Bois Island under low wind conditions to provide boundary conditions permitting the westward extension of the model limits to include all of East Mississippi Sound
3. In the event of a significant wind field during data collection, accurate wind records should be kept at each data station to provide the input for a variable wind field to the model
4. For calibration and verification of the model, some velocity stations should be located outside the ship channels, as these channels are difficult to represent with a two-dimensional model

Implementation of the field-data collection studies described above will provide the basis for developing this model, as well as the other Mobile Bay models, from a trend analysis tool to a truly predictive model. The integration

of the Mobile Bay-East Mississippi Sound model with models of the rest of the estuarine system of the Gulf Coast, supported by adequate field data, would provide an invaluable tool for the management of this important system.

## LIST OF REFERENCES

1. Department of the U.S. Army Corps of Engineers. Waterborne Commerce of the United States: Calendar Year 1976: Waterways and Harbors of the Gulf Coast, Mississippi River, and Antilles.
2. U.S. National Fisheries Service. Fisheries of the United States, 1977. Current Fishery Statistics No. 7500, 1978.
3. April, Gary C., Ng, Samuel C., and Hu, Chung-Shung. "Mobile Bay Hydrography under Flood Stage Conditions." Proceedings of the Symposium on Coastal Hazards II-Coastal Zone 78. 3 (1978):1783-1802.
4. Geological Survey of Alabama for the State Oil and Gas Board. The Environment of Offshore and Estuarine Alabama. by R. L. Chermock and Philip E. LaMoreaux, Information Series 51, 1974.
5. Hinwood, J. B. and Wallis, I. G. "Classification of Models of Tidal Waters." Journal of the Hydraulics Division ASCE 101 (October 1975):1315-31.
6. Hinwood, J. B. and Wallis, I. G. "Review of Models of Tidal Waters." Journal of the Hydraulics Division ASCE 101 (November 1975):1405-21.
7. Abraham, G. and Karelse, M. "Discussion of 'Classification of Tidal Waters' and 'Review of Models of Tidal Waters' by J. B. Hinwood and I. G. Wallis." Journal of the Hydraulics Division ASCE 102 (June 1976):808-11.
8. Abbot, M. B. "Discussion of 'Review of Models of Tidal Waters' by J. B. Hinwood and I. G. Wallis." Journal of the Hydraulics Division ASCE 102 (August 1976):1145-8.
9. Fisher, H. B. "Some Remarks on Computer Modeling of Coastal Flows." Journal of the Waterways, Harbors and Coastal Engineering Division ASCE 102 (December 1976):395-406.

10. Hinwood, J. B. and Wallis, I. G. "Closure to 'Classification of Models of Tidal Waters'." Journal of the Hydraulics Division ASCE 102 (December 1976):1776-7.
11. Hill, Donald O. "A Hydrodynamic and Salinity Model for Mobile Bay." Ph.D. dissertation, The University of Alabama, 1975.
12. Liu, Hua-An. "A Non-conservative Species Transport Model for Mobile Bay." M.S. thesis, The University of Alabama, 1975.
13. Ng, Samuel C. "Sediment Transportation in Mobile Bay: Correlation of Remote Sensing Data with the Hydrodynamic Model." M.S. thesis, The University of Alabama, 1977.
14. Hu, Chung-Shung. "Computer Simulation of Storm Surge and River Flooding in Mobile Bay." M.S. thesis, The University of Alabama, 1979.
15. Schroeder, William W. "The Impact of the 1973 Flooding of the Mobile River System on the Hydrography of Mobile Bay and East Mississippi Sound." Northeast Gulf Science 1 (December 1977):68-76.
16. Mississippi-Alabama Sea Grant Consortium. Physical Oceanography Section. Mississippi Sound Salinity Distributions and Indicated Flow Patterns. by Charles K. Eleuterius, 1976.
17. U.S. Army Engineers Waterways Experiment Station. WIFM II-WES Implicit Flooding Model: Theory and Program Documentation. by H. Lee Butler, vol. 2.
18. U.S. Department of Commerce. National Ocean Survey. U.S. Gulf Coast: Alabama: Mobile Bay, 1:80000 Mercator Projection at Lat. 30 25' (Sept 23/78).
19. U.S. Department of the Interior Geological Survey. Fort Morgan Quadrangle Alabama: 7.5 Minute Series (Topographic) NE/4 Fort Morgan 15' Quadrangle, 1958.
20. Mississippi-Alabama Sea Grant Program. Physical Environment Atlas of Coastal Alabama. by William W. Schroeder, 1976.

21. May, Edwin B. "Atlas: A Survey of the Oyster and Oyster Shell Resources of Alabama: Appendix B to Alabama Marine Resources Bulletin No. 4." Alabama Marine Resources Bulletin 4 (1971):12.
22. May, Edwin B. "A Survey of the Oyster and Oyster Shell Resources of Alabama." Alabama Marine Resources Bulletin 4 (February 1971):1-51.
23. May, Edwin B. "The Effect of Flood Waters on Oysters in Mobile Bay." Proceedings of the National Shellfisheries Association 62 (1972):67-71.
24. Hoese, H. D., Nelson, W. R., and Bechert. "Seasonal and Spatial Setting of Fouling Organisms in Mobile Bay and East Mississippi Sound." Alabama Marine Resources Bulletin 8 (June 1972):9-17.
25. Department of the Interior. Office of Water Resources Research. A Numerical Model for the Simulation of Tidal Hydrodynamics in Shallow Irregular Estuaries, by Frank D. Masch, N. J. Shankar, M. Jeffrey, R. J. Brandes, and W. A. White, February 1969.
26. U.S. Army Engineer District, Mobile Alabama. Mobile Bay Model: Report 1: Effects of Proposed Theodore Ship Channel and Disposal Areas on Tides, Currents, Salinities, and Dye Dispersion, by Raymond J. Lawing, Robert A. Boland, and William H. Bobb, September 1975.
27. U.S. Army Engineer District, New Orleans, Louisiana. An Open-Coast Mathematical Storm Surge Model with Coastal Flooding for Louisiana: Report 1: Theory and Application, by John J. Wanstrath, February 1978.
28. Wanstrath, John J., Butler, H. Lee, Vincent, C. L., Resio, D. T., and Whalin, R. W. "Use of Numerical Models for Computation of Coastal Water Levels." ASCE Fall Convention and Exhibit Preprint No. 3070 (October 1977).
29. The RAND Corp., Santa Monica, California. Aspects of a Computational Model for Long-Period Water-wave Propagation. by Jan J. Leendertse, May 1967.
30. Roache, Patrick J. Computational Fluid Dynamics. Albuquerque: Hermosa Publishers, 1972.
31. U.S. Department of Commerce. National Ocean Survey. Tide Tables: East Coast of North and South America including Greenland, 1972-3.

32. MacPhearson, Jr., Roland M. "The Hydrography of Mobile Bay and Mississippi Sound, Alabama." Journal of Marine Science 1 (August 1970):1-83.
33. Personal Communication from Lawrence R. Green , Chief of the Planning Division, U.S. Army Corps of Engineers, Mobile, Alabama to Dr. Gary C. April, Professor, The University of Alabama, University, Alabama.

## APPENDICES

A. Sample Input Data to WIFM II

B. Sample Output from WIFM II

For detailed program documentation see Butler (17).

APPENDIX A

Sample Input Data to WIFM II

EXAMPLE MAY OHED 2100 CELLS BLINE IMPUP 0100 4717 - 1300 6714/745

27	45	52	500	2	1	45	1	-1	-7	10	0	0	0	0	0	0	0	0	0
8:100	1666.7	1666.7	1666.7	1666.7	1666.7	1666.7	1666.7	1666.7	1666.7	1666.7	1666.7	1666.7	1666.7	1666.7	1666.7	1666.7	1666.7	1666.7	1666.7
5:	3	3	3	3	3	3	3	3	3	3	3	3	3	3	3	3	3	3	3
6:5	3	3	3	3	3	3	3	3	3	3	3	3	3	3	3	3	3	3	3
7:	600	20	100	1	1	30	0	20	0	0	0	0	0	0	0	0	0	0	0
1	4.0841327904	3.2612271677	2.7800234556	2.9562150512															
2	2.2198003909	2.0378003909	1.8921908402	1.7726004571															
3	1.6719336440	1.5879984540	1.5110801149	1.4453986138															
4	1.4631623725	1.3850567570	1.2886048411	1.2439784287															
5	1.2065492816	1.1705248071	1.1300531742	1.1074651812															
6	1.0794362128	1.0531786798	1.0245539561	1.0055150906															
7	1.1072579056	1.2146676366	1.3284865224	1.4480987256															
8	1.4719104897	1.7059902800	1.8494286719	1.9893188179															
9	2.1807571963	2.2981813949	2.0825104117	1.8916709721															
10	1.7227301508	1.5728943016	1.4190813549	1.3196379989															
11	1.2126706243	1.1145927202	1.0300794116	.9519937709															
12	1.5053629878	1.0608192008	1.1173603856	1.1760256588															
13	1.2144916358	1.2987763137	1.3628971577	1.4288713932															
14	1.4967164748	1.5648425644	1.6380049597	1.714416097															
15	1.7871358891	1.8649816562	1.9480011044	2.0254042149															
16	2.1080899089	2.197406645	2.2816057398	2.3711869688															
17	2.4627449883	2.5548018748	2.6521414287	2.7499910593															
18	2.8499681818	2.9520759583	3.0563912081	3.1627743840															
19	3.273899482	3.382023649	3.4952257216	3.6104743183															
20	3.7279621783	3.847031291	3.9700078117	3.5539772513															
21	4.181350470	4.289084793	4.402772894	3.0498705181															
22	4.932483402	4.833297799	4.7311606853	2.6350712478															
23	5.581961817	5.000000000	5.000000000	5.000000000															
24	6.000000000	5.000000000	5.000000000	5.000000000															
25	6.589281385	4.1935381293	3.8855985701	3.6223302166															
26	7.3945117491	3.1953156488	3.0194752918	2.8433066118															
27	8.271706859	2.5973324776	2.4811428210	2.3791878223															
28	9.2041253781	2.1968801572	2.1363976192	2.0420088596															
29	10.180585206	2.6188628078	2.4876003904	3.2994603217															
30	11.461617073	4.0937935099	4.5349137488	5.0102480531															
31	12.034872051	5.058643032	5.0245535919	5.8052723527															
32	13.278191802	5.184988793	5.1710524327	5.1920637488															
33	14.26505275	5.2328315073	5.2526241591	5.2720483606															
34	15.2911069989	5.3098244933	5.3282154567	5.3462879698															
35	16.371723330	4.4590399461	4.0630763578	3.7450904912															
36	17.4806350553	3.1685518612	2.9173861792	2.6923112959															
37	18.800757928	2.1028149511	2.1338238688	1.9781188536															
38	19.85572459	1.7099575830	1.5919722688	1.8838970356															
39	20.454872718	1.2932728529	1.2092170566	1.1337342311															
40	21.182330885	1.2322105169	1.2884568432	1.3384406269															
41	21.893762418	1.4505828870	1.5089204911	1.5687953383															
42	22.6302213571	1.6932362169	1.6256083711	1.5614539155															
43	23.401354248	1.8435070106	1.7887266887	1.3366332650															
44	24.2070712280	1.2198884187	1.1949482860	1.521114793															
45	25.045044443	1.4887250560	1.4119434970	1.8015100781															
46	25.91683538020	2.236814814	2.4879460878	2.7648668221															
47	26.8084556315	3.4024817929	3.7649107206	4.189199277															
48	27.7100855475	5.0893088579	5.6187027567	6.1885733521															
49	28.6218181818	5.000000000	5.000000000	5.000000000															
50	29.5436363636	5.000000000	5.000000000	5.000000000															
51	30.4654545454	5.000000000	5.000000000	5.000000000															
52	31.3872727272	5.000000000	5.000000000	5.000000000															
53	32.3090909090	5.000000000	5.000000000	5.000000000															
54	33.2309090909	5.000000000	5.000000000	5.000000000															
55	34.1527272727	5.000000000	5.000000000	5.000000000															
56	35.0745454545	5.000000000	5.000000000	5.000000000															
57	36.0000000000	5.000000000	5.000000000	5.000000000															













APPENDIX B

Sample Output from WIFM II





NO. OF FLOOD CELLS 372

MSD, TRD 75.14065 1-0.51516 179.61435 158.16130 154.30023 150.61522 162.29595 189.57571

167.20372 174.00722

376.34372

1.000000000000

1	0	1	000074000
2	1	2	03675-001
3	1	3	07009+000
4	2	4	09252+000
5	3	5	0A151+000
6	4	6	021007+000
7	5	7	05625-001
8	5	8	03122+000
9	7	9	03667-001
10	1	0	03279+000



INPUT DATA--CARD 1  
 OBJECTIVE COEFFICIENTS  
 OBJ1 34 17 16 10 73 55 36 74 12 53  
 OBJ2 25 27 19 72 73 26 17 32 32 24







N	1	23	45	50	44	47
1	5070	5070	5070	5070	5070	5070
2	5070	5070	5070	5070	5070	5070
3	5070	5070	5070	5070	5070	5070
4	5070	5070	5070	5070	5070	5070
5	5070	5070	5070	5070	5070	5070
6	5070	5070	5070	5070	5070	5070
7	5070	5070	5070	5070	5070	5070
8	5070	5070	5070	5070	5070	5070
9	5070	5070	5070	5070	5070	5070
10	5070	5070	5070	5070	5070	5070
11	5070	5070	5070	5070	5070	5070
12	5070	5070	5070	5070	5070	5070
13	5070	5070	5070	5070	5070	5070
14	5070	5070	5070	5070	5070	5070
15	5070	5070	5070	5070	5070	5070
16	5070	5070	5070	5070	5070	5070
17	5070	5070	5070	5070	5070	5070
18	5070	5070	5070	5070	5070	5070
19	5070	5070	5070	5070	5070	5070
20	5070	5070	5070	5070	5070	5070
21	5070	5070	5070	5070	5070	5070
22	5070	5070	5070	5070	5070	5070
23	5070	5070	5070	5070	5070	5070
24	5070	5070	5070	5070	5070	5070
25	5070	5070	5070	5070	5070	5070
26	5070	5070	5070	5070	5070	5070
27	5070	5070	5070	5070	5070	5070
28	5070	5070	5070	5070	5070	5070
29	5070	5070	5070	5070	5070	5070
30	5070	5070	5070	5070	5070	5070
31	5070	5070	5070	5070	5070	5070
32	5070	5070	5070	5070	5070	5070
33	5070	5070	5070	5070	5070	5070
34	5070	5070	5070	5070	5070	5070
35	5070	5070	5070	5070	5070	5070
36	5070	5070	5070	5070	5070	5070
37	5070	5070	5070	5070	5070	5070
38	5070	5070	5070	5070	5070	5070
39	5070	5070	5070	5070	5070	5070
40	5070	5070	5070	5070	5070	5070
41	5070	5070	5070	5070	5070	5070
42	5070	5070	5070	5070	5070	5070
43	5070	5070	5070	5070	5070	5070
44	5070	5070	5070	5070	5070	5070
45	5070	5070	5070	5070	5070	5070
46	5070	5070	5070	5070	5070	5070
47	5070	5070	5070	5070	5070	5070
48	5070	5070	5070	5070	5070	5070
49	5070	5070	5070	5070	5070	5070
50	5070	5070	5070	5070	5070	5070
51	5070	5070	5070	5070	5070	5070
52	5070	5070	5070	5070	5070	5070





P	1	41	42	43	44	45
1	10.0	10.6	10.0	10.0	10.6	10.6
2	10.0	10.0	10.0	10.0	10.0	10.0
3	10.0	10.0	10.0	10.0	10.0	10.0
4	10.0	10.0	10.0	10.0	10.0	10.0
5	10.0	10.0	10.0	10.0	10.0	10.0
6	10.0	10.0	10.0	10.0	10.0	10.0
7	10.0	10.0	10.0	10.0	10.0	10.0
8	10.0	10.0	10.0	10.0	10.0	10.0
9	10.0	10.0	10.0	10.0	10.0	10.0
10	10.0	10.0	10.0	10.0	10.0	10.0
11	10.0	10.0	10.0	10.0	10.0	10.0
12	10.0	10.0	10.0	10.0	10.0	10.0
13	10.0	10.0	10.0	10.0	10.0	10.0
14	10.0	10.0	10.0	10.0	10.0	10.0
15	10.0	10.0	10.0	10.0	10.0	10.0
16	10.0	10.0	10.0	10.0	10.0	10.0
17	10.0	10.0	10.0	10.0	10.0	10.0
18	10.0	10.0	10.0	10.0	10.0	10.0
19	10.0	10.0	10.0	10.0	10.0	10.0
20	10.0	10.0	10.0	10.0	10.0	10.0
21	10.0	10.0	10.0	10.0	10.0	10.0
22	10.0	10.0	10.0	10.0	10.0	10.0
23	10.0	10.0	10.0	10.0	10.0	10.0
24	10.0	10.0	10.0	10.0	10.0	10.0
25	10.0	10.0	10.0	10.0	10.0	10.0
26	10.0	10.0	10.0	10.0	10.0	10.0
27	10.0	10.0	10.0	10.0	10.0	10.0
28	10.0	10.0	10.0	10.0	10.0	10.0
29	10.0	10.0	10.0	10.0	10.0	10.0
30	10.0	10.0	10.0	10.0	10.0	10.0
31	10.0	10.0	10.0	10.0	10.0	10.0
32	10.0	10.0	10.0	10.0	10.0	10.0
33	10.0	10.0	10.0	10.0	10.0	10.0
34	10.0	10.0	10.0	10.0	10.0	10.0
35	10.0	10.0	10.0	10.0	10.0	10.0
36	10.0	10.0	10.0	10.0	10.0	10.0
37	10.0	10.0	10.0	10.0	10.0	10.0
38	10.0	10.0	10.0	10.0	10.0	10.0
39	10.0	10.0	10.0	10.0	10.0	10.0
40	10.0	10.0	10.0	10.0	10.0	10.0
41	10.0	10.0	10.0	10.0	10.0	10.0
42	10.0	10.0	10.0	10.0	10.0	10.0
43	10.0	10.0	10.0	10.0	10.0	10.0
44	10.0	10.0	10.0	10.0	10.0	10.0
45	10.0	10.0	10.0	10.0	10.0	10.0
46	10.0	10.0	10.0	10.0	10.0	10.0
47	10.0	10.0	10.0	10.0	10.0	10.0
48	10.0	10.0	10.0	10.0	10.0	10.0
49	10.0	10.0	10.0	10.0	10.0	10.0
50	10.0	10.0	10.0	10.0	10.0	10.0
51	10.0	10.0	10.0	10.0	10.0	10.0
52	10.0	10.0	10.0	10.0	10.0	10.0





10	1	1-	17	7	77	27
1	13.0	23.5	18.8	21.8	21.8	23.5
2	13.0	23.5	18.8	21.8	21.8	23.5
3	13.0	23.5	18.8	21.8	21.8	23.5
4	13.0	23.5	18.8	21.8	21.8	23.5
5	13.0	23.5	18.8	21.8	21.8	23.5
6	13.0	23.5	18.8	21.8	21.8	23.5
7	13.0	23.5	18.8	21.8	21.8	23.5
8	13.0	23.5	18.8	21.8	21.8	23.5
9	13.0	23.5	18.8	21.8	21.8	23.5
10	13.0	23.5	18.8	21.8	21.8	23.5
11	13.0	23.5	18.8	21.8	21.8	23.5
12	13.0	23.5	18.8	21.8	21.8	23.5
13	13.0	23.5	18.8	21.8	21.8	23.5
14	13.0	23.5	18.8	21.8	21.8	23.5
15	13.0	23.5	18.8	21.8	21.8	23.5
16	13.0	23.5	18.8	21.8	21.8	23.5
17	13.0	23.5	18.8	21.8	21.8	23.5
18	13.0	23.5	18.8	21.8	21.8	23.5
19	13.0	23.5	18.8	21.8	21.8	23.5
20	13.0	23.5	18.8	21.8	21.8	23.5
21	13.0	23.5	18.8	21.8	21.8	23.5
22	13.0	23.5	18.8	21.8	21.8	23.5
23	13.0	23.5	18.8	21.8	21.8	23.5
24	13.0	23.5	18.8	21.8	21.8	23.5
25	13.0	23.5	18.8	21.8	21.8	23.5
26	13.0	23.5	18.8	21.8	21.8	23.5
27	13.0	23.5	18.8	21.8	21.8	23.5
28	13.0	23.5	18.8	21.8	21.8	23.5
29	13.0	23.5	18.8	21.8	21.8	23.5
30	13.0	23.5	18.8	21.8	21.8	23.5
31	13.0	23.5	18.8	21.8	21.8	23.5
32	13.0	23.5	18.8	21.8	21.8	23.5
33	13.0	23.5	18.8	21.8	21.8	23.5
34	13.0	23.5	18.8	21.8	21.8	23.5
35	13.0	23.5	18.8	21.8	21.8	23.5
36	13.0	23.5	18.8	21.8	21.8	23.5
37	13.0	23.5	18.8	21.8	21.8	23.5
38	13.0	23.5	18.8	21.8	21.8	23.5
39	13.0	23.5	18.8	21.8	21.8	23.5
40	13.0	23.5	18.8	21.8	21.8	23.5
41	13.0	23.5	18.8	21.8	21.8	23.5
42	13.0	23.5	18.8	21.8	21.8	23.5
43	13.0	23.5	18.8	21.8	21.8	23.5
44	13.0	23.5	18.8	21.8	21.8	23.5
45	13.0	23.5	18.8	21.8	21.8	23.5
46	13.0	23.5	18.8	21.8	21.8	23.5
47	13.0	23.5	18.8	21.8	21.8	23.5
48	13.0	23.5	18.8	21.8	21.8	23.5
49	13.0	23.5	18.8	21.8	21.8	23.5
50	13.0	23.5	18.8	21.8	21.8	23.5
51	13.0	23.5	18.8	21.8	21.8	23.5
52	13.0	23.5	18.8	21.8	21.8	23.5





511	1.012	.712	16.570	11.380
512	.667	.667	16.570	11.380
513	.712	.567	16.570	11.380
514	.710	.677	16.570	11.370
515	.696	.772	16.570	11.370
516	1.007	.717	16.570	11.370
517	1.000	.792	16.570	11.380
518	1.017	.900	16.570	11.380
519	1.014	1.060	16.570	11.380
601	1.013	1.113	16.570	11.370
602	1.005	1.277	16.570	11.380
603	1.010	1.312	16.570	11.370
604	1.010	1.277	16.570	11.380
605	1.000	1.370	16.570	11.380
606	1.000	1.370	16.570	11.380
607	1.010	1.392	16.570	11.370
608	1.010	1.317	16.570	11.370
609	1.015	1.140	16.570	11.380
610	.670	1.060	16.570	11.380
701	.700	.763	16.570	11.380
702	.717	.767	16.570	11.380
703	.667	.732	16.570	11.380
704	.567	.717	16.570	11.380

\*\*\*\*\* END OF INPUT DATA\*\*\*\*\*













1	11	74	74	5510	2727010	66251010
2	11	41	42	5100	2467010	3023010
3	11	25	31	5403	2768011	1671011
				2-40	29.000	640.000
TOTAL						33.000

**THE UNIVERSITY OF ALABAMA  
COLLEGE OF ENGINEERING**

The College of Engineering at The University of Alabama has an undergraduate enrollment of more than 1,800 students and a graduate enrollment exceeding 100. There are approximately 100 faculty members, a significant number of whom conduct research in addition to teaching.

Research is an integral part of the educational program, and research interests of the faculty parallel academic specialities. A wide variety of projects are included in the overall research effort of the college, and these projects form a solid base for the graduate program which offers twelve different master's and five different doctor of philosophy degrees.

Other organizations on the University campus that contribute to particular research needs of the College of Engineering are the Charles L. Seebeck Computer Center, Geological Survey of Alabama, Marine Environmental Sciences Consortium, Mineral Resources Institute—State Mine Experiment Station, Mineral Resources Research Institute, Natural Resources Center, School of Mines and Energy Development, Tuscaloosa Metallurgy Research Center of the U. S. Bureau of Mines, and the Research Grants Committee.

This University community provides opportunities for interdisciplinary work in pursuit of the basic goals of teaching, research, and public service.